



PLACE IN RETURN BOX to remove this checkout from your record.
TO AVOID FINES return on or before date due.
MAY BE RECALLED with earlier due date if requested.

DATE DUE	DATE DUE	DATE DUE
MAY 06 2005		

**LONG-TERM EFFECTS OF PHENOL AND PHENOL PLUS
TRICHLOROETHENE APPLICATION ON MICROBIAL COMMUNITIES IN
AEROBIC SEQUENCING BATCH REACTORS**

By

Héctor Luis Ayala-del-Río

A DISSERTATION

Submitted to
Michigan State University
in partial fulfillment of the requirements
for the degree of

DOCTOR OF PHILOSOPHY

Department of Microbiology and Molecular Genetics

2002

ABSTRACT

LONG TERM EFFECTS OF PHENOL AND PHENOL PLUS TRICHLOROETHENE APPLICATION ON MICROBIAL COMMUNITIES IN AEROBIC SEQUENCING BATCH REACTORS

By

Héctor Luis Ayala-del-Río

One of the most common bioremediation strategies to treat contaminated effluents is the use of bioreactor systems. Although there is well established theory on the design and operation of bioreactors, there is scarce knowledge about the microbial ecology of these systems. The effects of more than two years of trichloroethene (TCE) application on the microbial communities of sequencing batch reactors were studied. One reactor was fed phenol and the other phenol and TCE in sequence. Exposure to TCE resulted in a community with reduced and relatively stable TCE transformation rates. Community analysis of the phenol plus TCE-fed reactor by terminal restriction fragment length polymorphism (T-RFLP) revealed that after initial changes in community structure, a stable community was selected. In contrast, the absence of TCE in the second bioreactor community resulted in higher but unstable TCE transformation rates. The community structure of the phenol-fed reactor was highly dynamic, showing only transient stability as revealed by T-RFLP analysis. In both reactors the changes in community structure correlated with changes in function. Scanning electron microscopy and fractionation of the suspended

solids revealed that TCE application induced major changes in the physiology of the system by increasing the accumulation of extracellular polymeric substances (EPS) and the formation of "star-like" flocs. In contrast, low amounts of EPS, and cells forming small aggregates were observed in the phenol-fed reactor. Isolation and phylogenetic analysis from both reactors revealed that the cultivable members of these communities belonged to the *Proteobacteria* (alpha, beta and gamma classes) *Firmicutes*, *Actinobacteria*, *Bacteroidetes*, and *Deinococcus-Thermus* phyla. Characterization of the phenol- and TCE-degrading capabilities of the isolates revealed that only 28 % degraded phenol under the conditions tested, and that 57 % of the phenol degraders cometabolized TCE. Enumeration of selected isolates from the communities by SYBR green real-time PCR revealed that a group of isolates belonging to the *Comamonadaceae* of the beta *Proteobacteria* were the predominant populations among the isolates tested in both reactors. These isolates, which contain phenol hydroxylase genes, grow on phenol and cometabolize TCE suggesting that long-term application of TCE does not result in the disappearance of TCE degrading phenotypes.

Copyright by
Héctor Luis Ayala-del-Río
2002

Dedication

To my family and my wife, for all their love, support and encouragement during this long journey. Thanks for helping me complete this dream.

ACKNOWLEDGEMENTS

I would like to express my deepest gratitude to many individuals who have helped me to complete this goal. First, I would like to thank my advisor Dr. James M. Tiedje, for his guidance, support, patience and encouragement during the completion of this dissertation. Thanks for giving me the creative freedom to pursue my own research path; I am sure the experiences I have gained under your guidance will help in my future career. I have always felt privileged to be here at MSU and for being your student. Special thanks to Dr. Craig S. Criddle, for allowing me to work in these microbial communities. Your creativity, encouragement and enthusiasm made my research more enjoyable and exciting. Thanks for introducing me to the world of environmental engineering. I have always considered you as my second advisor. Thanks to the other guidance committee members: Dr. Thomas Schmidt, Dr. Patrick Oriel and Dr. Greg Zeikus; for their constructive criticism that helped me to maintain focus on what was important, and for making my dissertation defense the most enjoyable discussion that I could ever imagine. Finally, thanks to Dr. Rawle Hollingsworth and Mindock, from the Department of Biochemistry at Michigan State University for helping me with the polysaccharide analysis.

I am indebted to Mr. Stephen J. Callister for operating the reactors during the duration of this experiment. Without your efforts in maintaining and monitoring these reactors none of this dissertation would have been possible. THANKS STEVE!!!. Thanks to past and present members of the Tiedje's lab; Ana Fernández, Shannon Flynn, Frank Loeffler, Klaus Nüsslein, Gesche Braker,

Bekki Helton, Ben Griffin, John Davis, John Urbance, James Cole, Alison Murray, Jorge Rodrigues, Vincent Deneff, Tamara Tsoi, Joon Park, David Treves, Monica Ponder, Krystal Baird, Robert SanInocencio... and many others for their friendship and help throughout my studies. Special thanks to past and present CME staff, Lisa Pline, Pat Englehart, Nikki Mulvaney and Brenda Minnot for making my life easier.

I would like to thank my friends; Lycely Sépulveda, Andres Chong, Verónica Grüntzig, Carlos Rodríguez, Claribel Cruz, Gustavo Bonaventura, Olga Hernández, Jaime Graulau, Vladimir Ferrer and Carmen M. Medina for being there in the good and bad times; and for being my family at MSU. I hope our friendship lasts forever!

None of this would have been possible without the love, support and encouragement of my family at home, Papi, Mami, Javier and Sarita. They always had cheering words when I needed them the most, and they did everything they could to help me complete this dream.

I own the greatest gratitude to my wife, Lizy Fernández. Although at the beginning you were far away, you always gave me strength and endless love to complete this journey. Thanks for being with me every day during the last two years, for encouraging me the days that things did not work out and for believing in me even when I had doubts in my abilities. Your patience and encouragement during this last stage were essential to complete this dissertation. I am grateful to have your love and I look forward to spend eternity together.

Last but not least, I want to thank God my lord, for your love, blessings, for giving me this opportunity and the strength to complete it. You were always with me, especially when I needed you the most. You have guided me through all my life, and especially during this last six years. You will remain my steward until the end of my days.

PREFACE

The work presented in this dissertation was a collaborative effort between the Center for Microbial Ecology and the Department of Civil and Environmental Engineering at Michigan State University. Mr. Stephen J. Callister, from the department of Civil and Environmental Engineering, was in charge of bioreactor operation, and in gathering the functional measurements presented in Chapter 2. The analysis of the polysaccharide fraction of the extracellular polymeric substances isolated from the phenol plus TCE-fed reactor presented on Chapter 3, was performed under the guidance of Dr. Rawle I. Hollingsworth and Dr. Carol C. Mindock, from the Department of Biochemistry at Michigan State University. Dr. Mindock, performed the GC-MS and NMR analyses. The scanning electron microscopy images presented on Chapter 4 were taken by Ewa Danielewicz, from the Center for Electron Microscopy at Michigan State University.

TABLE OF CONTENTS

LIST OF FIGURES	xiii
LIST OF TABLES	xviii

CHAPTER 1: TRICHLOROETHENE OXIDATION BY MICROBIAL COMMUNITIES..... 1

Trichloroethene.....	1
Characteristics and applications	1
Why TCE is a concern?	2
TCE biodegradation.....	3
Aerobic vs. Anaerobic	3
Cometabolism	5
Aerobic degradation pathways	6
Metabolic diversity	9
Toxicity	12
Bioreactors	14
General	14
Sequencing Batch Reactor	15
Microbial communities	19
The culture dependent era	19
Culture independent community analysis.....	20
Thesis Overview	24
Objectives	24
Experimental design	26
References	29

CHAPTER 2: SUCCESSIONAL AND FUNCTIONAL RESPONSES IN PHENOL AND PHENOL PLUS TCE FED REACTORS..... 36

Introduction.....	36
Materials and Methods	38
Reactor design and operation	38
TCE and phenol analysis	40
Reactor sampling and DNA extraction	41
PCR primers and conditions	42
PCR purification, restriction digest and gel separation.....	43
Analysis of T-RFLPs.	44
Results	45
TCE transformation rates	45
Phenol transformation rates	48
Community structure by T-RFLP	48
Discussion	63
References	68

CHAPTER 3: THE ABUNDANCE OF EXTRACELLULAR POLYMERIC SUBSTANCES AND THE SPATIAL DISTRIBUTION OF BACTERIA IN FLOCS IN PHENOL AND PHENOL PLUS TCE FED REACTORS. 72

Introduction.....	72
Materials and Methods	75
Reactor sampling	75
Scanning electron microscopy	75
Epifluorescent microscopy	76
Fractionation of the TSS	76
Purification and characterization of EPS	77
Results	78
Visual inspection and microscopy.....	78
EPS abundance	81
EPS composition.....	84
Discussion	88
References	92

CHAPTER 4: CHARACTERIZATION OF THE CULTIVABLE MEMBERS FROM PHENOL AND PHENOL PLUS TRICHLOROETHENE-FED REACTOR COMMUNITIES, AND THEIR DENSITIES OVER 2 YEARS OF REACTOR OPERATION..... 98

Introduction.....	98
Materials and Methods	100
Pure culture isolation and characterization	100
DNA isolation and purification	102
16S rDNA and phenol hydroxylase sequencing, and phylogenetic analyses	102
<i>In-silico</i> generation of terminal restriction fragments and community comparisons.....	104
SYBR green quantitative PCR	105
Results	109
Strain isolation and identification.....	109
Phylogeny of the isolated populations.....	112
Degradative characterization.	120
Primer design and specificity.	124
Sensitivity and reproducibility.....	124
Bacterial abundances.	129
Additional phylogenetic analysis of the dominant populations	137
Discussion	140
References	152

CHAPTER 5: CONCLUSIONS, SYNTHESIS AND FUTURE DIRECTIONS. 160

Conclusions	160
Synthesis	161

Future research	166
APPENDIX A: PROTOCOL FOR T-RFLP ANALYSIS OF MICROBIAL COMMUNITIES.....	171
APPENDIX B: HAEIII T-RFLP DATA.....	177
APPENDIX C: TRANSMISSION ELECTRON MICROGRAPHS.....	179

LIST OF FIGURES

Some of the figures in this dissertation are in color.

Figure 1.1. Proposed TCE degradation pathway catalized by aromatic degrading oxygenases. The toluene dioxygenase pathway was derived from studies in *Pseudomonas putida* F1 (Li and Wackett 1992), while the toluene 2-ortho monooxygenase pathway was determined from studies in *Burkholderia cepacia* G4 (Newman and Wackett 1997). Generation of CO₂ and cells from the TCE intermediates has been observed in mixed cultures.
..... 8

Figure 1.2. Normal operational cycles used in SBRs. Dashed lines indicate inflow or outflow of liquid, suspended solids or waste. Modified from Irvine et al. (1989).
..... 18

Figure 1.3. Overview of the molecular methods of community analysis based on rRNA genes. PCR, polymerase chain reaction; DGGE, denaturing gradient gel electrophoresis; TGGE, temperature gradient gel electrophoresis; ARDRA, amplified ribosomal DNA restriction analysis; T-RFLP, terminal restriction fragment length polymorphism; RFLP, restriction fragment length polymorphism; and FISH, fluorescent in-situ hybridization.
..... 23

Figure 1.4. Components of the Sequencing Batch Reactors. Phenol and TCE were fed via syringes to each reactor individually. For the phenol-fed reactor, the TCE syringe was replaced with a mineral medium syringe. The mineral medium, concomitantly fed with TCE, was fed from a carboy using a peristaltic pump. In order to provide oxygen, an air pump was used. To control temperature, a peristaltic pump was used to recycle water between a water bath and a cooling plate inside the reactor.
..... 28

Figure 1.5. Sequencing Batch Reactor cycling scheme. This cycle occurs twice a day. The cycle begins with the feed step, where phenol is fed. The phenol recharge stage is the period when cell grow and phenol degrading enzymes are activated. In the fill phase, TCE is added to the phenol plus TCE-fed reactor while the phenol-fed reactor receives the same volume of mineral medium. The react phase is when the second compound is consumed. In the settle phase, no aeration or mixing occurs to allow suspended solids to settle. Finally, the supernatant is removed on the decant phase before the cycle starts again.
..... 28

- Figure 2.1.** Long term functional responses of the phenol-fed and phenol plus TCE-fed reactors. (A), TCE transformation rates. (B), phenol degradation rates. 47
- Figure 2.2.** T-RFLP electropherograms of PCR amplified 16S rDNA bacterial genes from replicate reactor communities before TCE application to reactor B. Samples were digested with six different restriction enzymes individually 51
- Figure 2.3.** Changes in bacterial community structure over time. T-RFLP electropherograms were generated from a *CfoI* digest of the 16S rDNA PCR product. Shaded peaks indicate dynamic ribotypes. 55
- Figure 2.4.** Correspondence analysis of T-RFLP data from reactor communities. Results from independent digests with *CfoI* and *HaeIII*, were combined for the analysis. Circles with letters indicate periods where the community structure of the two reactors was similar. (A) phenol-fed reactor days 50-198, 605-811; phenol plus TCE-fed reactor 50-104. (B) phenol-fed reactor days 357-541; phenol plus TCE-fed reactor days 294-361, 399, and 414-811. T=0, day 0 of each reactor before TCE application to one of them. Dim, dimension. 56
- Figure 2.5.** Relative abundance of Bacterial T-RF's from reactor samples after digestion with *CfoI*. Numbers in the legend indicate the sizes of the T-RF's in base pairs..... 59
- Figure 2.6.** Correspondence analysis of T-RFLP data for each reactor community individually. (A), phenol-fed reactor; (B) phenol plus TCE-fed reactor. Numbers in the legend next to a symbol indicate day periods that were grouped together to facilitate interpretation. Arrows and numbers inside the graph indicate the order of the changes in community structure. Results from independent digests with *CfoI* and *HaeIII* were combined for the analysis. Circles delineate the different clusters formed. Dim, dimension..... 60
- Figure 2.7.** Community restriction patterns of PCR amplified phenol hydroxylase genes digested with *RsaI* and *MspI*. Numbers on top of each lane indicate time in days. Bars on tops represent the samples with similar fingerprinting pattern within and between reactors as determined from cluster analysis. 62
- Figure 3.1.** Electron scanning micrographs of reactor suspended solids. Images were taken after 900 days of reactor operation. Micrographs A-C and D-F represent different levels of resolution for the phenol-fed and the

phenol plus TCE-fed reactors, respectively. EPS, extracellular polymeric substances..... 79

Figure 3.2. Epifluorescence microscopy of the phenol plus TCE-fed reactor flocs. Samples were stained with SYTO-9. Panel A, 100X magnification, panel B, 700X magnification. 80

Figure 3.3. Fractionation of the TSS (A) and percentage of the fractions relative to the TSS (B). Values represent means \pm 95 % confidence intervals ($n=6$). 82

Figure 3.4. Gas chromatogram of alditol acetates from the phenol plus TCE-fed reactor purified EPS. The identities of the peaks were determined by coelution with standards and analysis of mass spectra. The peak before rhamnose is an unidentified compound. N-acetylglucosamine is not shown due to its long retention time. 85

Figure 3.5. ^1H NMR spectrum of the extracellular polysaccharide. Signals characteristic of rhamnose include two singlets between 1.2 and 1.5 ppm that were assigned to the 6-deoxy groups and signals between 5.0 and 5.5 ppm that were assigned to the alpha linkages of rhamnose. The two singlets between 2.0 and 2.2 ppm correspond to N-acetyl groups of N-acetylglucosamine and the signals between 4.7 and 4.9 ppm correspond to beta linkages of N-acetylglucosamine. Signals between 3.4 and 4.3 ppm correspond to the remaining sugar protons. PPM, part per million. 86

Figure 3.6. Composition of the EPS from the phenol plus TCE-fed reactor. Values represent averages \pm one standard deviation of triplicate injections. 87

Figure 4.1. OTU composition of the isolate collection from the two reactors. An OTU was defined as one or more sequences with more than 97 % sequence similarity..... 113

Figure 4.2. Phylogenetic tree of 16S rDNA sequences of isolates that belonged to the α -*Proteobacteria* class. The tree was constructed from 605 unambiguously aligned positions using the maximum-likelihood method, and was rooted using *Nitrosomonas eutropha*. Numbers at nodes represent the percentage of 100 bootstraps. The nodes without bootstraps values represent either nodes with bootstrap values below 50 %, or inconsistent branch order when compared against the consensus tree. The scale bar represents the number of substitutions per nucleotide position. T, type strain. 115

Figure 4.3. Phylogenetic tree of 16S rDNA sequences of isolates that belonged to the *β-Proteobacteria* class. The tree was constructed from 677 unambiguously aligned positions using the maximum-likelihood method, and was rooted using *Rhizobium* sp. Numbers at nodes represent the percentage of 100 bootstraps. The nodes without bootstraps values represent either nodes with bootstrap values below 50 %, or inconsistent branch order when compared against the consensus tree. The scale bar represents the number of substitutions per nucleotide position. T, type strain. 116

Figure 4.4. Phylogenetic tree of 16S rDNA sequences of isolates that belonged to the *Deinococcus-Thermus* phylum, *γ-Proteobacteria* class, and *Bacteroidetes* phylum. The tree was constructed from 659 unambiguously aligned positions using the maximum-likelihood method. Numbers at nodes represent the percentage of 100 bootstraps. The nodes without bootstraps values represent either nodes with bootstrap values below 50 %, or inconsistent branch order when compared against the consensus tree. The scale bar represents the number of substitutions per nucleotide position. T, type strain. 118

Figure 4.5. Phylogenetic tree of 16S rDNA sequences of isolates that belonged to *Actinobacteria* and *Firmicutes* phylums. The tree was constructed from 449 unambiguously aligned positions using the maximum-likelihood method, and was rooted using *Acidovorax avenae*. Numbers at nodes represent the percentage of 100 bootstraps. The nodes without bootstraps values represent either nodes with bootstrap values below 50 %, or inconsistent branch order when compared against the consensus tree. The scale bar represents the number of substitutions per nucleotide position. T, type strain. 119

Figure 4.6. Unrooted phylogenetic tree of the phenol hydroxylase amino acid sequences of the isolates. The tree was constructed using 169 aligned amino acids, between positions 83 and 252 of *Pseudomonas* sp. CF600 *dmpN* gene, using the protein maximum-likelihood method. Numbers at nodes represent the percentage of 100 bootstraps. The nodes without bootstraps values represent either nodes with bootstrap values below 50 %, or inconsistent branch order when compared against the consensus tree. The scale bar represents the number of substitutions per amino acid position. The asterisk indicates strains that degrade TCE. 123

Figure 4.7. Specificity of the SYBR green PCR reaction at 1.8 (A), and 1.5 (B), mM MgCl₂ using melting peak analysis. $-dF/dT$, negative derivative of fluorescence with respect to temperature. Data points shown represent every tenth measurement. 125

- Figure 4.8.** SYBR green I real time PCR calibration curves using cell lysates as template. Values represent averages of duplicate reactions \pm one standard deviation. C_T , cycle at which the fluorescence crosses an arbitrary threshold determined using a reference dye. 126
- Figure 4.9.** Reproducibility of SYBR green I real time PCR. Two different primer sets were used for the test. Values represent averages \pm 95 % confidence intervals ($n = 8$). 128
- Figure 4.10.** Abundance of phenol degraders in the phenol-fed reactor. Values represent averages \pm one standard deviation from duplicate reactions. ... 131
- Figure 4.11.** Abundance of phenol degraders in the phenol plus TCE-fed reactor. Values represent averages \pm one standard deviation from duplicate reactions. 133
- Figure 4.12.** Abundance of non-phenol degraders in the phenol-fed reactor. Values represent averages \pm one standard deviation from duplicate reactions. 135
- Figure 4.13.** Abundance of non-phenol degraders in the phenol plus TCE-fed reactor. Values represent averages \pm one standard deviation from duplicate reactions. 136
- Figure 4.14.** Phylogenetic tree of 16S rDNA sequences of the unidentified β *Proteobacteria* group. The tree was constructed from 1336 unambiguously aligned positions using the maximum-likelihood method, and was rooted using *Nitrosomonas europaea*. Numbers at nodes represent the percentage of 100 bootstraps. The nodes without bootstraps values represent either nodes with bootstrap values below 50 %, or inconsistent branch order when compared against the consensus tree. The scale bar represents the number of substitutions per nucleotide position. 138
- Figure 5.1.** Summary of community analysis results. Ph-RFLP, phenol hydroxylase restriction fragment length polymorphism analysis. *, phenol degrader; **, phenol and TCE degrader. Grey, white and black bars represent time periods when the community structure was similar within and between reactors (based on multivariate analysis). 164

LIST OF TABLES

Table 1.1. Examples of substrates, microorganisms and enzymes involved in TCE cometabolism*. α , alpha <i>Proteobacteria</i> ; β , beta <i>Proteobacteria</i> ; and γ , gamma <i>Proteobacteria</i>	11
Table 2.1. Reproducibility of the T-RFLP data. Means and 95% confidence intervals (CI) for Sørensen and Steinhaus similarity indexes were calculated from pairwise comparisons. The TAMRA GS2500 standard is a molecular weight marker used to determine the sizes of the fragments in the gel.	52
Table 3.1. Relative abundance of the EPS fraction in the phenol-fed and the phenol plus TCE-fed reactor. Values represent the percentage of the EPS relative to the TSS.....	83
Table 4.1. Primers and magnesium concentrations used for SYBR green quantitative PCR of the isolates. β proteo, beta proteobacteria	108
Table 4.2. Assignment of isolate T-RFs to community T-RFLPs. Isolate names in bold, indicate strains that T-RFs from both enzymes matched a community T-RF. NR, no restriction site. NM, no match with community T-RFLPs using a ± 3 bp window.....	110
Table 4.3. Percentages of community T-RFs that matched the isolates T-RFs. <i>n</i> , number of isolates.....	112
Table 4.4 Phenol and TCE degrading properties of the reactor isolates. Values represent percentage of removal. For the TCE degradation test fresh phenol medium at the appropriate concentration and TCE were mixed simultaneously. SBR-P, phenol-fed reactor; SBR-T, phenol plus TCE-fed reactor. NT, not tested. WV, Wolin's vitamins.	121
Table 4.5. Sequence similarity values of selected sequences from Figure 4.14.	139

CHAPTER 1

TRICHLOROETHENE OXIDATION BY MICROBIAL COMMUNITIES

Trichloroethene

Characteristics and applications

Trichloroethene (TCE) is a non-polar chlorinated compound widely used by industry as a solvent. TCE has been found in marine algae and volcanoes (Gribble 1994), but its major source is industrial production. It was first synthesized by Fisher in 1864 by the reduction of hexachloroethane with hydrogen (Hewer 1975). Ever since, TCE has been popular for industrial uses. Although the US government has imposed severe restrictions on the use and release of TCE, the demand for this chemical remains high. The U.S. demand for TCE increased from 128 million pounds in 1995 to 171 million pounds in 1998, an increase of 33 % (HSIA 1996, 2001).

The increased use of TCE is because of its favorable physico-chemical properties which include low flammability, high stability, non-corrosiveness, low specific heat and solubility with other industrial solvents. TCE is mainly used as a degreasing agent and for chemical synthesis of other products (HSIA 2001; ATSDR 2002; U.S.-EPA 2002). For instance, high purity TCE is used as a precursor to synthesize hydrofluorocarbon 134a, a replacement for the ozone depleting chlorofluorocarbon 113. As a cleaning and degreasing agent, TCE is fast and efficient, being used by the metal industry to clean steel before galvanizing, and previously by the United States Air Force to clean jet engines.

USCE:

אשר

act,

Why T

A

172

250

33

3.07

7.00

33

400

33a

32

250

23

20

11

3

ذکر

Miscellaneous uses of TCE include as an extraction solvent, waterless dying in the textile industry, dry cleaning, a component of paint, spot and paint removers and typewriter correction fluid.

Why TCE is a concern?

Although TCE is an excellent industrial solvent it is toxic to humans and animals. Acute short term exposure to TCE vapors can affect the central nervous system causing headaches, vertigo, drowsiness, irritation of the respiratory system and unconsciousness (ATSDR 1994). However, the most severe adverse effects are caused by oral ingestion. Animal studies on rodents revealed an increase on the incidence of liver, lung and kidney tumors (Bruckner et al. 1989). Re-analyses and interpretation of previous toxicological studies suggest that the effects of TCE on rodents can not be extrapolated to humans because of differences in the metabolism of TCE between the two groups (Green 2001). Large epidemiological studies, however, have found an association between TCE exposure and increased risk of different types of cancer (U.S.-EPA 2001). Nevertheless, the International Agency for Research on Cancer currently considers TCE to be “probably carcinogenic to humans” (W.H.O. 1993), while the US-EPS is currently reassessing the cancer classification of TCE (U.S.-EPA 2002).

The widespread use of TCE by industry comes with some consequences. The lack of early government regulation and inappropriate handling and disposal caused TCE to be one of the most frequently detected soil and groundwater

pollutants in the United States. In 1994, TCE was the most prevalent contaminant found on the National Priorities List (NPL), being identified in 37 % of all NPL sites ($n=951$), and was a groundwater contaminant in 34 % of them (ATSDR 1994). Furthermore, 87 % of the contaminated plumes ($n=322$) were active sources of drinking water representing a major hazard for the human population. For these reasons, TCE is listed on the top 20 priority pollutant list of US-EPA.

TCE biodegradation

Aerobic vs. Anaerobic

Biodegradation is the biologically catalyzed conversion of a pollutant into biomass or less toxic products. Microbes play the major role in the biodegradation of pollutants since they possess a wide variety of enzymes and physiological adaptations that allow them to metabolize various toxic compounds. Studies in the mid 1980's provided the first evidence that TCE can be degraded biologically by microorganisms (Vogel and McCarty 1985; Wilson and Wilson 1985). Anaerobic degradation of TCE occurs by a process known as reductive dehalogenation (Mohn and Tiedje 1992). In this process, TCE serves as an electron acceptor, due to its highly oxidized state, and Cl is removed simultaneously in the process. Although the process can completely dechlorinate the substrate to ethene, it carries the risk that daughter products generated from the dechlorination, i.e. cis-DCE, 1,1-DCE and vinyl chloride may accumulate. These dechlorination products are more toxic than TCE, and hence maybe even more problematic.

Aerobic biodegradation of TCE was first demonstrated by Wilson and Wilson in 1985, when they observed a significant reduction in the concentration of TCE in soil enriched with natural gas (77% methane) compared to the TCE in non-enriched soils. Subsequent studies by other investigators demonstrated that methanotrophic bacteria were responsible for the aerobic degradation of TCE (Fogel et al. 1986; Little et al. 1988; Tsien et al. 1989). Following this discovery methane was successfully used to stimulate TCE degradation both in bioreactors and in soils and aquifers (Phelps et al. 1990; Semprini et al. 1990; Alvarez-Cohen and McCarty 1991b).

Aerobic bacteria that grow on aromatic hydrocarbons are another group of microbes capable of TCE degradation. Nelson and coworkers isolated the first aerobic TCE degrader, *Burkholderia cepacia* G4, from a waste treatment facility at the Naval Air Station in Pensacola, FL (Nelson et al. 1986). They noted that oxygen and an unidentified component in the wastewater, latter identified as phenol, were essential for TCE oxidation. In subsequent studies they demonstrated that enzymes from the aromatic degradation pathway of G4 and other phenol and toluene degraders were involved in the degradation of TCE (Nelson et al. 1987; Nelson et al. 1988). A key observation made by Nelson's group was the requirement of phenol for TCE degradation. Similar results were obtained by Little and coworkers, who showed that active metabolism of the growth substrate (methane) by the methanotrophic isolate 46-1 was necessary for the degradation of TCE (Little et al. 1988). These findings, and the fact that no pure culture was able to grow on TCE as the sole carbon source lead to the

200

200

Com

100

100

100

100

100

100

100

100

100

100

100

100

100

100

100

100

100

100

conclusion that TCE is degraded aerobically by a process known as cometabolism.

Cometabolism

Cometabolism is defined as the transformation of an organic compound by a microbe, with a non-specific enzyme, that does not result in energy or carbon for cell growth (Alexander 1994). This means that cometabolism will not provide any direct nutritional benefit to the microorganisms degrading the compound, i.e. a fortuitous transformation. Cometabolism represents a dilemma for bacteria since the oxidation of a non-growth compound may require energy that could otherwise be devoted to growth (Chang 1996). Alexander (1994), suggests three possible explanations for this phenomenon: (a) the metabolites generated from the fortuitous reaction can not be further transformed by other enzymes to yield intermediates that could be used for growth; (b) the initial transformation generates products that inhibit the activity of later enzymes; and (c) the organism needs a second substrate in order to metabolize the intermediate generated. Although the first alternative is the most probable one, the potential toxic effects of the cometabolic transformation products can not be disregarded since it could result in a tradeoff for the microorganism carrying out cometabolic reactions. For cometabolism to occur the microorganisms will always require a growth substrate, which besides providing carbon and energy for growth, may be needed to activate the enzyme required for the fortuitous reaction. Hence, the enzymes involved should possess a broad substrate range to recognize

0000

0000

0000

0000

0000

0000

0000

0000

0000

0000

0000

0000

0000

0000

0000

0000

0000

0000

0000

0000

0000

different compounds. As described earlier, phenol and methane are two compounds that serve both as growth and inducing substrates for TCE cometabolism. The broad substrate range enzymes involved in this case are known as oxygenases, enzymes that activate molecular oxygen and incorporate it into organic and inorganic compounds as part of the catalyzed transformation.

Aerobic degradation pathways

Since the first reports on the biological degradation of TCE, there have been extensive efforts to determine how this compound is metabolized. Knowledge of the metabolic pathway of TCE degradation is necessary to understand how microbes perform this reaction, and to determine the final fate of TCE in the environment (Wackett 1995). The first insights into the mechanism of TCE degradation were provided by Little et al. using a pure culture of a methanotrophic bacterium (Little et al. 1988). Using ^{14}C -TCE they obtained preliminary data that suggests that the products generated from TCE cooxidation were glyoxylic and dichloroacetic acids. They proposed that TCE was converted to an unstable epoxide that decomposes in aqueous solution to yield the products mentioned above. However, in other studies, chloral, carbon monoxide and glyoxylate were observed as products from TCE cometabolism by methanotrophs, suggesting the existence of multiple TCE degradative pathways within this bacterial group (Fox et al. 1990; Newman and Wackett 1991). The majority of these products can be consumed by other heterotrophic bacteria to

190

334

0 שנה

၁၆

331

750

34

35

xca

2007

21

32

Des

15A

700

10

知

35.

22

50.

yield CO₂ and cells (Little et al. 1988; Uchiyama et al. 1992), and hence might provide a positive growth response.

As described earlier, the involvement of aromatic degradative pathways in the degradation of TCE was established early on by Nelson and coworkers using strain G4 (Nelson et al. 1987). Further support for this observation was provided by Wackett and Gibson using *todC* mutants of *Pseudomonas putida* F1 (Wackett and Gibson 1988). Defects in the *todC* gene, which produces the iron-sulfur protein of the dioxygenase component of the toluene dioxygenase, resulted in no TCE oxidation, while spontaneous revertants recovered the TCE oxidation ability. Using purified F1 toluene dioxygenase generated from recombinant *Escherichia coli* strains and ¹⁴C TCE, Li and Wackett (1992) found that glyoxylic and formic acids were the products of TCE oxidation, and by using deuterated TCE, formic acid was the main product. This pathway does not involve the formation of an epoxide (Figure 1.1).

The fact that no epoxide was formed during the degradation of TCE by F1 does not mean that all aromatic oxygenases will exhibit the same phenomenon. Newman and Wackett (1997) confirmed that indeed there are differences in the metabolism of TCE between a toluene dioxygenase and a toluene monooxygenase. Using purified toluene 2-monooxygenase from *Burkholderia cepacia* G4, they determined that the major oxidation products were formate, glyoxylate and carbon monoxide (Figure 1.1). Although the products are similar to the ones found in F1, they proposed that in G4 the TCE was converted to an epoxide intermediate that spontaneously decomposed to the major oxidation

products observed (Newman and Wackett 1997). Different from the dioxygenase, that incorporates two oxygen atoms to one TCE molecule, the monooxygenase reaction incorporates only one oxygen atom which leads to the formation of the epoxide.

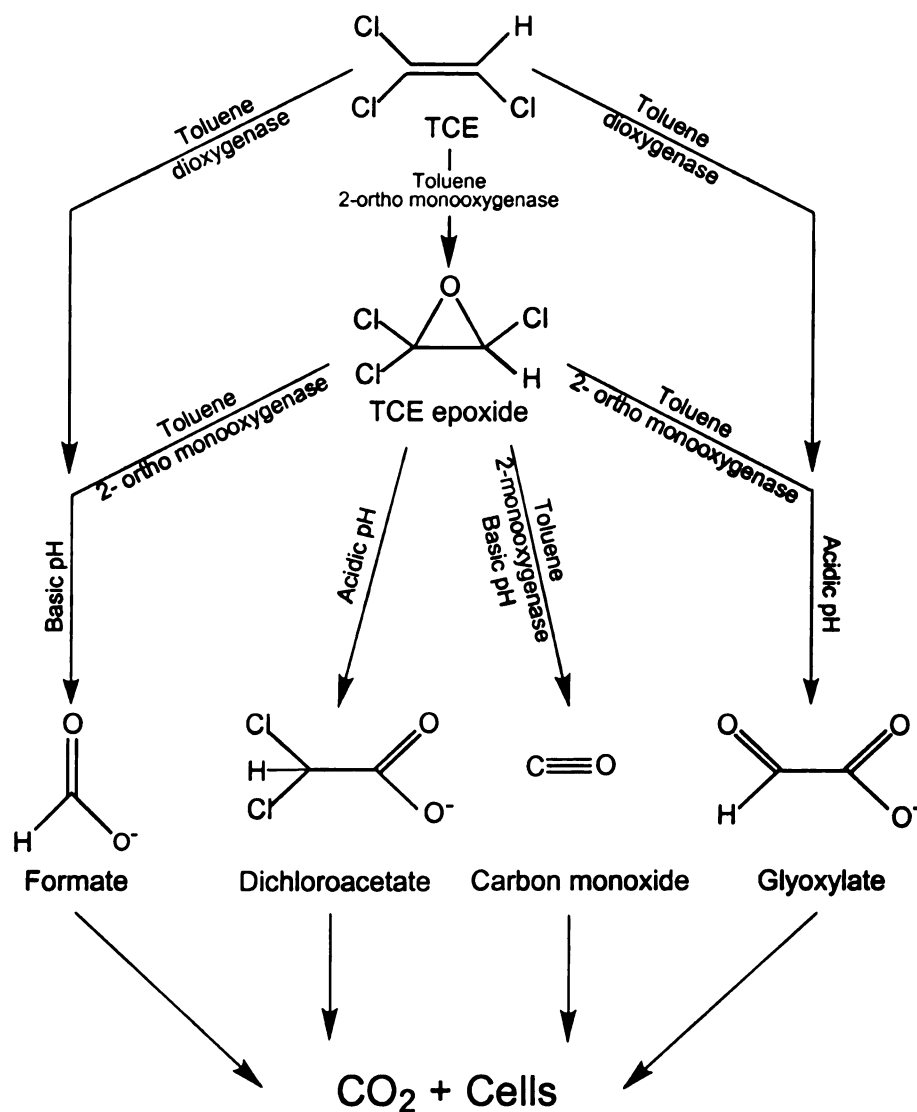


Figure 1.1. Proposed TCE degradation pathway catalyzed by aromatic degrading oxygenases. The toluene dioxygenase pathway was derived from studies in *Pseudomonas putida* F1 (Li and Wackett 1992), while the toluene 2-ortho monooxygenase pathway was determined from studies in *Burkholderia cepacia* G4 (Newman and Wackett 1997). Generation of CO₂ and cells from the TCE intermediates has been observed in mixed cultures.

Meta

TOE

Sim

Sim

Sim

Sim

Sim

TOE

Sim

Sim

Sim

Sim

TOE

Sim

Sim

Sim

Sim

Sim

Sim

Sim

Sim

Metabolic diversity

Although methane and toluene are two of the most studied substrates for TCE cometabolism, a diverse collection of compounds have been found to stimulate TCE degradation (Table 1.1). Ammonia, butane, 2,4-dichlorophenoxyacetate, isopropylbenzene, ethylene, phenol, propane and propylene are all the substrates known to stimulate TCE cometabolism, and in an equally diverse range of microbes. Members of the *Actinobacteria* and the alpha, beta and gamma classes of the *Proteobacteria*, are able to cometabolize TCE, indicating that this is a widespread phenomenon.

While oxygenases have the common characteristic of activating oxygen for catalysis, a survey of broad-substrate oxygenases revealed that many of them can not cometabolize TCE (Wackett et al. 1989), although later, a variety of enzymes were found to perform this reaction (Table 1.1). This enzymatic diversity is further accentuated by the fact that different enzymes that degrade the same growth substrate can oxidize TCE. For instance, there are five different pathways for toluene oxidation if judged by the position of the initial attack to the molecule, and three of them are capable of degrading TCE (Fries 1995). PCR amplification, cloning and sequencing of multicomponent phenol hydroxylase genes from pure cultures and aquifer samples revealed substantial sequence diversity for an enzyme with a common reaction mechanism (Watanabe et al. 1998; Futamata et al. 2001b). These authors found that different clades of sequence correlated with different affinities for TCE, i.e. K_m . Diversity can also be seen at the strain level, since some strains contain multiple

and V

stop

and a

tegra

and very different metabolic pathways capable of degrading TCE. *Ralstonia eutropha* JMP134, possesses a chromosomally encoded phenol hydroxylase and a plasmid encoded 2,4-dichlorophenol hydroxylase, both capable of TCE degradation but at different rates (Harker and Kim 1990).

2
5
10

2000

2000

2000

2000

2000

2000

2000

2000

2000

2000

2000

2000

2000

2000

2000

2000

2000

2000

2000

2000

Table 1.1. Examples of substrates, microorganisms and enzymes involved in TCE cometabolism*. α , alpha *Proteobacteria*; β , beta *Proteobacteria*; and γ , gamma *Proteobacteria*.

Growth substrate	Bacterial class†	Microorganism	Enzyme	Reference
Ammonia	α	<i>Nitrosomonas europaea</i>	Ammonia monooxygenase	(Arciero et al. 1989) (Rasche et al. 1991)
Butane	γ	<i>Pseudomonas butanavora</i>	Butane monooxygenase	(Hamamura et al. 1997)
Ethylene/propylene	α	<i>Xanthobacter</i> Py2	Alkene monooxygenase	(Ensign et al. 1992) (Reij et al. 1995)
Isopropylbenzene	<i>Actinobacteria</i>	<i>Rhodococcus erythropolis</i>	Isopropylbenzene dioxygenase	(Dabrock et al. 1992) (Pflugmacher et al. 1996)
Methane	α	<i>Methylosinus trichosporium</i> OB3b	Particulate methane monooxygenase	(DiSpirito et al. 1992) (Lontoh et al. 1999)
Methane	α	<i>Methylosinus trichosporium</i> OB3b	Soluble methane monooxygenase	(Tsien et al. 1989) (Oldenhuis et al. 1989)
Phenol and 2,4-dichloro-phenoxyacetate	β	<i>Ralstonia eutropha</i> JMP 134	Phenol hydroxylase, 2,4-dichlorophenol hydroxylase	(Harker and Kim 1990)
Phenol	β	<i>Comamonas testosteroni</i> R5	Phenol hydroxylase	(Futamata et al. 2001a)
Phenol	β	<i>Variovorax</i> sp. HAB-29	Phenol hydroxylase	(Futamata et al. 2001b)
Phenol	β	<i>Ralstonia</i> sp. E2	Phenol hydroxylase	(Futamata et al. 2001b)
Propane	<i>Actinobacteria</i>	<i>Mycobacterium vaccae</i> JOB5	Propane monooxygenase	(Wackett et al. 1989)
Propylene	<i>Actinobacteria</i>	<i>Rhodococcus corallinus</i> B-276	Alkene monooxygenase	(Saeki et al. 1999)
Toluene	γ	<i>Pseudomonas putida</i> F1	Toluene dioxygenase	(Wackett and Gibson 1988) (Zylstra et al. 1989)
Toluene	β	<i>Burkholderia cepacia</i> G4	Toluene 2-monooxygenase	(Newman and Wackett 1995) (Shields et al. 1995)
Toluene	β	<i>Ralstonia pickettii</i> PKO 1	Toluene 3-monooxygenase	(Olsen et al. 1994) (Johnson and Olsen 1995)
Toluene	γ	<i>Pseudomonas mendocina</i> KR	Toluene 4-monooxygenase	(Yen et al. 1991)

* Modified from Arp et al. (2001). †, according to the taxonomic outline of the Bergey's Manual for Systematic Bacteriology (Garrrity et al. 2001).

Toxicity

The major hurdle for sustained TCE cometabolism is from the toxicity of the metabolites generated. One of the first observations of TCE metabolite toxicity was with *Pseudomonas putida* F1, in which the initial TCE degradation rate decreased 98 % during the first 20 min of TCE exposure leading to the conclusion that TCE related toxicity was occurring (Wackett and Gibson 1988). Subsequent studies using ^{14}C -TCE revealed that the decrease in degradation rates observed was caused by cytotoxicity of glyoxylic and formic acid, the major products generated from TCE (Wackett and Householder 1989). Furthermore, an F1 mutant defective in the oxygenase component of the toluene dioxygenase did not show any signs of toxicity when exposed to TCE, confirming that the TCE metabolites were responsible for the toxic effects.

The cytotoxic effects of TCE metabolites have also been observed on different microorganisms and oxygenases. Multiple studies on strain G4 indicate that this strain suffers from metabolite toxicity. Newman and Wackett (1997), using purified enzyme preparations of G4, concluded that similar to F1, the TCE metabolites damage the active enzyme which results in enzyme inactivation. This result was different from previous studies using whole cells that indicated that the TCE degrading ability of this strain was not lost during TCE exposure (Folsom et al. 1990). However, Mars et al. (1996) found that G4 grown in a chemostat on toluene had higher maintenance energy costs when exposed to TCE. Cells, exposed to TCE in the absence of toluene produced a number of mutants unable to grow on toluene. The G4 mutants had lost the TOM plasmid

2004

2005

2006

2007

2008

2009

2010

2011

2012

2013

2014

2015

2016

2017

2018

2019

2020

2021

2022

2023

2024

2025

2026

2027

involved in toluene monooxygenase formation. Recently, Yeager and coworkers (Yeager et al. 2001) measured cell cultivability, TCE activity and general respiratory activity of G4 cells exposed to toluene. A decrease in respiration rates and cultivability was observed after TCE exposure confirming that the cometabolic transformation of TCE damages cells and reduces viability.

Microbial communities have also been used to measure the toxic effects of TCE. Mu and Scow (1994) measured the effects of toluene and TCE on bacterial densities in soil exposed to these compounds. An increase in TCE concentration from 1 to 20 µg/ml resulted in a decrease in TCE degradation rates and densities of TCE degraders in soil (Mu and Scow 1994). Alvarez-Cohen and McCarty (1991a), using a mixed methanotrophic culture, also observed a decrease in methane consumption rates after methanotrophic reactors were exposed to TCE.

Although the majority of the studies suggest that the toxicity of the TCE intermediates is very high, it will vary among different microbes. Zylstra and Gibson (1989), who cloned the toluene dioxygenase of strain F1 in *Escherichia coli*, noted that the wild type strain had higher initial TCE degradation rates than the genetic construct. However, the degradation rates of the wild-type strain decreased rapidly after TCE exposure but remained stable at degradation rates lower than that of the genetic construct, suggesting that different hosts will have different sensitivities to TCE toxicity. Recently, studies on a constitutive mutant of *Ralstonia eutropha* JMP 134 revealed that this strain does not suffer TCE mediated toxicity (Ayoubi and Harker 1998). No reduction in TCE degradation

rates was observed at TCE concentrations as high as 800 μM (~ 100 mg/l), *indicating* that some microorganisms can avoid TCE toxicity. The explanation *for the* important difference is not known.

Bioreactors

General

Since the discovery that TCE can be degraded by microbes, many **approaches** have been tried for using this process to remove TCE contamination **from** the environment. The design and implementation of bioreactors has been **one** of the approaches that has received major attention. A bioreactor is a **controlled** environment where microorganisms are supplied with all the **necessary** substrates and environmental conditions that allow them to grow and **perform** a specific function in an optimal manner. Bioreactors are frequently **used** for biotechnological applications such as the production of biomass, **antibiotics** and other metabolites due to the high degree of environmental **control**, high substrate conversion efficiency and high reaction rates among **other** favorable characteristics (Scragg 1991).

Bioreactors are also used for biodegradation, since they convert pollutants **into** biomass and innocuous products. Ideally, bioreactors should be used to **prevent** future contamination by processing waste streams before release into **the** environment. However, prevention of contamination was not always the **case**, especially in years before effective government environmental regulations. **Hence**, bioreactors are frequently used to treat previously contaminated

mate

groun

groun

s tre

aquife

estab

piece

l

groun

teach

be de

confi

with c

Sequ

subst

the T

teach

be m

move

was

aware

subst

material. For instance, bioreactors have been used to treat contaminated ground water using a pump and treat strategy. In this approach, contaminated ground water is pumped from the contaminated plume into a bioreactor where it is treated to remove the contaminant before being re-injected into a clean aquifer. To avoid the cost of extraction of the groundwater, a bioreactor can be established *in-situ* using recirculation wells to create a mixing zone where biodegradation can occur (Semprini 1997).

Bioreactors are usually classified based on feeding strategy and type of growth. The two main feeding strategies are: continuous feeding i.e. chemostat reactor; and intermittent feeding, i.e. batch feed reactor. Microbial growth can be classified as dispersed or attached growth (biofilm). A variety of bioreactor configurations have been created based on these reactor types in combination with different physical implementations.

Sequencing Batch Reactor

One of the challenges presented by TCE cometabolism is that the primary substrate and TCE compete for the active site of the oxygenase, thereby making the TCE degradation inefficient (Alvarez-Cohen and Speitel 2001). Thus, a reactor system that separates the addition of growth substrate and TCE should be more efficient. Previous attempts to solve this problem employed the movement of cells through different reaction chambers, where each compound was applied individually to avoid competitive inhibition (Phelps et al. 1990; Alvarez-Cohen and McCarty 1991b). The other strategy is to separate the substrates in time, such as accomplished with Sequencing Batch Reactor

SBR

altern

The s

with t

re m

remo

aporo

Waste

reac

Waste

Long

Thro

Segra

Para

Sece

Bece

Wate

Atou

Bece

Wate

The e

Comp

(SBR). The SBR system was introduced in 1977 by Irvine and coworkers as an alternative, cost-effective system for waste water treatment (Irvine et al. 1977). The system, different from typical activated sludge systems, consists of one tank with five different sequential periods of operation (Figure 1.2). This means that the multiple stages of waste treatment, i.e. mixing, aeration, decant and solids removal, were accomplished in a single tank but at different time periods. This approach differs from the continuous flow strategy usually employed in wastewater treatment plants that requires multiple tanks for each stage of treatment (Irvine and Ketchum jr. 1989).

A typical SBR cycle begins with a FILL period, the stage where new wastewater is added to the reactor. The reactor could be mixed or remain static during this stage depending on the waste requirements and the type of microorganisms to be selected. The REACT phase is when most of the waste degradation occurs. Similar to the FILL phase, aeration and mixing are parameters that can be adjusted depending on the operational needs. Solids separation is achieved in the SETTLE phase, the period where no mixing or aeration occurs to allow the biomass fraction to settle. DECANT is the phase when the clean effluent is removed from the system by pumping a predefined amount of the clarified surface liquid. Finally, the IDLE phase is when the reactor is ready to receive new wastewater before the cycle begins again. Wasting (i.e., removal) of suspended solids usually occurs during this period. The length of the periods will be determined by the operational needs and the composition of the influent wastewater.

A

Wre

Sh

and

at R

has be

grou

the

the

the

the

the

the

the

As described by Shih, SBRs could be easily adapted for TCE cometabolism by the addition of a RECHARGE step during the IDDL period (Shih 1995). The RECHARGE step is the period when growth substrate is added for cell growth and enzyme activation, to be followed by FILL with TCE and REACT, thus minimizing competitive inhibition. The SBR operation mode has been successfully used for TCE cometabolism using phenol or methane as growth substrates in bioreactors with attached growth (Speitel and Leonard 1992; Segar et al. 1995), and dispersed growth (Chang 1996). Although these studies have provided a wealth of information about the kinetics and efficiency of TCE cometabolism, knowledge of the microbial communities involved is still missing. Microorganisms are the key components of these systems, and determine the success or failure of the reactors. Information about the microbial communities could be helpful for designing better systems and operational conditions that could favor the beneficial microbial populations.

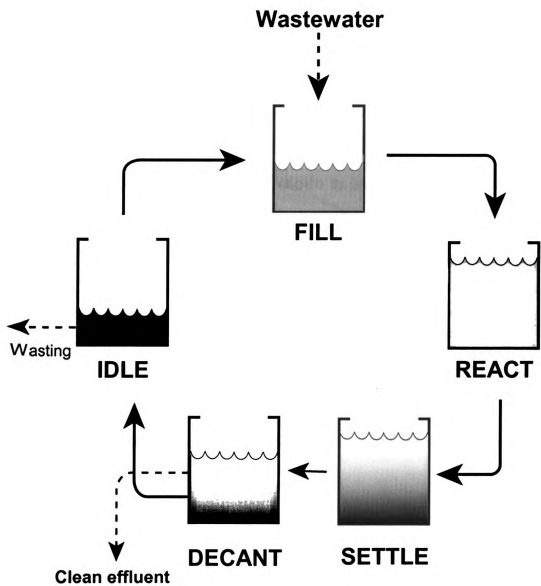


Figure 1.2. Normal operational cycles used in SBRs. Dashed lines indicate inflow or outflow of liquid, suspended solids or waste. Modified from Irvine et al. (1989).

The c

D

subje

Intro

inform

offere

has b

One

enro

enro

enro

enro

enro

enro

enro

enro

enro

enro

enro

enro

enro

enro

enro

Microbial communities

The culture dependent era

Different from disciplines such as macroecology, botany and zoology, the subjects of study in microbial ecology can not be observed or enumerated without using a microscope. If used, this methodology usually provides limited information about the structure of natural communities since physiologically different microbes often have similar morphologies. Thus, isolation of microbes has been the long-standing method of choice to study microbial communities. One of the pioneers in the isolation of important microorganisms from the environment was Martinus Beijerinck, who popularized the technique of enrichment culture. He isolated important microorganisms by tailoring culture conditions to favor only microbes with a particular metabolism. This methodology led to the discovery of important microbial processes such as nitrate reduction, methanogenesis and methanotrophy (Atlas and Bartha 1988). Physiological studies of pure cultures helped us understand the isolates' role in different environments.

Although isolation by enrichment or direct plating methods has provided a wealth of information about metabolic diversity in nature, it only provides a limited view of the composition of natural communities. Microorganisms live in unique niches determined by a variety of physical, chemical and biological factors. Niche, specialization reduces competition and promotes coexistence of diverse microbes, resulting in high microbial diversity. On the other hand, niche specialization is one of the factors that limit our ability to characterize

communities by cultivation. Many microbes live in unique niches that are hard, if not impossible to replicate in laboratory. Hence, the use of synthetic medium usually selects for a small group of microorganisms that is not representative of the entire microbial community. To gain a comprehensive view of a microbial community, methods that do not rely on cultivation are needed.

Culture independent community analysis

In the last decade, molecular techniques have been used to overcome the limitations of culture isolation for community structure analysis. Biological markers such as DNA, RNA and cellular components can be readily extracted from natural communities and used to distinguish many of the members. The ribosomal RNA genes (rRNA) have been the most frequently used molecular marker to study microbial communities since they provide an evolutionary framework that phenotypic methods do not provide (Olsen and Woese 1993). All forms of life can be divided in three major evolutionary lineages: Bacteria, Archaea and Eucarya, each with distinctive rRNA sequences. The strength of the rRNA gene for community analysis is because (Olsen et al. 1986; Muyzer and Ramsing 1995): (1) rRNA genes are necessary for protein synthesis, hence they are present in all known organisms; (2) they possess variable and conserved regions, providing different levels of resolution; (3) sequence information is sufficient to be used as a phylogenetic marker to estimate evolutionary relatedness among microorganisms; (4) rRNA is abundant in the cell, making it easily extractable, and (5) the rate of change of these genes is slow.

Furthermore, the availability of large databases that include both sequence and taxonomic information facilitate the use of this methodology for community analysis (Maidak et al. 2001).

Since the advent of using rRNA genes as a biomarker, a variety of strategies to analyze microbial communities have been developed (Figure 1.3). The choice of method will depend on the question asked, information available and level of resolution desired. For instance, if the purpose of the investigation is to assess changes in community composition across different samples or treatments, rDNA community fingerprinting and rDNA clone libraries will provide two different levels of resolution to answer the same question. Community fingerprinting methods rely on the generation of a representative mixture of rDNA amplicons from the community by PCR, which is further resolved based on the melting behavior of the entire product (DGGE and TGGE), or size differences of the products after restriction digestion (T-RFLP, ARDRA) (Figure 1.3). Fingerprinting methodologies provides a quick way to compare microbial communities under different treatments, although no first glance identification of the individuals is possible. On the other hand, cloning and sequencing of the rRNA genes either directly from the sample, or after PCR amplification provides detailed information about the phylogenetic composition of the community, but is very labor intensive.

When the focus of the research is to determine the abundance of different phylogenetic groups, hybridization and quantitative PCR are the methods of choice. Hybridization methods are based on the use of a labeled, single

stranded nucleic acid probe that binds to a complementary region of the target gene. Since the probes are labeled, the intensity of the signals can be used to quantify the abundance of the target. rRNA genes are relatively stable in cells, hence this method will provide an estimate of the abundance of microorganisms without the need for cultivation. However, it is difficult to relate rRNA abundance to cell densities since knowledge about the average rRNA content per cell is needed. Fluorescent in situ hybridization (FISH) uses the same principle of membrane hybridization but instead of using extracted nucleic acids, whole cells are hybridized with the probe. Since the probe is fluorescently labeled, cells will fluoresce under the proper excitation. The levels of resolution of the hybridization methods range from division to genus level depending on the availability of discriminatory regions in the rRNA sequence. Finally, quantitative PCR, similar to the hybridization methods, relies on discriminatory regions to amplify a specific target gene from a mixture. However, due to the exponential nature of PCR, the amount of product can not be directly related to initial copy number. The first approach to overcome this limitation was the addition of an internal standard to the reaction, a method known as competitive PCR. The addition of known amounts of a competitor, a plasmid with the target gene containing a 50-100 bp deletion, allows the quantification of the initial copy number relative to known amounts of the standard. This method, while reliable, is slow and laborious. A more recent approach has been the monitoring of the reaction progress over time with the aid of fluorescent reporters, a method known as real-time PCR. This method allows the identification of the linear

range of amplification, i.e. the period where the amount of PCR product will be proportional to the initial amount of template. Using the appropriate calibration curves, this method could quantify very low numbers of targets in environmental samples (Grüntzig et al. 2001).

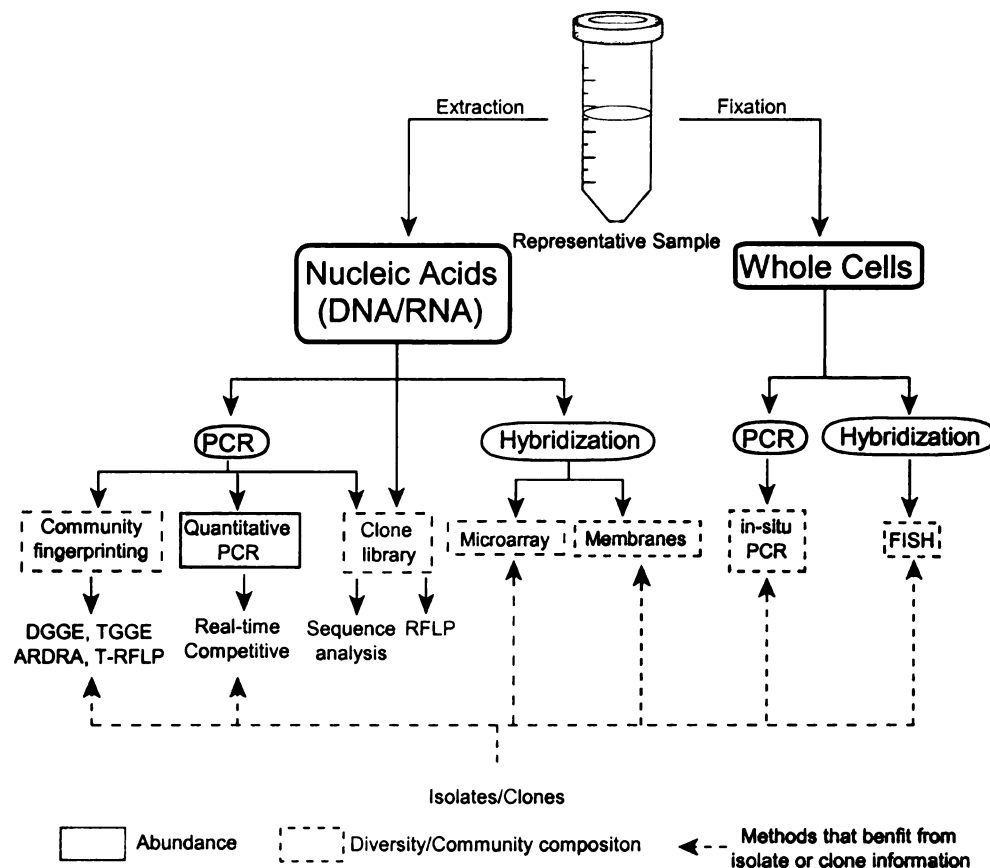


Figure 1.3. Overview of the molecular methods of community analysis based on rRNA genes. PCR, polymerase chain reaction; DGGE, denaturing gradient gel electrophoresis; TGGE, temperature gradient gel electrophoresis; ARDRA, amplified ribosomal DNA restriction analysis; T-RFLP, terminal restriction fragment length polymorphism; RFLP, restriction fragment length polymorphism; and FISH, fluorescent in-situ hybridization.

Although methods based on the rRNA have been extremely useful and powerful for microbial community analysis, isolation of community members is required for a more complete understanding of microbial communities (Wagner *et al.* 1993; Tiedje 1995; Dahllöf 2002). Physiological analyses of isolates from microbial communities provide clues about their possible role in the community. Furthermore, all molecular methods of community analysis could benefit from the study of isolates from the environment (Figure 1.3). The isolates could serve to test the specificity of primers or probes for quantification; and more importantly, to aid in interpretation since frequently a sequence does not reveal much information about the physiology of the organism. I adopted this strategy and I used a combination of cultivation and cultivation-independent molecular techniques to analyze community structure.

Thesis Overview

Objectives

The biodegradation of toxic compounds by microorganisms has been a major area of research for economic and health reasons. The use of microorganisms for waste processing is one of the most efficient and cost-effective approaches available. In this regard, microbial communities are essential since they provide a range of ecotypes and metabolic diversity resulting in a more robust process (Tiedje *et al.* 1995). These characteristics have been exploited in sewage treatment plants around the globe, where microbial communities are the key component of wastewater treatment. Microbial communities are also important in the degradation of toxic compounds;

because the range of ecotypes and the metabolic diversity allows synergistic interactions to occur. Microbial interactions such as metabolite transfer, allows microbial communities to completely mineralize compounds that pure cultures can only partially degrade (Slatter and Lovatt 1984). The biodegradation of pollutants by microbes can result in cleaner environments and reduced health risks to the human population.

Previous studies suggest that TCE cometabolism is a viable approach for the degradation of this pollutant. Although various reactors have been developed for this purpose, there is not much information about the microbial communities involved. Information about community structure, dynamics and abundance of different members may lead to improved design and operation of bioreactor systems. For example, integration of community structure data with reactor operation could be used to link microbial populations with reactor efficiency, including anticipating functional changes from community structure data. Furthermore, once key members of microbial communities are identified, environmental parameters, e.g. temperature, pH and substrate, could be optimized to meet the requirements of the relevant community members, thereby increasing process control and efficiency. The overall aim of this dissertation was to determine the long-term effects of TCE application on microbial communities in sequencing batch reactors. This study was organized around the following questions:

1. Does long-term TCE application decrease, increase or cause no change in TCE removal efficiency?

Experi

To

were us

percent

TC2 (5

scheme

and TC2

2. Does TCE application results in a shift in community structure?
3. How stable is the microbial community structure in the TCE and non-TCE treated reactors? If there is community succession, are there distinguishable patterns to the succession?
4. Does TCE application affect the physiology of the microbial community? If so, does it affect the spatial arrangement of bacteria?
5. What portion of the community can be obtained in culture? How many that grow on the primary substrate (phenol) can also cometabolize TCE?
6. How diverse are the isolates? Which have phenol hydroxylase genes and how diverse they are? Are any of the isolates dominant members of the microbial community?
7. Does long-term TCE application results in the extinction of TCE degrading phenotypes?

Experimental design

To address the questions stated above, two bench scale SBRs reactors were used (Figure 1.4). The control reactor was fed phenol (100 mg/l final concentration), while the experimental reactor was fed phenol (100 mg/l) and TCE (5 mg/l final concentration). The reactors were operated using the cycle scheme developed by Shih (1995) that involved the separate addition of phenol and TCE at different times during the reactor cycle (Figure 1.5). In Chapter 2

the function

assays from

communities

using the

phenol hy

of TCE ap

combinati

Chapter 4

of commu

physiolog

DNA seq

hydroxyla

target con

SBR com.

the function of the reactors was determined by phenol and TCE degradation assays from samples taken from the reactor during the REACT phase. The community structure and stability of the microbial communities were assessed using the T-RFLP community fingerprinting technique. Additionally, RFLP of phenol hydroxylase genes was used to validate the T-RFLP results. The effects of TCE application on EPS accumulation and aggregation were evaluated by a combination of solids fractionation and microscopy in Chapter 3. Finally, in Chapter 4 the diversity of the microbial communities was determined by isolation of community members. The isolates obtained were characterized physiologically for phenol and TCE degradation, and phylogenetically by 16S rDNA sequencing and tree construction. Additionally the diversity of phenol hydroxylase genes among the isolates was determined using PCR primers that target conserved regions of the gene. Selected isolates were enumerated in the SBR communities by SYBR green quantitative real-time PCR.

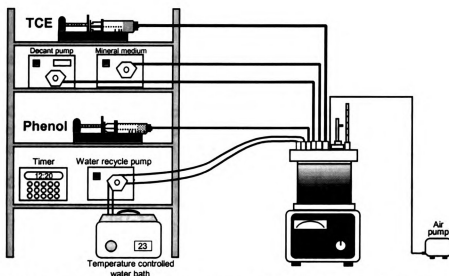


Figure 1.4. Components of the Sequencing Batch Reactors. Phenol and TCE were fed via syringes to each reactor individually. For the phenol-fed reactor, the TCE syringe was replaced with a mineral medium syringe. The mineral medium, concomitantly fed with TCE, was fed from a carboy using a peristaltic pump. In order to provide oxygen, an air pump was used. To control temperature, a peristaltic pump was used to recycle water between a water bath and a cooling plate inside the reactor.

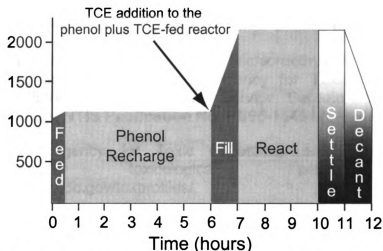


Figure 1.5. Sequencing Batch Reactor cycling scheme. This cycle occurs twice a day. The cycle begins with the feed step, where phenol is fed to a final concentration of 100 mg/l. The phenol recharge stage is the period when cell growth and phenol degrading enzymes are activated. In the fill phase, TCE is added to the phenol plus TCE-fed reactor (final concentration of 5 mg/l) while the phenol-fed reactor receives the same volume of mineral medium. The react phase is when the second compound is consumed. In the settle phase, no aeration or mixing occurs to allow suspended solids to settle. Finally, the supernatant is removed on the decant phase before the cycle starts again.

References

- Alexander, M.** (1994). Biodegradation and Bioremediation. San Diego, Academic Press.
- Alvarez-Cohen, L. and P. L. McCarty.** (1991a). Effects of toxicity, aeration, and reductant supply on trichloroethylene transformation by a mixed methanotrophic culture. *Appl. Environ. Microbiol.* **57**: 228-235.
- Alvarez-Cohen, L. and P. L. McCarty.** (1991b). Two-stage dispersed-growth treatment of halogenated aliphatic compounds by cometabolism. *Environ. Sci. Technol.* **25**: 1387-1393.
- Alvarez-Cohen, L. and G. E. Speitel.** (2001). Kinetics of aerobic cometabolism of chlorinated solvents. *Biodegradation* **12**: 105-126.
- Arciero, D., T. Vannelli, M. Logan and A. B. Hooper.** (1989). Degradation of trichloroethylene by the ammonia-oxidizing bacterium *Nitrosomonas-europaea*. *Biochem. Biophys. Res. Commun.* **159**: 640-643.
- Arp, D. J., C. M. Yeager and M. R. Hyman.** (2001). Molecular and cellular fundamentals of aerobic cometabolism of trichloroethylene. *Biodegradation* **12**: 81-103.
- Atlas, R. M. and R. Bartha.** (1988). Microbial Ecology: fundamentals and applications. Menlo Park, Benjamin Cummings science publishing.
- ATSDR.** (1994). National exposure registry. Trichloroethylene (TCE) subregistry baseline technical report (revised). Agency for Toxic Substances and Disease Registry, U.S. Public Health Service, Department of Health and Human Services. **NTIS Publication No. PB95-154589**: Atlanta, Georgia.
- ATSDR.** (2002). Agency for Toxic Substance and Disease Registry. Trichloroethene toxicological profile. [Online] <http://www.atsdr.cdc.gov/toxprofiles/>.
- Ayoubi, P. J. and A. R. Harker.** (1998). Whole-cell kinetics of trichloroethylene degradation by phenol hydroxylase in a *Ralstonia eutropha* JMP134 derivative. *Appl. Environ. Microbiol.* **64**: 4353-4356.
- Bruckner, J. V., B. D. Davis and J. N. Blancato.** (1989). Metabolism, toxicity, and carcinogenicity of trichloroethylene. *Crit. Rev. Toxicol.* **20**: 31-50.
- Chang, W.** (1996). Kinetics characterization of cometabolizing communities and adaptation to nongrowth substrate. Ph. D. dissertation. Michigan State University, East Lansing, MI.

- Dabrock, B., J. Riedel, J. Bertram and G. Gottschalk.** (1992). Isopropylbenzene (cumene) - a new substrate for the isolation of trichloroethene-degrading bacteria. *Arch. Microbiol.* **158**: 9-13.
- Dahllöf, I.** (2002). Molecular community analysis of microbial diversity. *Curr. Opin. Biotechnol.* **13**: 1-5.
- DiSpirito, A. A., J. Gullledge, A. K. Shiemke, J. C. Murrel, M. E. Lidstrom and C. L. Krema.** (1992). Trichloroethylene oxidation by the membrane associated methane monooxygenase in type I, type II and type X methanotrophs. *Biodegradation* **2**: 151-164.
- Ensign, S. A., M. R. Hyman and D. J. Arp.** (1992). Cometabolic degradation of chlorinated alkenes by alkene monooxygenase in a propylene-grown *Xanthobacter* strain. *Appl. Environ. Microbiol.* **58**: 3038-3046.
- Fogel, M. M., A. R. Taddeo and S. Fogel.** (1986). Biodegradation of chlorinated ethenes by a methane-utilizing mixed culture. *Appl. Environ. Microbiol.* **51**: 720-724.
- Folsom, B. R., P. J. Chapman and P. H. Pritchard.** (1990). Phenol and trichloroethylene degradation by *Pseudomonas cepacia* G4: kinetics and interactions between substrates. *Appl. Environ. Microbiol.* **56**: 1279-1285.
- Fox, B. G., J. G. Borneman, L. P. Wackett and J. D. Lipscomb.** (1990). Haloalkene oxidation by the soluble methane monooxygenase from *Methylosinus trichosporium* OB3b: mechanistic and environmental implications. *Biochemistry* **29**: 6419-6427.
- Fries, M.** (1995). Diversity of mono aromatic hydrocarbon degrading bacteria and their TCE co-oxidation potential. Ph. D. Dissertation, East Lansing, MI.
- Futamata, H., S. Harayama and K. Watanabe.** (2001a). Diversity in kinetics of trichloroethylene-degrading activities exhibited by phenol-degrading bacteria. *Appl. Microbiol. Biotechnol.* **55**: 248-253.
- Futamata, H., S. Harayama and K. Watanabe.** (2001b). Group-specific monitoring of phenol hydroxylase genes for a functional assessment of phenol-stimulated trichloroethylene bioremediation. *Appl. Environ. Microbiol.* **67**: 4671-4677.
- Garrity, G. M., M. Winters and D. B. Searles.** (2001). Taxonomic outline of the prokaryotic genera bergey's manual of systematic bacteriology. [Online] Bergey's manual of systematic bacteriology. Second edition. <http://www.cme.msu.edu/bergeys/april2001-genus.pdf>.
- Green, T.** (2001). Trichloroethylene and human cancer. *Human and Ecological Risk Assessment* **7**: 677-685.

- Gribble, G.** (1994). The natural production of chlorinated compounds. *Environ. Sci. Technol.* **28**: 311A-3119A.
- Grüntzig, V., S. C. Nold, J. Z. Zhou and J. M. Tiedje.** (2001). *Pseudomonas stutzeri* nitrite reductase gene abundance in environmental samples measured by real-time PCR. *Appl. Environ. Microbiol.* **67**: 760-768.
- Hamamura, N., C. Page, T. Long, L. Semprini and D. J. Arp.** (1997). Chloroform cometabolism by butane-grown CF8, *Pseudomonas butanovora*, and *Mycobacterium vaccae* JOB5 and methane-grown *Methylosinus trichosporium* OB3b. *Appl. Environ. Microbiol.* **63**: 3607-3613.
- Harker, A. R. and Y. Kim.** (1990). Trichloroethylene degradation by two independent aromatic-degrading pathways in *Alcaligenes eutrophus* JMP134. *Appl. Environ. Microbiol.* **56**: 1179-1181.
- Hewer, C. L.** (1975). Trichloroethylene. *Anesthesia* **30**: 483-487.
- HSIA.** (1996). Halogenated Solvents Industry Alliance Inc. Trichloroethylene white paper. [Online] <http://www.hsia.org/trichloro.htm>.
- HSIA.** (2001). Halogenated Solvents Industry Alliance Inc. Trichloroethylene white paper. [Online] <http://www.hsia.org/trichloro.htm>.
- Irvine, R. L., T. P. Fox and R. O. Richter.** (1977). Investigation of fill and batch periods of sequencing batch biological reactors. *Water Res.* **11**: 713-717.
- Irvine, R. L. and L. H. Ketchum jr.** (1989). Sequencing batch reactors for biological wastewater treatment. *CRC crit. rev. env. cont.* **18**: 255-294.
- Johnson, G. R. and R. H. Olsen.** (1995). Nucleotide-sequence analysis of genes encoding a toluene benzene-2-monooxygenase from *Pseudomonas* sp. strain JS150. *Appl. Environ. Microbiol.* **61**: 3336-3346.
- Li, S. and L. P. Wackett.** (1992). Trichloroethylene oxidation by toluene dioxygenase. *Biochem. Biophys. Res. Commun.* **185**: 443-451.
- Little, C. D., A. V. Palumbo, S. E. Herbes, M. E. Lidstrom, R. L. Tyndall and P. J. Gilmer.** (1988). Trichloroethylene biodegradation by a methane-oxidizing bacterium. *Appl. Environ. Microbiol.* **54**: 951-956.
- Lontoh, S., A. A. DiSpirito and J. D. Semrau.** (1999). Dichloromethane and trichloroethylene inhibition of methane oxidation by the membrane-associated methane monooxygenase of *Methylosinus trichosporium* OB3b. *Arch. Microbiol.* **171**: 301-308.

- Maidak, B. L., J. R. Cole, T. G. Lilburn, C. T. J. Parker , P. R. Saxman, R. J. Farris, G. M. Garrity, G. J. Olsen, T. M. Schmidt and J. M. Tiedje.** (2001). The RDP-II (Ribosomal Database Project). *Nucleic Acids Res.* **29**: 173-174.
- Mars, A. E., J. Houwing, J. Dolfig and D. B. Janssen.** (1996). Degradation of toluene and trichloroethylene by *Burkholderia cepacia* G4 in growth-limited fed-batch culture. *Appl. Environ. Microb.* **62**: 886-891.
- Mohn, W. W. and J. M. Tiedje.** (1992). Microbial reductive dehalogenation. *Microbiol. Rev.* **56**: 482-507.
- Mu, D. Y. and K. M. Scow.** (1994). Effect of trichloroethylene (TCE) and toluene concentrations on TCE and toluene biodegradation and the population-density of TCE and toluene degraders in soil. *Appl. Environ. Microbiol.* **60**: 2661-2665.
- Muyzer, G. and N. B. Ramsing.** (1995). Molecular methods to study the organization of microbial communities. *Water. Sci. Technol.* **32**: 1-9.
- Nelson, M. J. K., S. O. Montgomery, W. R. Mahaffey and P. H. Pritchard.** (1987). Biodegradation of trichloroethylene and involvement of an aromatic biodegradative pathway. *Appl. Environ. Microbiol.* **53**: 949-954.
- Nelson, M. J. K., S. O. Montgomery, E. J. O'Neill and P. H. Pritchard.** (1986). Aerobic metabolism of trichloroethylene by a bacterial isolate. *Appl. Environ. Microbiol.* **52**: 383-384.
- Nelson, M. J. K., S. O. Montgomery and P. H. Pritchard.** (1988). Trichloroethylene metabolism by microorganisms that degrade aromatic compounds. *Appl. Environ. Microbiol.* **54**: 604-606.
- Newman, L. M. and L. P. Wackett.** (1991). Fate of 2,2,2-trichloroacetaldehyde (chloral hydrate) produced during trichloroethylene oxidation by methanotrophs. *Appl. Environ. Microbiol.* **57**: 2399-2402.
- Newman, L. M. and L. P. Wackett.** (1995). Purification and characterization of toluene 2-monooxygenase from *Burkholderia-cepacia* G4. *Biochemistry* **34**: 14066-14076.
- Newman, L. M. and L. P. Wackett.** (1997). Trichloroethylene oxidation by purified toluene 2- monooxygenase: products, kinetics, and turnover-dependent inactivation. *J. Bacteriol.* **179**: 90-96.
- Oldenhuis, R., R. L. J. M. Vink, D. Janssen and B. Witholt.** (1989). Degradation of chlorinated aliphatic hydrocarbons by *Methylosinus trichosporium* OB3b expressing soluble methane monooxygenase. *Appl. Environ. Microbiol.* **55**: 2819-2826.

- Olsen, G. J., D. J. Lane, S. J. Giovannoni, N. R. Pace and D. A. Stahl.** (1986). Microbial ecology and evolution: a ribosomal RNA approach. *Ann. Rev. Microbiol.*
- Olsen, G. J. and C. R. Woese.** (1993). Ribosomal RNA: a key to the phylogeny. *FASEB* 7: 113-123.
- Olsen, R. H., J. J. Kukor and B. Kaphammer.** (1994). A novel toluene-3-monooxygenase pathway cloned from *Pseudomonas Picketti* PK01. *J. Bacteriol.* 176: 3749-3756.
- Pflugmacher, U., B. Averhoff and G. Gottschalk.** (1996). Cloning, sequencing, and expression of isopropylbenzene degradation genes from *Pseudomonas* sp. strain JR1: identification of isopropylbenzene dioxygenase that mediates trichloroethene oxidation. *Appl. Environ. Microbiol.* 62: 3967-3977.
- Phelps, T. J., J. J. Niedzielski, R. M. Schram, S. E. Herbes and D. C. White.** (1990). Biodegradation of trichloroethylene in continuous-recycle expanded-bed bioreactors. *Appl. Environ. Microbiol.* 56: 1702-1709.
- Rasche, M. E., M. R. Hyman and D. J. Arp.** (1991). Factors limiting aliphatic chlorocarbon degradation by *Nitrosomonas europaea*: cometabolic inactivation of ammonia monooxygenase and substrate specificity. *Appl. Environ. Microbiol.* 57: 2986-2994.
- Reij, M. W., J. Kieboom, J. A. M. DeBont and S. Hartmans.** (1995). Continuous degradation of trichloroethylene by *Xanthobacter* sp., strain PR2 during growth on propane. *Appl. Environ. Microbiol.* 61: 2936-2942.
- Saeki, S., S. Mukaia, K. Iwasaki and O. Yagi.** (1999). Production of trichloroacetic acid, trichloroethanol and dichloroacetic acid from trichloroethylene degradation by *Methylocystis* sp. strain M. *Biocatal. Biotransform.* 17: 347-357.
- Scragg, A. H., Ed.** (1991). Bioreactors in biotechnology: a practical approach. *Biochemistry and Biotechnology*. West Sussex, Ellis Horwood limited.
- Segar, R. L., S. L. Dewys and G. E. Speltel.** (1995). Sustained trichloroethylene cometabolism by phenol-degrading bacteria in sequencing biofilm reactors. *Water Environ. Res.* 67: 764-774.
- Semprini, L.** (1997). Strategies for the aerobic co-metabolism of chlorinated solvents. *Curr. Opin. Biotechnol.* 8: 296-308.
- Semprini, L., P. V. Roberts, G. D. Hopkins and P. L. McCarty.** (1990). A field evaluation of in situ biodegradation of chlorinated ethenes. Part 2. Results of

biostimulation and biotransformation experiments. *GROUND WATER* **28**: 715-727.

Shields, M. S., M. J. Reagin, R. R. Gerger, R. Campbell and C. Somerville. (1995). *Tom*, a new aromatic degradative plasmid from *Burkholderia (Pseudomonas) cepacia* G4. *Appl. Environ. Microbiol.* **61**: 1352-1356.

Shih, C. C. (1995). Experimental and numerical evaluations of cometabolism in sequencing batch reactors. Ph.D. dissertation. Michigan State University, East Lansing, MI.

Slatter, J. H. and D. Lovatt. (1984). Biodegradation and the significance of microbial communities. *In* Microbial degradation of organic compounds. D. T. Gibson. New York, Marcel Dekker, Inc 439-485.

Speitel, G. E. and J. M. Leonard. (1992). A sequencing biofilm reactor for the treatment of chlorinated solvents using methanotrophs. *Water Environ. Res.* **64**: 712-719.

Tiedje, J. M. (1995). Approaches to the comprehensive evaluation of prokaryote diversity of a habitat. *In* Microbial diversity and ecosystem function. D. Allsopp, R. R. Colwell and D. L. Hawksworth. Wallingford, CAB international.

Tiedje, J. M., R. M. Sanford and A. A. Massol-Deya. (1995). Advantages and disadvantages of consortia in bioremediation. *In* Bioremediation: The Tokyo '94 Workshop. Paris, OECD 357-367.

Tsien, H. C., G. A. Brusseau, R. S. Hanson and L. P. Wackett. (1989). Biodegradation of trichloroethylene by *Methylosinus trichosporium* OB3b. *Appl. Environ. Microbiol.* **55**: 3155-3161.

U.S.-EPA. (2001). Trichloroethylene health risk assessment: synthesis and characterization. Office of Research and Development **August**.

U.S.-EPA. (2002). Trichloroethylene. [Online] <http://www.epa.gov/ttn/atw/hlthef/tri-ethy.html>.

Uchiyama, H., T. Nakajima, O. Yagi and T. Nakahara. (1992). Role of heterotrophic bacteria in complete mineralization of trichloroethylene by *Methylocystis* sp. strain M. *Appl. Environ. Microbiol.* **58**: 3067-3071.

Vogel, T. M. and P. L. McCarty. (1985). Biotransformation and tetrachloroethylene to trichloroethylene, dichloroethylene, vinyl chloride and carbon dioxide under methanogenic conditions. *Appl. Environ. Microbiol.* **49**: 1080-1083.

W.H.O. (1993). World Health Organization. Guidelines for drinking-water quality. Vol 1. Recommendations. Geneva.

- Wackett, L. P.** (1995). Bacterial cometabolism of halogenated organic compounds. *In* Microbial transformations and degradation of toxic organic chemicals. L. Y. Young and C. E. Cerniglia. New York, Wiley-Liss 217-241.
- Wackett, L. P., G. A. Brusseau, S. R. Householder and R. S. Hanson.** (1989). Survey of microbial oxygenases: trichloroethylene degradation by propane-oxidizing bacteria. *Appl. Environ. Microbiol.* **55**: 2960-2964.
- Wackett, L. P. and D. T. Gibson.** (1988). Degradation of trichloroethylene by toluene dioxygenase in whole-cell studies with *Pseudomonas putida* F1. *Appl. Environ. Microbiol.* **54**: 1703-1708.
- Wackett, L. P. and S. R. Householder.** (1989). Toxicity of trichloroethylene to *Pseudomonas putida* F1 is mediated by toluene dioxygenase. *Appl. Environ. Microbiol.* **55**: 2723-2725.
- Wagner, M., R. I. Amman, H. Lemmer and K. H. Schleifer.** (1993). Probing activated sludge with oligonucleotides specific for *Proteobacteria*: inadequacy of culture-dependent methods for describing microbial community structure. *Appl. Environ. Microbiol.* **59**: 1520-1525.
- Watanabe, K., M. Teramoto, H. Futamata and S. Harayama.** (1998). Molecular detection, isolation, and physiological characterization of functionally dominant phenol-degrading bacteria in activated sludge. *Appl. Environ. Microbiol.* **64**: 4396-4402.
- Wilson, J. T. and B. H. Wilson.** (1985). Biotransformation of trichloroethylene in soil. *Appl. Environ. Microbiol.* **49**: 242-243.
- Yeager, C. M., P. J. Bottomley and D. J. Arp.** (2001). Cytotoxicity associated with trichloroethylene oxidation in *Burkholderia cepacia* G4. *Appl. Environ. Microbiol.* **67**: 2107-2115.
- Yen, K. M., M. R. Karl, L. M. Blatt, M. J. Simon, R. B. Winter, P. R. Fausset, H. S. Lu, A. A. Harcourt and K. K. Chen.** (1991). Cloning and characterization of a *Pseudomonas Mendocina* KR1 gene cluster encoding toluene-4-monooxygenase. *J. Bacteriol.* **173**: 5315-5327.
- Zylstra, G. J., L. P. Wackett and D. T. Gibson.** (1989). Trichloroethylene degradation by *Escherichia coli* containing the cloned *Pseudomonas putida* F1 toluene dioxygenase genes. *Appl. Environ. Microbiol.* **55**: 3162-3166.

CHAPTER 2

SUCCESSIONAL AND FUNCTIONAL RESPONSES IN PHENOL AND PHENOL PLUS TCE FED REACTORS

Introduction

Trichloroethylene (TCE) is a potentially carcinogenic, volatile, chlorinated solvent that is one of the most common groundwater pollutants in the United States (Bruckner et al. 1989; ATSDR 1994). TCE can be degraded anaerobically by reductive dechlorination, but the degradation is often incomplete yielding cis-dichloroethene and vinyl chloride, a carcinogen (Infante and Tsongas 1987; Mohn and Tiedje 1992). However, TCE can be degraded aerobically by cometabolism, a fortuitous oxidation that does not result in energy or carbon for cell growth (Alexander 1994). Cometabolism of TCE produces an epoxide that is spontaneously converted to innocuous products such as formate and glyoxylate (Vogel et al. 1987; Wackett 1995), but some epoxide reacts with the catalytic enzyme destroying these cells (Wackett and Householder 1989). Hence, long-term TCE exposure can select against TCE degraders (Mars et al. 1996), or possibly for a more active TCE degrading community if active organisms grow on formate and glyoxylate.

Cometabolism, has been successfully used for the degradation of TCE in bioreactors (Segar et al. 1995; Chang 1996) and in ground water communities (Hopkins and McCarty 1995; McCarty et al. 1998) provided the appropriate growth substrate. However, the majority of the studies have focused on the kinetics and efficiency of TCE degradation without considering the microbial

communities involved. Only one study has investigated the dynamics and **diversity** of microbial communities undergoing TCE cometabolism in a test **aquifer** (Fries et al. 1997a; Fries et al. 1997b). Understanding the structure and **stability** of microbial communities is of extreme importance for the success of **bioremediation** strategies, since microbial communities are responsible for the **success** or failure of the process. Insights into processes such as community **succession** are necessary to understand and predict future changes in **community** structure in natural and managed ecosystems. Often, bioreactor **systems** are operated for extended periods of time assuming that the microbial **community** structure will remain unchanged. However, studies on a functionally **stable** methanogenic reactor revealed that microbial communities can be very **dynamic**, suggesting that stable function is not always correlated with stable **community** structure (Fernández et al. 1999). On the other hand, perturbation **studies** using 1,1-dichlorethene, a very toxic compound (Dolan and McCarty 1995; Anderson and McCarthy 1997), suggest that microbial communities can **be** quite resilient since the community structure recovered to its original state (Fries et al. 1997b). Hence, is clear that the dynamics and stability of microbial **communities** will depend on many environmental factors.

In the study reported here, we compared the structure and function of two **reactor** communities; one fed phenol only and the other phenol plus TCE over **two** years of continuous operation. Our objectives were to determine the effect **of** long-term TCE application on community structure, succession, and reactor **Performance**, the latter measured as rates of phenol and TCE degradation. We

used sequencing batch reactors (SBR) so that the phenol consumption phase **was** temporally separated from the TCE degradation phase to avoid competitive **inhibition** between the two substrates. Periodic changes in community structure **and** function were observed in the SBR that received phenol alone. These **changes** were not observed in the phenol plus TCE-fed community, where long-**term** exposure to the TCE selected for a community that was more stable in **structure** and function. Overall, long-term exposure to TCE did not result in a **community** with higher TCE transformation rates.

Materials and Methods

Reactor design and operation

Two aerobic bench scale SBRs (Chang 1996) were inoculated from a **phenol** fed reactor that showed high and stable phenol and TCE kinetics (Shih et **al.** 1996). Each reactor consisted of a 2.2 l glass vessel and mixer system (**W**heaton minijar fermentor M-100, Millville, NJ.). Reactors were mixed at 180 **rpm**, except during the settling phase, and the temperature was maintained at **22°± 1°C** by water re-circulation from a temperature controlled water bath **through** a cooling plate inside the vessel. Reactors were operated aerobically by **pumping** air at a flow rate of 220-280 ml/min. Both vessels were covered from **light** to avoid photosynthetic growth. Phenol and TCE solutions were fed using **60** ml syringes and syringe pumps (Harvard Apparatus Inc., Holliston, Mass.). **Supernatant** was decanted and mineral medium was added by peristaltic pumps (**W**atson-Marlow, Wilmington, Md.). Peristaltic, air and syringe pumps were

controlled by a programmable timer (Fisher Scientific, Pittsburgh, Penn.). Both reactors were fed phenol for 30 days before adding TCE to one of them. Reactor operation was as follows: initially, both reactors received 25 ml of a mixture of phenol (7,200 mg/l) and mineral medium (2.13 g of Na_2HPO_4 , 2.04 g of KH_2PO_4 , 1 g of $(\text{NH}_4)_2\text{SO}_4$, 0.067 g of $\text{CaCl}_2 \cdot 2\text{H}_2\text{O}$, 0.248 g of $\text{MgCl}_2 \cdot 6\text{H}_2\text{O}$, 0.5 mg of $\text{FeSO}_4 \cdot 7\text{H}_2\text{O}$, 0.4 mg of $\text{ZnSO}_4 \cdot 7\text{H}_2\text{O}$, 0.002 mg of $\text{MnCl}_2 \cdot 4\text{H}_2\text{O}$, 0.05 mg of $\text{CoCl}_2 \cdot 6\text{H}_2\text{O}$, 0.01 mg of $\text{NiCl}_2 \cdot 6\text{H}_2\text{O}$, 0.015 mg of H_3BO_3 , and 0.25 mg of EDTA per liter) over a 0.5 h interval for a final concentration of 100 mg phenol/l. This concentration was selected because it was sufficient for cell growth and the fortuitous oxidation TCE in the next stage. Higher concentrations of phenol could result in growth inhibition. Six hours after phenol addition the TCE-fed reactor received 25 ml of TCE mixed with mineral medium (0.2 mg/ml) and additional mineral medium (1 l) during 1 h for a final concentration of 5 mg TCE/l, while the phenol-fed reactor received mineral medium only. The TCE concentration of 5 mg/l was chosen because pure culture studies indicate that values below this concentration were sufficient to observe TCE mediated toxicity. Three hours later, suspended solids were allowed to settle for 30 min, and the supernatant (~1.1 l) was removed before another 12 h cycle began. Suspended solids (200 ml) were removed every other day 1.5 h after phenol injection to maintain a mean cell residence time of 11 days.

TCE and phenol analysis

Reactor performance was evaluated by calculation of kinetics for phenol and TCE removal in batch assays. Samples from each reactor (5 ml) were taken 1.5 h after the end of the phenol addition step of the cycle and were transferred to three 20-ml glass vials and crimp sealed with Teflon-coated butyl rubber stoppers. For TCE removal measurements, different amounts of TCE in water (~ 1,000 mg/l) were injected (10-50 µl) into the vials which were then incubated at 120 rpm in a rotary shaker, at room temperature. Periodically, 0.1 ml of headspace was removed using a 0.5 ml Pressure-Lok Series A-2 gas syringe (Hamilton company, Reno, Nev.) and injected into a Hewlett-Packard 5890A gas chromatograph (GC) equipped with a capillary column (DB624, 30 m x 0.53 mm I.D.), a flame ionization detector (FID) and a electron capture detector (ECD). The GC was operated isothermally at 90°C with helium as carrier gas (12 ml/min) and the injection port was set at 250°C. The temperature of the FID and ECD were 250°C and 350°C respectively. Second order rate constants for TCE removal, which normalize for biomass, were calculated from the TCE concentrations as described previously (Chang 1996). For phenol removal rates, different amounts of phenol were injected into each of the vials which were then incubated as described above. Periodically, samples were removed with a syringe and filtered through 0.2 µm nylon syringe filters (Wheaton). Filtrate was collected (2 ml) to measure phenol concentrations by an HPLC equipped with a C18 column (Waters, Milford, Mass.) and a UV detector set to 235 nm. The solvent used was an acetonitrile water mixture

(60:40) at a 1 ml/min flow rate. Zero order kinetic transformation coefficients for phenol removal were calculated from the phenol concentrations as described previously (Chang 1996).

Reactor sampling and DNA extraction

Samples of suspended solids (~ 12 ml) were taken for community analysis at the same time the kinetic assays were performed. Samples were centrifuged for 15 min at 6,000 x g (4°C), the supernatant fraction was decanted, and cell pellets were stored at -80°C. No major wall growth was observed in the reactor.

For nucleic acid extraction, cells were resuspended in TE buffer (10 mM Tris [pH 8.0] and 1 mM EDTA [pH 8.0]) and ATL lysis buffer (Qiagen, Chatsworth, Calif.) before being mixed by a vortex mixer. The cell suspension was subjected to two freeze-thaw cycles before being digested with lysozyme (50 µl of a 100 mg/ml solution, Gibco BRL, Gaithersburg, Md.) and achromopeptidase (10 µl of a 25 mg/ml solution, Sigma, St. Louis, Mo.). The cell lysate was digested with RNase (10 mg/ml Boehringer Mannheim, Indianapolis, Ind.) followed by proteinase K (45 µl of a 25 mg/ml, Gibco BRL) for 1 h at 60°C. Nucleic acids were purified by three phenol-chloroform-isoamyl alcohol extractions and were precipitated overnight at -20°C by addition of NaOAc (3M pH 5.3) and 0.8 volumes of 100% isopropanol. The DNA pellet was resuspended in 100 µl of sterile deionized water. Purity and quantity of the DNA were determined by UV spectrophotometry at 260 and 280 nm. DNA was stored at -20°C.

PCR primers and conditions

Amplification of bacterial 16S rDNA genes from community DNA was performed with primers 8F (5'-AGAGTTTGATCMTGGCTCAG-3' where M was A or C) (Giovannoni 1991), fluorescently labeled at the 5' end with the phosphoramidite dye 5-hexachlorofluorescein (Operon Inc., Alameda, Calif.), and 1392R (5'-ACGGGCGGTGTGTACA-3') (Amann et al. 1995). PCR reactions were carried out as described previously (Braker et al. 2001) with the following modifications: 20 ng of template DNA was added to each PCR reaction, and 25 cycles of amplification were performed. Amplification of the phenol hydroxylase genes from the community was performed with primers FD2 (5'-GGCATCAARATYNNNGACTGG-3' where N was a mixture of A,C,G,T; R was A or G; and Y was C or T) and Phe212 (5'-GTTGGTCAGCACGTACTCGAAGGAGAA-3') (Watanabe et al. 1998). These primers produce a 490 bp PCR product from the large subunit (α) of the multicomponent phenol hydroxylase gene family. Primer FD2 was designed by comparative analysis of amino acid sequences of this protein from *Pseudomonas* sp. str. CF600, *Pseudomonas putida* str. H, *Pseudomonas putida*, P35X, *Burkholderia cepacia* G4 and *Burkholderia* sp. str. JS150. Primer specificity was tested using a collection of isolates known to degrade phenol, and *Burkholderia cepacia* G4. The PCR products were sequenced, and were found to be highly similar to phenol hydroxylase genes from known phenol degraders. PCR amplification was performed using the same thermal cycler and reaction mixture described previously (Braker et al. 2001), with the modification

that 25 pmol of each primer was used and five replicate reactions were prepared for each sample. The following touch down thermal profile was used for the amplification: an initial denaturation step of 5 min at 95°C, followed by 10 cycles at 94°C 30s, 30s of annealing (where the temperature started at 58°C and decreased 1°C every cycle) and 45 s at 72°C. In addition, 25 more cycles were carried out using an annealing temperature of 55°C. The quality and quantity of the PCR products was determined by electrophoresis of an aliquot (10 µl) of each PCR reaction on a 2.0 % (wt/vol) agarose gel (Gibco BRL) in 1X TAE (Tris acetate-EDTA).

PCR purification, restriction digest and gel separation.

PCR purification, restriction digest and gel separation for T-RFLP of 16S rRNA genes were performed as described previously (Braker et al. 2001) with *Hae*III and *Cfo*I restriction enzymes (Gibco BRL).

For the phenol hydroxylase genes the PCR products from the five replicate reactions were combined and concentrated by roto-evaporation. The concentrated PCR product was separated in a 2.5% (wt/vol) agarose gel (Gibco BRL) in 1X TAE, and the band of correct size was excised from the gel and eluted in 60 µl of sterile filtered distilled water using a QIAquick gel extraction kit (Qiagen). The purified PCR products were concentrated by roto-evaporation and digested with 15 U of *Msp*I and *Rsa*I restriction enzymes combined (Gibco BRL). The resulting fragments were separated in a 4% (wt/vol) Metaphor agarose gel (FMC, Indianapolis, Ind.) in 1X TBE (Tris borate-EDTA) buffer at

140 volts for 3.5 h at 4°C, and then stained with ethidium bromide (0.5 µg/ml). Gel images were analyzed using GelCompar 4.5 (Applied Maths, Kortrijk, Belgium).

Analysis of T-RFLPs.

Electropherograms from each sample from both reactors were manually aligned against each other using Genotyper 2.5 (Applied Biosystems Instruments, Foster City, Calif.). To avoid primer artifacts, fragments smaller than 35 base pairs were excluded from the analysis. The alignment resulted in a matrix in which different peaks were considered to be indicative of different ribotypes present in the community, and the peak heights were used as a measure of ribotype abundance. After alignment, samples where the sum of the peak heights was less than 10,000 units were re-digested and separated, since data below this threshold is unreliable for statistical analysis (Blackwood 2001). Histograms with the abundance of each peak normalized by the total signal in each sample were used to compare the changes in community structure in each reactor. Similarity between samples from the same reactor and between the two reactors was determined by Correspondence Analysis (CA) (ter Braak 1995; Legendre and Legendre 1998) with the software package ADE-4 (<http://biomserv.univ-lyon1.fr/ADE-4.html>) (Thioulouse et al. 1997). CA was chosen for the analysis of the T-RFLP profiles because this ordination method recovers the underlying structure of the data by analysis of the proportional changes in species abundances, providing a global view of the community

structure without being severely affected by noise. For CA, peak height was used as described above and the data analysis was performed in a step-wise process. CA was initially performed on all the samples (from both reactors) to compare the two reactors (between and within treatment variability). Subsequently, each reactor data set was analyzed individually to evaluate within treatment variability.

To evaluate the reproducibility of the T-RFLP methodology nine replicate samples from each reactor (taken after 811 days of operation) and 32 lanes of internal standard were analyzed with two similarity indices. Similarity indices were used because they generate direct sample to sample comparisons, providing more precise estimates of the variability. The Sørensen similarity index takes into account presence or absence of peaks while the Steinhaus similarity index takes into account the abundance of each peak (Legendre and Legendre 1998). Similarity matrixes were generated for each set of nine replicates and 32 lanes of the internal standard (Gene scan 2500, Applied Biosystems, Alameda, Calif.) with the SIMIL module of the R-package 4.0 (<http://www.fas.umontreal.ca/BIOL/legendre/>) (Legendre and Legendre 1998). Means, 95 % confidence intervals and coefficients of variation were calculated from the similarity values.

Results

TCE transformation rates

Reactor communities showed different TCE transformation rates after long-term phenol and phenol plus TCE application (Figure 2.1, panel A). From days 60 to

100 both reactors showed similar TCE transformation rates, that were as high as 0.22 and 0.24 $\text{I mg}^{-1} \text{ d}^{-1}$ for the phenol and phenol plus TCE fed reactors, respectively. By day 109, TCE transformation rates decreased to 0.03 $\text{I mg}^{-1} \text{ d}^{-1}$ for the phenol-fed reactor, and to 0.05 $\text{I mg}^{-1} \text{ d}^{-1}$ for the phenol plus TCE-fed reactor. At this point, the TCE transformation rates of the reactors diverged. The phenol-fed reactor had variable TCE transformation rates ranging from 0.01 to 0.24 $\text{I mg}^{-1} \text{ d}^{-1}$. In contrast, the TCE transformation rates in the phenol plus TCE-fed reactor were less variable in the range of 0.01 to 0.12 $\text{I mg}^{-1} \text{ d}^{-1}$. Visual inspection of the TCE transformation rates in the phenol-fed reactor suggests that changes TCE kinetics occur periodically in this reactor (Figure 2.1, panel A). Unimodal TCE transformation rates were observed approximately between days 60-109, 400-500 and 575-725 in the phenol-fed reactor. On the other hand, the phenol plus TCE-fed reactor did not show continuous periodicity, with only marked changes in transformation rates during the first 110 days, and minor changes afterwards (Figure 2.1, panel A). The average TCE transformation rates from 150-825 days were 0.082 ± 0.12 and 0.044 ± 0.05 $\text{I mg}^{-1} \text{ d}^{-1}$ for the phenol and the phenol plus TCE-fed reactor, respectively. Analyses of headspace from the phenol plus TCE-fed reactor indicate that the injected TCE was completely degraded before the settle and decant phases.

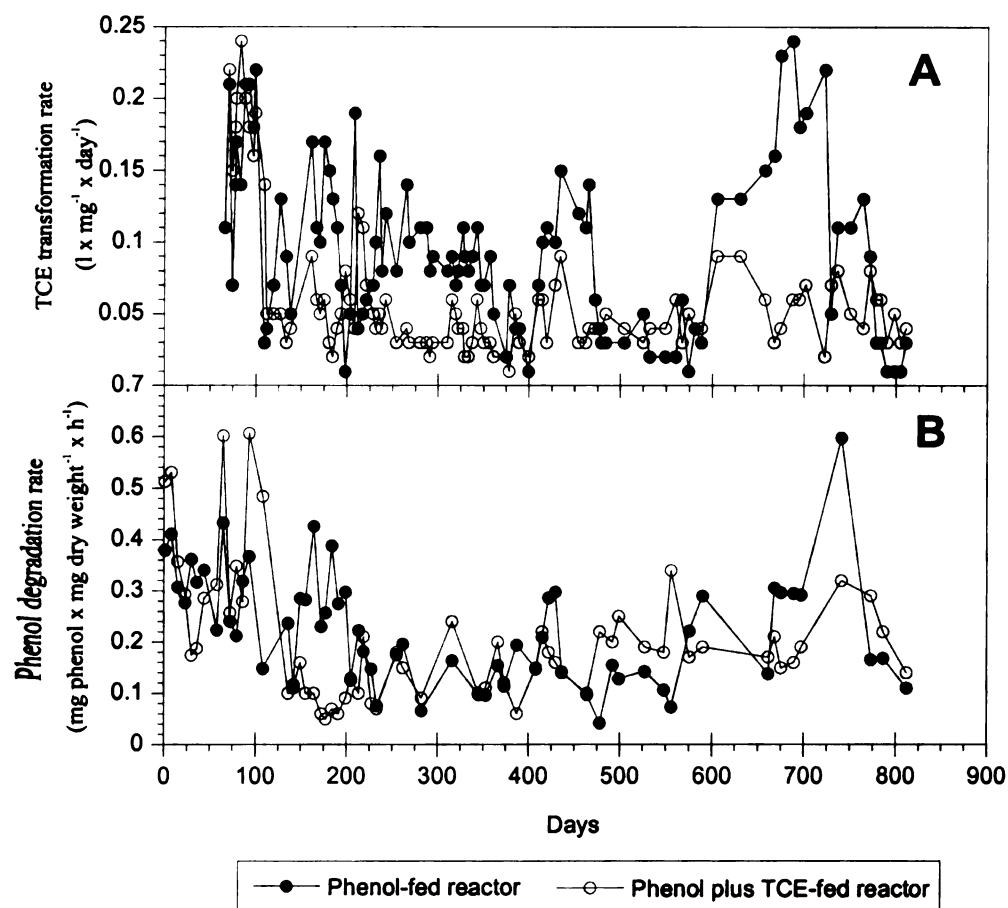


Figure 2.1. Long term functional responses of the phenol-fed and phenol plus TCE-fed reactors. (A), TCE transformation rates. (B), phenol degradation rates.

Phenol degradation rates

The maximum specific rates of phenol degradation for the phenol-fed reactor were variable during the first 200 days of operation, ranging from 0.1 to 0.4 mg phenol x mg dry weight⁻¹ x h⁻¹ (Figure 2.1, panel B). After 200 days of operation, the phenol degradation rates were stable in the range of 0.1-0.3 mg phenol x mg dry weight⁻¹ x h⁻¹, except for day 747 when for unexplained reasons the rates increased to 0.6 mg phenol x mg dry weight⁻¹ x h⁻¹. Visual inspections of the phenol degradation did not reveal any marked periodicity, such as in the TCE transformation rates (Figure 2.1, panel A).

In the phenol plus TCE-fed reactor, phenol degradation rates started at an initial value of 0.5 mg phenol x mg dry weight⁻¹ x h⁻¹ and then cycled, with conspicuous decreases (0.19 and 0.22 mg phenol x mg dry weight⁻¹ x h⁻¹) and increases (0.6 mg phenol x mg dry weight⁻¹ x h⁻¹) (Figure 2.1, panel B). After day 145 the phenol degradation rates did not increase as high as before, and less pronounced changes occurred. No periodicity on the phenol degradation rates was observed in the phenol-fed reactor. Analyses of samples from both reactors after phenol injection indicate that phenol concentrations decreased to zero after the first 2 h of the phenol recharge stage. No major wall growth was observed.

Community structure by T-RFLP

To determine if the two reactor communities were similar after 30 days of operation on phenol, and before TCE was applied to one of them, T-RFLP was

performed with six different tetrameric restriction enzymes (Figure 2.2). Each of the enzymes tested produced almost identical patterns for each of the two reactors, with only minor differences in the height of some small peaks.

In the T-RFLP procedure, enzyme selection is critical to judge if changes in community structure have occurred. Therefore, to select the best restriction enzymes for the analysis, a subset of all the samples was tested with the six enzymes previously used. Restriction enzymes *HaeIII* and *CfoI* were selected for community analysis because they generated the highest number of sharp and distinguishable fragments in all the samples tested. Restriction enzymes such as *MspI* and *RsaI* were initially promising (Figure 2.2), but in later samples several peaks overlapped.

To assess if T-RFLP is a suitable method to monitor population dynamics, a reproducibility analysis was conducted (Table 2.1). The indices used measured similarity based on the presence or absence of a fragment (Sørensen) and abundance of each fragment (Steinhaus). To have some reference for comparison, 32 lanes from the DNA marker GS2500 were analyzed. For the two indices the GS2500 standard resulted in the highest values as expected (Sørensen 1.0, Steinhaus 0.931), and the phenol and phenol plus TCE-fed reactors T-RFLP patterns showed good reproducibility (Table 2.1). Variability of the community measurements was lower than from previous studies (Dunbar et al. 2000; Osborn et al. 2000; Scala and Kerkhof 2000; Braker et al. 2001), with percentages of variation that ranged from 3.3 % to 6.2 %. This is an important finding since in previous studies there were some disagreements

on the reproducibility of the T-RFLP method (Osborn et al. 2000; Scala and Kerkhof 2000; Braker et al. 2001), probably caused by the limited number of samples analyzed.

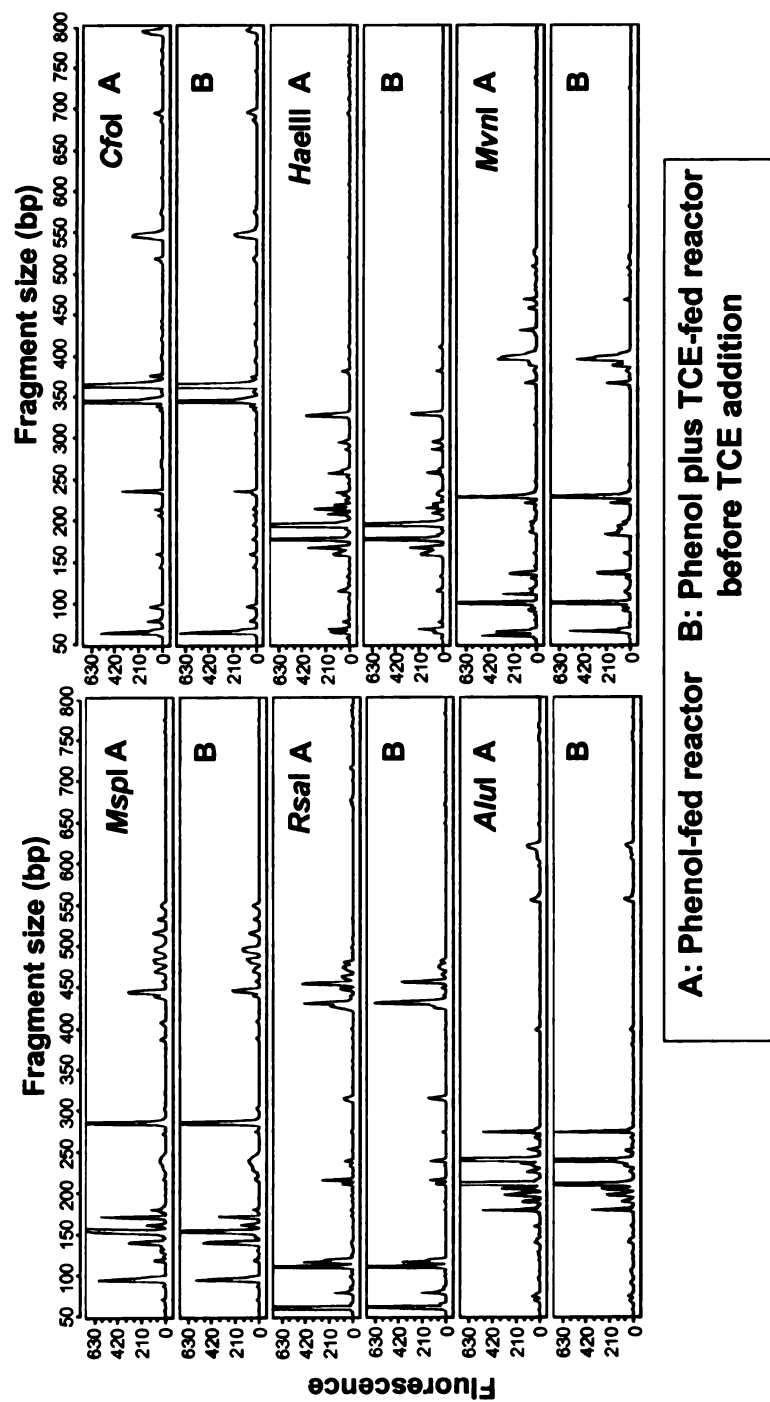


Figure 2.2. T-RFLP electropherograms of PCR amplified 16S rDNA bacterial genes from replicate reactor communities before TCE application to reactor B. Samples were digested with six different restriction enzymes individually.

Table 2.1. Reproducibility of the T-RFLP data. Means and 95 % confidence intervals (CI) for Sørensen and Steinhaus similarity indexes were calculated from pairwise comparisons. The TAMRA GS2500 standard is the molecular weight marker used to determine the sizes of the fragments in the gel.

Samples	<u>n</u>	Sørensen		Steinhaus		Coefficient of variation	
		Mean	95% CI	Mean	95% CI	Sørensen	Steinhaus
Phenol-fed reactor	9	0.966	± 0.012	0.921	± 0.013	3.5%	4.3%
Phenol plus TCE-fed reactor	9	0.937	± 0.010	0.851	± 0.018	3.3%	6.2%
TAMRA GS2500 Standard	32	1		0.931	± 0.003	0.0%	3.4%

The samples from the phenol plus TCE-fed reactor have a notable amount of polymer (Chapter 3) that could have affected DNA extraction procedures and might account for the slightly higher variability in this reactor. Nevertheless, good reproducibility was observed for the nine replicate samples from each reactor indicating that the samples were homogenous and representative of the microbial community in each system.

T-RFLP analysis of the two reactors showed marked changes in community structure over time (Figure 2.3). Fragments between 340-375 bp had different peak heights for the two reactors. Other fragments increased in relative peak height over time (200 bp fragment in the phenol plus TCE-fed reactor) or remained relatively stable (58 bp fragment in the phenol-fed reactor).

To determine if there were similarities between both reactor communities, CA was applied to data from both reactors combined. CA is a multivariate method that reveals the underlying structure of the data by taking into account both the peaks present in each sample and proportional changes in peak intensity. The analysis will result in a graphical representation of the samples along two or more axis of reference (dimensions) that will contain a fraction of the total variability. Each dimension represents the possible environmental factors that affect species distributions. Samples with similar community structure will be closer together in the multidimensional plot. The amount of data scatter in the multidimensional plot represents the variability of the community. CA resulted in data points forming an arch structure, typical of systems undergoing succession (ter Braak 1995) (Figure 2.4). CA data from the two

reactors before TCE addition ($T=0$) were nearly identical and different from all the other samples, indicating that the reactor communities were almost identical at the beginning of the experiment, and then diverged. Sample data from the phenol-fed reactor were scattered in the plot, which suggests that the phenol-fed community was highly variable. On the other hand, the data from the phenol plus TCE-fed reactor were more confined to the left arm of the arch, suggesting that the community in the phenol plus TCE-fed reactor was more stable than the community in the phenol-fed reactor. Both reactor communities were similar at different periods (Figure 2.4, circles A and B). Data points from days 50-104 of the phenol plus-TCE-fed reactor grouped with data from days 50-198, and 605-811 of the phenol-fed reactor (Figure 2.4, circle A). Interestingly, the highest TCE transformation rates were observed in both reactors during those days with similar community structure suggesting that some community structures were beneficial for high TCE transformation rates. Similarities were also observed between days 357-567 of the phenol-fed reactor and days 294-361, 399, 414-811 of the phenol plus TCE-fed reactor (Figure 2.4, circle B), periods with intermediate to low TCE degradation rates. All these data together indicate that the communities of the two reactors were similar at different functional stages.

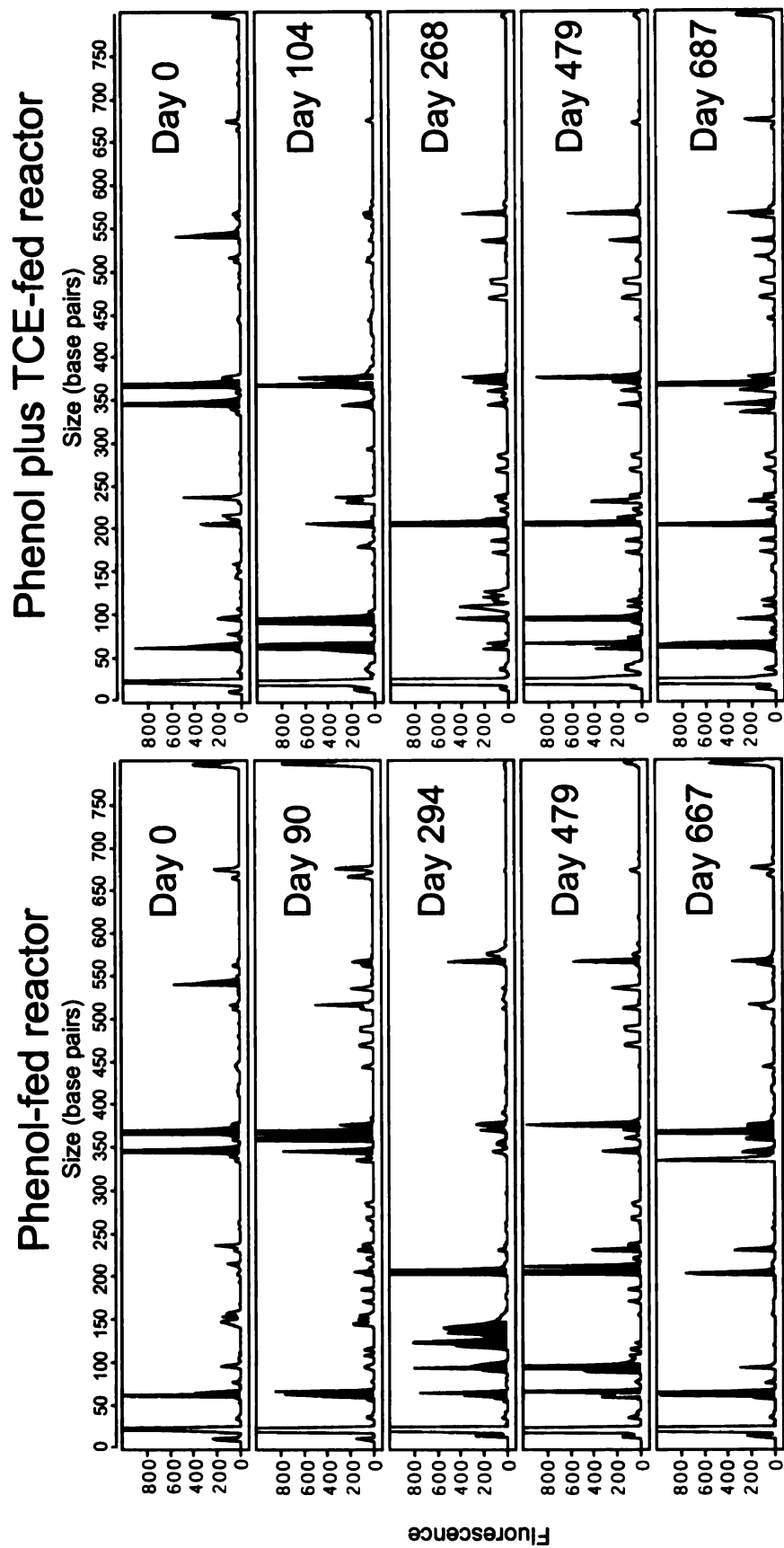


Figure 2.3. Changes in bacterial community structure over time. T-RFLP electropherograms were generated from a Cfol digest of the 16S rDNA PCR product. Shaded peaks indicate dynamic ribotypes

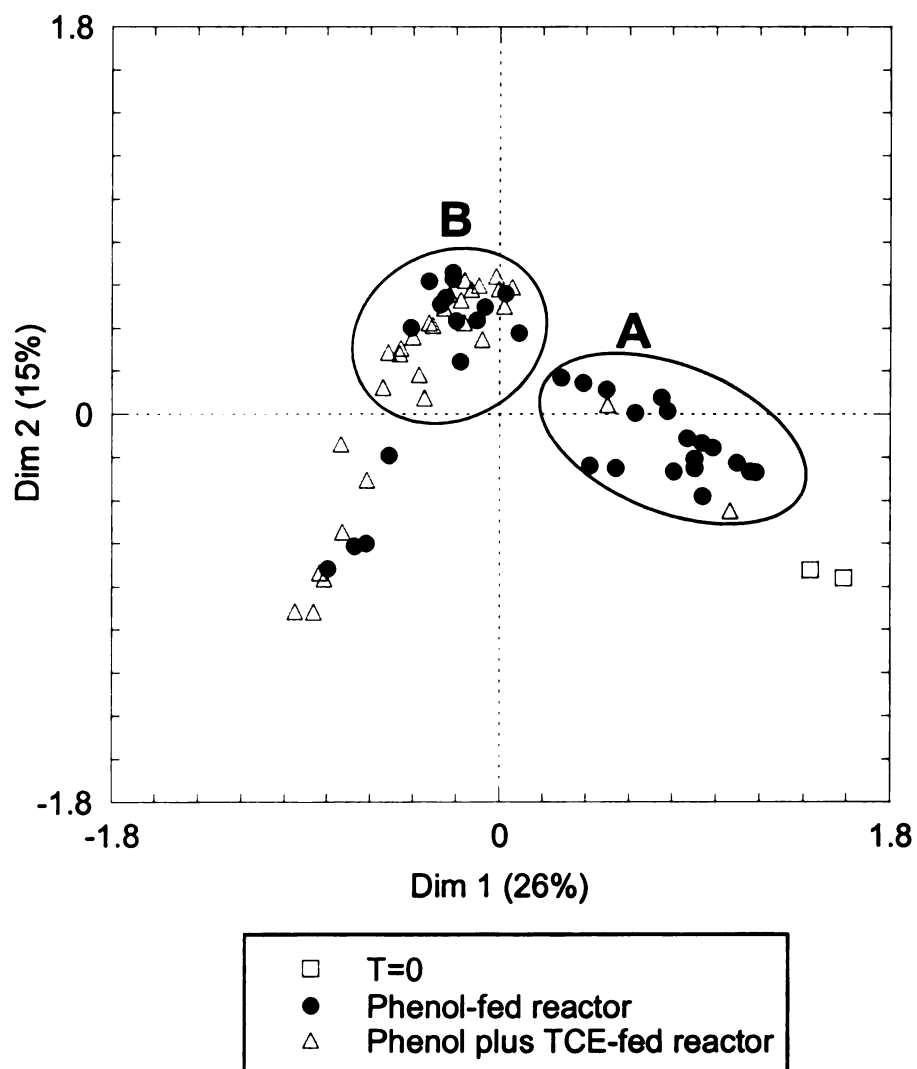


Figure 2.4. Correspondence analysis of T-RFLP data from reactor communities. Results from independent digests with *CfoI* and *HaeIII*, were combined for the analysis. Circles with letters indicate periods where the community structure of the two reactors was similar. (A) phenol-fed reactor days 50-198, 605-811; phenol plus TCE-fed reactor 50-104. (B) phenol-fed reactor days 357-541; phenol plus TCE-fed reactor days 294-361, 399, and 414-811. T=0, day 0 of each reactor before TCE application to one of them. Dim, dimension.

Changes in community structure can be seen in more detail in histograms that show the relative proportions of each fragment over time (Figure 2.5, Appendix B). The appearance or disappearance of fragments indicates that the community in the phenol-fed reactor was dynamic. For example, fragment 367 disappeared or was below detection limit after 198 days and simultaneously fragment 206 appeared and was present from day 127 until day 616. Fragment 367 reappeared after 605 days of operation. CA of each reactor separately was used to discern temporal patterns in each reactor community individually. CA confirmed that there were differences in community dynamics between the two reactors, and the relationship between community structure and function (Figure 2.6). In the phenol-fed reactor, the community structure changed at least three times converging back to its original state (Figure 2.6, panel A). T-RFLP patterns of samples from days 0-198 clustered with samples from days 605-811 indicating that the communities from those two periods of high TCE transformation rates were very similar. The T-RFLP profiles from days 226-310 and 357-567, periods with intermediate to low TCE transformation rates, formed distinct clusters.

The community in the phenol plus TCE-fed reactor was less dynamic than in the phenol-fed reactor (Figure 2.5). Most of the changes in community structure occurred in the first 100 days of operation. Fragment 367 disappeared during the first 100 days while fragment 206 appeared after 127 days and was present until the end of the sampling period. In addition to fragment 206, fragments 60, 66, 95, 376 and 567 were present most of time during days 127-

811. CA analysis revealed the majority of the changes occurred during days 0-104 (Figure 2.6, panel B), while in days 127-811 points tend to cluster together near the origin indicating that the community structure was similar and relatively stable during this lengthy period.

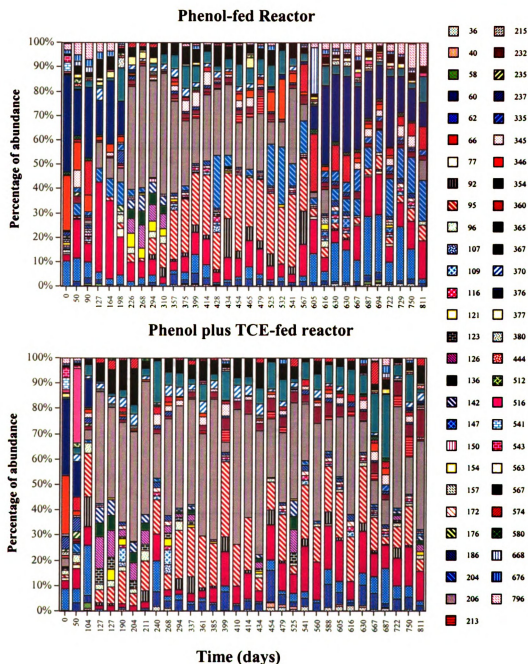


Figure 2.5. Relative abundance of Bacterial T-RF's from reactor samples after digestion with *CfoI*. Numbers in the legend indicate the sizes of the T-RF's in base pairs.

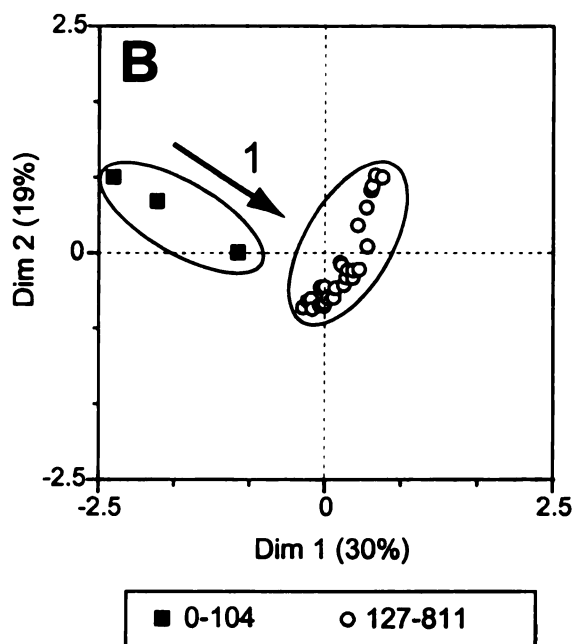
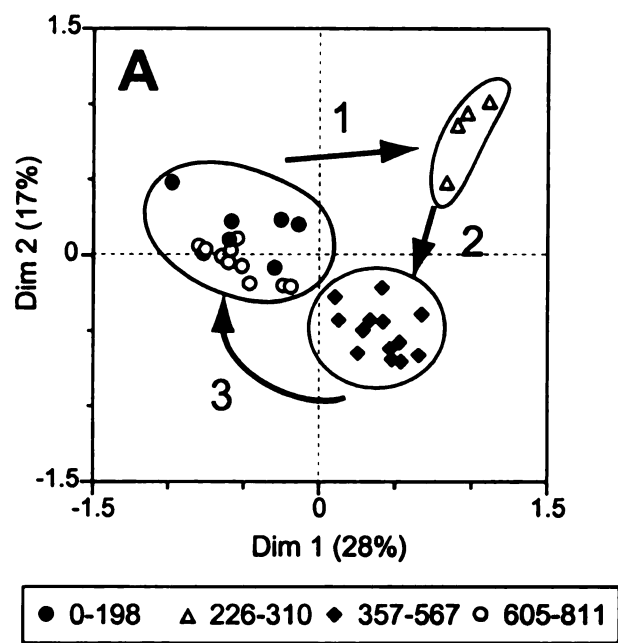


Figure 2.6. Correspondence analysis of T-RFLP data for each reactor community individually. (A), phenol-fed reactor; (B) phenol plus TCE-fed reactor. Numbers in the legend next to a symbol indicate day periods that were grouped together to facilitate interpretation. Arrows and numbers inside the graph indicate the order of the changes in community structure. Results from independent digests with *CfoI* and *HaeIII* were combined for the analysis. Circles delineate the different clusters formed. Dim, dimension.

To investigate changes in community structure at the functional level, phenol hydroxylase genes were amplified by PCR, digested with two restriction enzymes, and separated by electrophoresis (Figure 2.7). Cluster analysis of the phenol hydroxylase fingerprints revealed that populations with the gene in the phenol-fed reactor exhibit periods that correspond approximately to the periods found by T-RFLP (Figure 2.7, black and gray bars). Fingerprints from days 0-198 of the phenol-fed reactor were different from days 226-525, where the intensity of a ~135 bp band increased and a band between 89 and 104 bp appeared. Furthermore, fingerprints from days 630-811 were similar to days 0-198 profiles, consistent with the T-RFLP data (Figure 2.5 and 2.6, panel A). The phenol hydroxylase bearing populations in the phenol plus TCE-fed reactor showed two periods of change (Figure 2.7). During the first 50 days the community was stable and then changed with the emergence of a band of ~135 bp and the disappearance of two bands of ~210 and ~230 bp. This profile remained stable until the end of the experiment (day 811). Cluster analysis of the phenol hydroxylase fingerprints from both reactors confirmed that both communities were similar during the initial days and the latter period of the phenol-fed reactor (black bars), when the highest TCE transformation rates were observed. The communities were also similar during days 226-525 and days 127-811 of the phenol-fed and the phenol plus TCE-fed reactors respectively (Figure 2.7, grey bars), periods with low or intermediate TCE transformation rates.

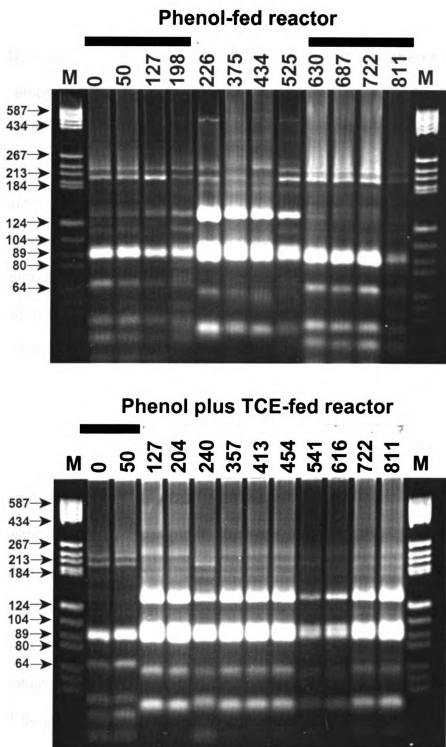


Figure 2.7. Community restriction patterns of PCR amplified phenol hydroxylase genes digested with *RsaI* and *MspI*. Numbers on top of each lane indicate time in days. Bars on tops represent the samples with similar fingerprinting pattern within and between reactors as determined from cluster analysis.

Discussion

Shih et al. previously showed that pulse feeding of phenol selected for a more efficient TCE degrading community than continuous feeding of phenol (Shih et al. 1996). However, the efficiency of TCE degradation was determined by assays on reactor samples, where the effects of TCE application on the community were not measured. In the current study, we employed the phenol feeding strategy of Shih et al. modified by the addition of a TCE feeding step to determine the long-term effects of TCE application. Long-term TCE application resulted in a microbial community with reduced TCE transformation rates (0.093 vs. 0.049 l mg⁻¹ d⁻¹ for the phenol and phenol plus TCE fed reactors respectively), but the rates were relatively stable over two years. Toxicity from the TCE epoxide is well documented in *Pseudomonas putida* F1 and *Burkholderia cepacia* G4 (Wackett and Householder 1989; Newman and Wackett 1997; Yeager et al. 2001). Although, the effects of TCE toxicity can be seen within 1 h of exposure, long-term effects have not been studied. Mars et al. (1996) suggested that TCE epoxide toxicity resulted in an increase in maintenance energy cost and the appearance of variants of *Burkholderia cepacia* G4 in batch culture which had lost the catabolic plasmid for TCE cooxidation. After 100 days of operation we observed low but relatively stable phenol degradation rates in the phenol plus TCE-fed reactor. In contrast, the phenol-fed community experienced frequent changes in phenol degradation rates that were linked to changes in TCE degradation rates (Figure 2.1, panel A and B). Our findings indicate that long-term TCE application in a sequential

feeding mode resulted in a slower though more stable TCE degrading community. It has been proposed that one of the adaptations to TCE toxicity is reduced rates of TCE cometabolism (Ishida and Nakamura 2000). Apparently, TCE application selected against the fast TCE degrading organisms but allowed slower TCE degraders to succeed.

Community analysis by T-RFLP of 16S rDNA genes revealed that there was correspondence between community structure and function in these reactors. Changes in TCE transformation rates for the phenol-fed reactor occurred periodically, and corresponded to changes in community structure. CA of all the fragments from two enzymes (*HaeIII* *CfoI*) showed that different day periods had particular community structures associated with them, and when TCE transformation rates were high the community structure was similar (Figure 2.6, panel A). Fragment 367 was present in days 0-198 and 605-729 in the phenol-fed reactor, when the highest TCE transformation rates were registered. In contrast, fragments 206 and 95 were present during days 226-567, when TCE transformation rates were intermediate to lower. Interestingly, a similar pattern was observed in the phenol plus TCE-fed reactor where fragment 367 was present when the transformation rates were high (days 0-104) and it was replaced by fragments 206 and 95 when the transformation rates were low (127-811 days). Changes in the distribution of phenol degrading populations can result from adaptations to phenol degradation or interactions between community members, e.g. predation by protozoa which were present in both reactors. Mutations in the promoter region of the phenol degradation genes

(Burchhardt et al. 1997), repression by organic acids (Müller et al. 1996; Ampe et al. 1998) or activity of unknown gene repressors (Arai et al. 1998) are events possible in a mixed community and could affect the fitness of phenol degrading populations causing changes in community structure.

While the T-RFLP data suggests that there was a community structure-function relationship, it is possible that the changes observed at the 16S rDNA level were not related to changes in the functional genes. Analysis of phenol hydroxylase genes (an enzyme often involved in TCE cooxidation) from selected samples from the two reactors revealed that the changes in community structure resulted and corresponded to changes in the phenol hydroxylase fingerprints. Different phenol hydroxylase genotypes were present when the reactors had higher transformations rates (days 0-198 and 630-811, of the phenol-fed reactor; and days 0-50 of the phenol plus TCE-fed reactor) suggesting that some phenol hydroxylases were more efficient in TCE cooxidation (Figure 2.7_). Furthermore, some phenol hydroxylase genotypes disappeared shortly after TCE was injected into one of the reactors suggesting that genotypes that were efficient in TCE cometabolism were also sensitive to TCE toxicity.

Understanding community succession has been one of the most challenging topics in contemporary ecology. Current ecological theories of succession predict contrasting outcomes of the process. Succession, as defined by Clements (1916), is an ordered unidirectional process of species replacements that culminate in a stable community, i.e. a climax community. On the other hand, more recent theories propose that during succession,

disturbances are frequent, and communities never reach a climax stage. Our findings suggest that microbial community succession was continuous in the phenol-fed reactor, while a relatively stable community was formed in the phenol plus TCE-fed reactor. Furthermore, CA of the phenol plus TCE-fed reactor community revealed that most of the changes in the community occurred during the first 100 days (Figure 2.6, panel B) and then, the community stabilized for 700 days suggesting that the community reached the climax stage Clements proposed (Clements 1916). In contrast, the community from the phenol-fed reactor changed periodically over the two year period and never reached a stable phase. Interestingly, the community structure of the phenol-fed reactor during the initial days (0-198) was similar to the community structure at the end of the experiment (days 605-811). The similarity was mainly caused by T-RFs present in those periods that were apparently displaced during the intermediate days (226-567). This is unusual in ecology since lost species usually do not return to the community. In our case, species were probably never entirely displaced from the community because they could remain as a refugia and below the detection limit of our methodologies (Massol-Deyá et al. 1997; Fernández et al. 1999). Nevertheless, it can be hypothesized from the changes in community structure that some microbial communities are dynamic and never reach a climax stage, but rather are a shifting mosaic where changes are unpredictable, as observed in some plant communities (McCune and Cottam 1985), and only limited temporal stability occurs.

The remaining question now is why the phenol plus TCE-fed community is more stable than the phenol-fed community. Cook (Cook 1996) reviewed modern successional theory and concluded that one of the points of commonality between the new theories is that disturbances are frequent and they likely affect the outcome of succession. It is possible that the changes in community structure seen in the phenol-fed reactor are a response to random disturbances that occur as part of any normal reactor operation. However, the way the reactors were designed and operated, random disturbance should affect both communities. Then, why should one of our communities be more stable? A possible answer of this question lies in the effects of TCE on the community. Toxicity studies on pure cultures suggest that the epoxide generated from TCE cometabolism damages cellular components, rendering cells inactive (Wackett and Householder 1989). Furthermore, recent studies on *Burkholderia cepacia* G4 suggest that G4 secretes toxic soluble intermediates from the degradation of TCE, which affect inactive cells (Yeager et al. 2001). Therefore, it is reasonable to hypothesize that TCE application selected for a community that is more resistant to TCE toxicity, and depending on the protection mechanism, the community could be more resistant to environmental disturbances. For instance, an increase in EPS accumulation was observed in the phenol plus TCE-fed reactor (Chapter 3), a phenomenon that resulted in the formation of “star-like” flocs, which to some extent resemble biofilms. Biofilm communities are very stable and resilient to perturbations suggesting that an analogous mechanism could be conferring increased stability to the TCE-fed community.

The results of this study suggest that the stability of the microbial communities could be dependent upon random disturbances and the selective pressure applied to the ecosystem. More than two years of phenol and TCE application resulted in a community with reduced but stable TCE degradation rates and relatively stable community structure. On the other hand, long-term application of phenol resulted on a different community with higher TCE transformation rates but with continuous and unpredictable changes in community structure and function. These findings suggest that microbial communities in nature in similar niches could have contrasting dynamics depending upon particular physical, chemical or biological conditions imposed.

References

- Alexander, M.** (1994). Biodegradation and bioremediation. San Diego, Academic Press.
- Amann, R. I., W. Ludwig and K. H. Schleifer.** (1995). Phylogenetic identification and in situ detection of individual microbial cells without cultivation. *Microbiol. Rev.* **59**: 143-69.
- Ampe, F., D. Léonard and N. Lindley.** (1998). Repression of phenol catabolism by organic acids in *Ralstonia eutropha*. *Appl. Environ. Microbiol.* **64**: 1-6.
- Anderson, J. E. and P. L. McCarthy.** (1997). Transformation yields of chlorinated ethenes by a methanotrophic mixed culture expressing particulate methane monooxygenase. *Appl. Environ. Microbiol.* **63**: 687-693.
- Arai, H., S. Akahira, T. Ohishi, M. Maeda and T. Kudo.** (1998). Adaptation of *Comamonas testosteroni* TA441 to utilize phenol: organization and regulation of the genes involved in phenol degradation. *Microbiol.* **144**: 2895-2903.
- ATSDR.** (1994). National exposure registry. Trichloroethylene (TCE) subregistry baseline technical report (revised). Agency for Toxic Substances and Disease Registry, U.S. Public Health Service, Department of Health and Human Services. **NTIS Publication No. PB95-154589**: Atlanta, Georgia.

- Blackwood, C. B.** (2001). Spatial organization in soil bacterial communities. Ph. D. dissertation. Michigan State University, East Lansing, MI.
- Braker, G., H. L. Ayala-del-Rio, A. H. Devol, A. Fesefeldt and J. M. Tiedje.** (2001). Community structure of denitrifiers, Bacteria and Archaea along redox gradients in Pacific Northwest marine sediments by T-RFLP analysis of amplified nitrite reductase (*nirS*) and 16 rRNA genes. *Appl. Environ. Microbiol.* **67**: 1893-1910.
- Bruckner, J. V., B. D. Davis and J. N. Blancato.** (1989). Metabolism, toxicity, and carcinogenicity of trichloroethylene. *Crit. Rev. Toxicol.* **20**: 31-50.
- Burchhardt, G., I. Schmidt, H. Cuypers, L. Petruschka, A. Völker and H. Herrmann.** (1997). Studies on spontaneous promoter-up mutations in the transcriptional activator-encoding gene *phlR* and their effects on the degradation of phenol in *Escherichia coli* and *Pseudomonas putida*. *Mol. Gen. Genet.* **254**: 539-547.
- Chang, W.** (1996). Kinetics characterization of cometabolizing communities and adaptation to nongrowth substrate. Ph. D. dissertation. Michigan State University, East Lansing, MI.
- Clements, F. E.** (1916). Plant succession: An analysis of the development of vegetation. Carnegie Inst. Publ. Washington, DC. **242**.
- Cook, J. E.** (1996). Implications of modern successional theory for habitat typing: A review. *Forrest Sci.* **42**: 67-75.
- Dolan, M. E. and P. L. McCarty.** (1995). Small Column Microcosm for Assessing Methane-Stimulated Vinyl- Chloride Transformation in Aquifer Samples. *Environ. Sci. Technol.* **29**: 1892-1897.
- Dunbar, J., O. Ticknor Lawrence and C. Kuske.** (2000). Assessment of microbial diversity in four southwestern United States soils by 16S rRNA gene terminal restriction fragment analysis. *Appl. Environ. Microbiol.* **66**: 2943-2950.
- Fernández, A., S. Huang, S. Seston, J. Xing, R. Hickey, C. Criddle and J. Tiedje.** (1999). How stable is stable? Function versus community composition. *Appl. Environ. Microbiol.* **65**: 3697-3704.
- Fries, M. R., L. J. Forney and J. M. Tiedje.** (1997a). Phenol- and toluene-degrading microbial populations from an aquifer in which successful trichloroethene cometabolism occurred. *Appl. Environ. Microbiol.* **63**: 1523-1530.
- Fries, M. R., G. D. Hopkins, P. L. McCarty, L. J. Forney and J. M. Tiedje.** (1997b). Microbial succession during a field evaluation of phenol and

t
f

Gio

Hop

Inf

Ishi

Leg

Mar

Mas

McC

McC

Moh

Müll

(
P
1

- toluene as the primary substrates for trichloroethene cometabolism. *Appl. Environ. Microbiol.* **63**: 1515-1522.
- Giovannoni, S. J.** (1991). The polymerase chain reaction. *In* *Nucleic acids techniques in bacterial systematics*. E. Stackebrandt. New York, John Wiley & Sons 177-201.
- Hopkins, G. D. and P. L. McCarty.** (1995). Field-Evaluation of in-Situ Aerobic Cometabolism of Trichloroethylene and 3 Dichloroethylene Isomers Using Phenol and Toluene as the Primary Substrates. *Environ. Sci. Technol.* **29**: 1628-1637.
- Infante, P. F. and T. A. Tsongas.** (1987). Mutagenic and oncogenic effects of chloromethanes, chloroethenes, and halogenated analogs of vinyl chloride. *Environ. Sci. Res.* **25**: 301-327.
- Ishida, H. and K. Nakamura.** (2000). Trichloroethylene degradation by *Ralstonia* sp. KN1-10A constitutively expressing phenol hydroxylase: transformation products, NADH limitation and product toxicity. *J. Biosc. Bioeng.* **5**: 438-445.
- Legendre, P. and L. Legendre.** (1998). *Numerical Ecology*. Amsterdam, Elsevier Science B. V.
- Mars, A. E., J. Houwing, J. Dolfing and D. B. Janssen.** (1996). Degradation of toluene and trichloroethylene by *Burkholderia cepacia* G4 in growth-limited fed-batch culture. *Appl. Environ. Microbiol.* **62**: 886-891.
- Massol-Deyá, A., R. Weller, L. Ríos-Hernández, J. Z. Zhou, R. F. Hickey and J. M. Tiedje.** (1997). Succession and Convergence of Biofilm communities in Fixed-Film reactors treating aromatic hydrocarbons in groundwater. *Appl. Environ. Microbiol.* **63**: 270-276.
- McCarty, P. L., M. N. Goltz, G. D. Hopkins, M. E. Dolan, J. P. Allan, B. T. Kawakami and T. J. Carrothers.** (1998). Full scale evaluation of in situ cometabolic degradation of trichloroethylene in groundwater through toluene injection. *Environ. Sci. Technol.* **32**: 88-100.
- McCune, B. and G. Cottam.** (1985). The successional status of a southern Wisconsin oak woods. *Ecology* **66**: 1270-1278.
- Mohn, W. W. and J. M. Tiedje.** (1992). Microbial Reductive Dehalogenation. *Microbiol. Rev.* **56**: 482-507.
- Müller, C., L. Petruschka, H. Cuypers, G. Burchhardt and H. Herrmann.** (1996). Carbon catabolite repression of phenol degradation in *Pseudomonas putida* is mediated by the inhibition of the activator protein PhIR. *J. Bacteriol.* **178**: 2030-2036.

- Newman, L. M. and L. P. Wackett.** (1997). Trichloroethylene oxidation by purified toluene 2-monooxygenase: products, kinetics, and turnover-dependent inactivation. *J. Bacteriol* **179**: 90-96.
- Osborn, A. M., E. R. B. Moore and K. N. Timmis.** (2000). An evaluation of terminal-restriction fragment length polymorphism (T-RFLP) analysis for the study of microbial community structure and dynamics. *Environ. Microbiol.* **2**: 39-50.
- Scala, D. J. and L. J. Kerkhof.** (2000). Horizontal heterogeneity of denitrifying bacterial communities in marine in marine sediments by terminal-restriction fragment length polymorphism analysis. *Appl. Environ. Microbiol.* **66**: 1980-1986.
- Segar, R. L., S. L. Dewys and G. E. Speitel.** (1995). Sustained Trichloroethylene Cometabolism by Phenol-Degrading Bacteria in Sequencing Biofilm Reactors. *Water Environ. Res.* **67**: 764-774.
- Shih, C. C., M. E. Davey, J. Zhou, J. M. Tiedje and C. S. Criddle.** (1996). Effects of phenol feeding pattern on microbial community structure and cometabolism of trichloroethylene. *Appl. Environ. Microbiol.* **62**: 2953-2960.
- ter Braak, C. J. F.** (1995). Ordination. *In* Data analysis in community and landscape ecology. R. H. G. Jongman, C. J. F. ter Braak and v. Torgeren. Cambridge, UK, Cambridge University Press 91-105.
- Thioulouse, J., D. Chessel, S. Dolédec and J. M. Olivier.** (1997). ADE-4: a multivariate analysis and graphical display software. *Stat. Comp.* **7**: 75-83.
- Vogel, T. M., C. S. Criddle and P. L. McCarty.** (1987). Transformations of halogenated aliphatic compounds. *Environ. Sci. Technol.* **21**: 722-736.
- Wackett, L. P.** (1995). Bacterial cometabolism of halogenated organic compounds. *In* Microbial transformations and degradation of toxic organic chemicals. L. Y. Young and C. E. Cerniglia. New York, Wiley-Liss 217-241.
- Wackett, L. P. and S. R. Householder.** (1989). Toxicity of trichloroethylene to *Pseudomonas putida* F1 is mediated by toluene dioxygenase. *Appl. Environ. Microbiol.* **55**: 2723-2725.
- Watanabe, K., M. Teramoto, H. Futamata and S. Harayama.** (1998). Molecular detection, isolation, and physiological characterization of functionally dominant phenol-degrading bacteria in activated sludge. *Appl. Environ. Microbiol.* **64**: 4396-4402.
- Yeager, C. M., P. J. Bottomley and D. J. Arp.** (2001). Cytotoxicity associated with trichloroethylene oxidation in *Burholderia cepacia* G4. *Appl. Environ. Microbiol.* **67**: 2107-2115.

CHAPTER 3

THE ABUNDANCE OF EXTRACELLULAR POLYMERIC SUBSTANCES AND THE SPATIAL DISTRIBUTION OF BACTERIA IN FLOCS IN PHENOL AND PHENOL PLUS TCE FED REACTORS.

Introduction

The majority of the microorganisms in bioreactor systems live in aggregates often termed as granules, flocs or biofilms. This lifestyle is convenient for microbes because the close proximity between them allows interactions such as metabolite transfer, communication via diffusible factors and horizontal gene transfer (Davey and O'Toole 2000). Aggregate formation can also serve as a protection mechanism against undesirable environmental conditions such as predation (Decho and Lopez 1993) and the presence of toxic compounds (Gilber and Brown 1995). For instance, the addition of ethanol to liquid and solid cultures of *Pseudomonas aeruginosa* enhances the production of alginate, leading to the formation of mucoid cells and biofilms that are resistant to antibiotics (DeVault et al. 1990; Costerton et al. 1999). Starvation is another condition that favors aggregation. Cells form aggregates under starvation in order to trap nutrients from the surrounding environment making them available to the cells in the floc or biofilm (Lewis and Gattie 1990; Davey and O'Toole 2000; Flemming and Wingender 2001). Aggregate formation is also an important process for efficient wastewater treatment, where good settling

sludge is essential to obtain clean effluents (Urbain et al. 1993; Bossier and Verstrate 1996; Sponza 2002).

Bacteria form aggregates by attaching to each other forming a microcolony, a structure that will be colonized by other species of bacteria, and if stable, will eventually result in the formation of a floc or a biofilm (Watnick and Kolter 2000). This process will also be strongly affected by physical and chemical features of the environment. Extracellular polymeric substances (EPS) serve as the “glue” that maintain cells attached to each other and to solid surfaces (Li and Ganzarczyk 1990; Urbain et al. 1993; Bossier and Verstrate 1996; Wingender et al. 1999).

Microbial EPS is a mixture of organic compounds secreted by cells either in aggregates or in isolation. EPS is usually composed of polysaccharides, proteins, DNA and some lipids (Frolund et al. 1996; Neu 1996; Dignac et al. 1998), with polysaccharides being the most abundant representing 40-90% of the total organic matter in biofilms (Urbain et al. 1993; Flemming and Wingender 2001; Sutherland 2001). In pure cultures EPS can be found as a capsule surrounding the cell resulting in a mucoid appearance, or secreted into the medium (Grobe et al. 1995; Kachlany et al. 2001). Diverse groups of bacteria are capable of secreting EPS under a variety of conditions. Some of the genera known to secrete EPS include: *Burkholderia*, *Streptococcus*, *Bacillus*, *Flavobacterium*, *Rhizobium*, *Mycobacterium*, *Lactobacillus*, *Pseudomonas*, *Sphingomonas*, *Nitrosomonas*, *Klebsiella*, *Desulfovibrio*, and *Enterobacter* (Graber et al. 1988; Stehr et al. 1995; Cerantola et al. 2000; Denner et al. 2001).

EPS production could be a major factor in bioremediation applications. Bacteria that produce EPS and attach to surfaces in large quantities affect ground water flow reducing the success of the bioremediation strategy. In other cases EPS could help protect cells from the toxic effects of some pollutants. For instance, studies on a mucoidal strain of *Rhodococcus rhodochlorus* revealed that EPS conferred tolerance to 10 % (vol/vol) n-hexadecane and allowed cells to degrade crude oil (Iwabuchi et al. 2000). EPS production is also important for the success of bioreactors. In biofilm reactors EPS is essential for retention of the biocatalyst populations on solid surface. In batch reactors EPS is also needed for good settling and hence retention of the biomass. Despite the importance of biofilms, generalizations about the conditions that cause EPS secretion and its role in bioremediation are not yet clear.

Previous studies in activated sludge have examined the abundance of EPS during normal operation and during anaerobic storage, as well as its physico-chemical properties (Urbain et al. 1993; Nielsen et al. 1996; Liao et al. 2001; Sponza 2002). However, there are no studies on the effects of chlorinated compounds on the EPS content of bioreactor communities. The purpose of this study was to determine the effects of long-term TCE application on the EPS content of phenol-fed sequencing batch reactors. Our objectives were: (i) to determine if the EPS content was affected by TCE addition; (ii) determine the spatial distribution of bacteria in the different reactors; and (iii) determine the composition of the EPS. We had noted an increase in EPS abundance and the

formation of “star like” flocs in the phenol plus TCE-fed reactor, but not in the phenol-fed reactor suggesting this phenomenon might be important.

Materials and Methods

Reactor sampling

Samples of total suspended solids (TSS) were obtained from two bench scale sequencing batch reactors (SBR), one was fed-phenol and the other was fed phenol and TCE in alternate cycles (Chapter 2). Initially, six samples (~ 10 ml each) from each reactor were taken and processed the same day for EPS extraction. Samples frozen at -80° C were used to analyze the changes in EPS content during reactor operation. For scanning electron microscopy (SEM), samples (~5 ml) were fixed with one volume of 4% glutaraldehyde in 0.1M sodium phosphate buffer (pH 7.4) for 30 min before processing.

Scanning electron microscopy

One drop of fixed sample was placed on a 12 mm round glass cover slip pre-coated with 1 % poly-l-lysine (Sigma Aldrich, St. Louis, Missouri), and air dried for 5 min. The slide was gently washed in water before dehydration by successive transfers in ethanol baths (25 %, 50 %, 75 %, 95 %), and three final changes in 100% ethanol. The sample was critical point dried in a Balzers critical point dryer (Balzers, Lichtenstein) and then coated with gold in an emscope sputter coater (Emscope, UK). Images were taken in a JEOL 6400V scanning electron microscope (JEOL, Ltd., Tokyo, Japan).

Ep

(M

for

mic

with

Fra

solu

mod

with

min

cer

fiite

We

W

C

W

fr

fre

untr

weigh

Epifluorescent microscopy

Reactor samples (1 ml) were mixed with the nucleic acid stain SYTO-9 (Molecular Probes, Eugene, Oreg.) to a 1 μ M final concentration, and incubated for 15 min at 25° C. An aliquot (5 μ l) was placed on a 6 mm well of a microscope slide (Cel-line associates, Newfield, New Jersey) and was observed with a Leitz Orthoplan 2 microscope equipped with a 50 W mercury lamp.

Fractionation of the TSS

The EPS was recovered from the TSS by the potassium hydroxide solubilization method described by Kim et al. (Kim et al. 2000) with the following modifications: fresh TSS samples (~ 10 ml) were transferred to a beaker, diluted with two volumes of 10 % potassium hydroxide (1.8 M) and mixed slowly for 30 min at 25° C. The biomass fraction was separated from the mixture by centrifugation (2000 x g at 25° C for 15 min), resuspended in distilled water and filtered through a 0.22 μ m Durapore filter (Millipore, Bedford, Mass.) for dry weight measurement. The supernatant was transferred to a flask and mixed with three volumes of 95 % ethanol to precipitate the EPS fraction. After centrifugation (2000 x g at 25° C for 15 min), the EPS was dried at 42° C and weighted as described previously (De Vuyst et al. 1998). The efficiency of the fractionation method was determined by comparing the sum of the masses of the different fractions against the TSS of untreated samples. The TSS of untreated samples was measured by filtering six replicate samples and dry weight measurements were obtained as described above.

Purification and characterization of EPS

Precipitated EPS was purified by dialysis against distilled water (two water changes daily) in a 12,000-14,000 Dalton molecular weight cutoff membrane (Spectrum Laboratories, Rancho Dominguez, Calif.) for 10 days at 22° C. The purified EPS was frozen to -80° C before being lyophilized. The composition of the EPS was determined by analysis of alditol acetate derivatives (Wang and Hollingsworth 1994). Approximately 0.1 mg of sample was hydrolyzed in 2 M trifluoroacetic acid (TFA) for 1 h at 120° C. The solution was dried under a stream of nitrogen while heated at 50° C, dissolved in distilled water, and dried again. This procedure was repeated two times to remove traces of TFA. The dried product was reduced to form alditol acetates by incubation with sodium borohydrate at 25° C for 24 h. To remove the excess of sodium borohydrate one volume of distilled water and one drop of concentrated hydrochloric acid were added to the vial and the solution was incubated at 25° C for 10 min before being dried under a stream of nitrogen as described above. Water, concentrated acetic acid and methanol were added to the vial, mixed and dried under nitrogen. Methanol was added and dried three more times to remove traces of boric acid. The dried product was paracetylated with acetic anhydride and pyridine, and analyzed by gas chromatography (GC) and gas chromatography followed by mass spectrometry (GC-MS) as described previously (Wang and Hollingsworth 1994). The temperature program employed began with an initial temperature of 170° C for 2 min, followed by an increase to 220° C at a rate of 2° C/min and held for 60 min at that temperature. To further

support the GC-MS findings H^1 NMR of non-hydrolyzed samples was performed in D_2O using a Varian VXR500 spectrometer at 500 MHz.

Results

Visual inspection and microscopy.

Marked differences in the appearance of the suspended solids were observed between the phenol and the phenol plus TCE-fed reactors. The suspended solids of the phenol-fed reactor formed loose granules by visual inspection of reactor samples. On the contrary, the suspended solids from the phenol plus TCE-fed reactor formed large and dense cell floccules of slimy appearance.

Scanning electron microscopy revealed major differences between the phenol-fed and the phenol plus TCE-fed reactors communities (Figure 3.1). The microbial community of the phenol-fed reactor formed small aggregates of 50-60 μm in diameter with low amounts of EPS connecting the cells (Figure 3.1, A and C). The aggregate was composed of rod shaped bacteria of different sizes, some of which were pleomorphic. In contrast, the microbial community of the phenol plus TCE-fed reactor formed a "star-like" structure (Figure 3.1, D) with bacteria embedded within an EPS matrix that together made up the long filament (Figure 3.1, E and F). The filaments were composed mainly of small rods ($\sim 1.2 \mu m$ in length) and some longer rods positioned towards the outside of the filament (Figure 3.1, F).

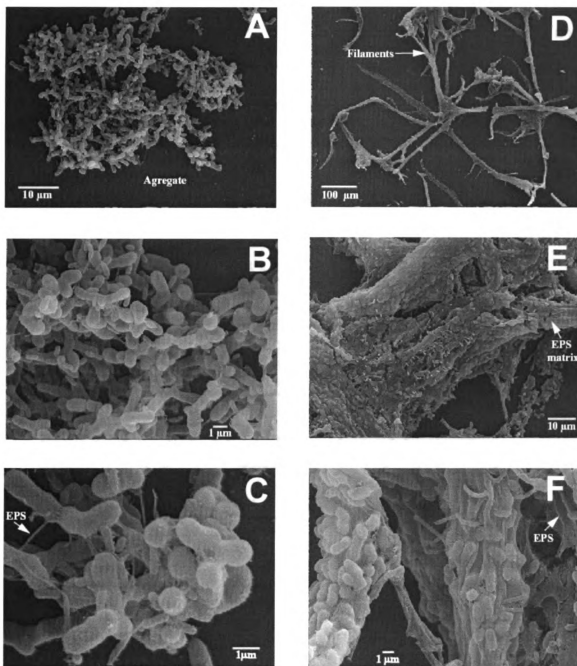


Figure 3.1. Electron scanning micrographs of reactor suspended solids. Images were taken after 900 days of reactor operation. Micrographs A-C and D-F represent different levels of resolution for the phenol-fed and the phenol plus TCE-fed reactors, respectively. EPS, extracellular polymeric substances.

This star-like structure could also be observed under epifluorescence microscopy (Figure 3.2); the filaments were also arranged in conical structures with relatively similar diameters. The cells are uniform in shape and arrangement in these filaments (Figure 3.2, B). The aforementioned structures were observed in different samples throughout the 120 to 811 day period. They may have formed sooner than 120 days but no samples were examined for the 0 to 120 days period of operation.

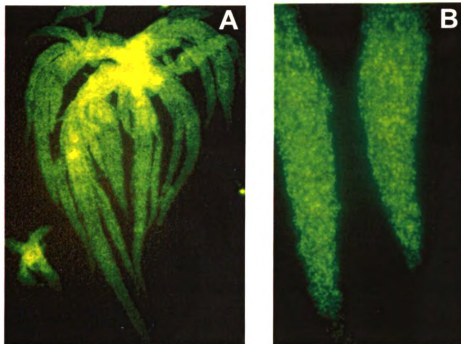


Figure 3.2. Epifluorescence microscopy of the phenol plus TCE-fed reactor flocs. Samples were stained with SYTO-9. Panel A, 100X magnification, panel B, 700X magnification.

EPS abundance

Analysis of the TSS by dry weight revealed that there were marked differences between the two reactors (Figure 3.3, panel A). The TSS of the phenol-fed reactor was $1,002 \pm 39.7$ mg/l, 30 % less than the TSS of the phenol plus TCE-fed reactor which was 1462 ± 24.5 mg/l. Fractionation of the TSS in EPS and biomass revealed that the differences observed between the TSS of the two reactors were caused by a significant increase in the EPS content of the phenol plus TCE-fed reactor. The concentration of EPS in the phenol plus TCE-fed reactor, measured as polymer dry mass (PDM), was 589 ± 88.2 mg PDM/l or 40 % of the TSS (Figure 3.3 panel B). In contrast the EPS concentration in the phenol-fed reactor was 121 ± 33.8 mg PDM/l or only 12% of the TSS. No major differences were observed between the biomass fractions of each reactor, with concentrations of 862 ± 68.9 and 735 ± 87.3 mg/l in the phenol-fed and the phenol plus TCE-fed reactors respectively. However, due to the major amount of EPS in the phenol plus TCE-fed reactor, the biomass fraction only represented 50% of the TSS (Figure 3.3, panel B). In contrast the biomass fraction of the phenol-fed reactor represented 86 % of the TSS.

In order to determine the changes in EPS content during the duration of the experiment, selected frozen samples were used for biomass and EPS fractionation (Table 3.1). The values were expressed as the percentage of EPS relative to the TSS previously measured (Chapter 2). Analysis of the phenol-fed reactor samples shows that the proportion of EPS was relatively stable over the duration of the experiment with an average of 10 % of the TSS. In contrast, the

proportion of EPS in the phenol plus TCE-fed reactor increased during the first 90 days of operation and stabilized at an average of 45 % of the TSS.

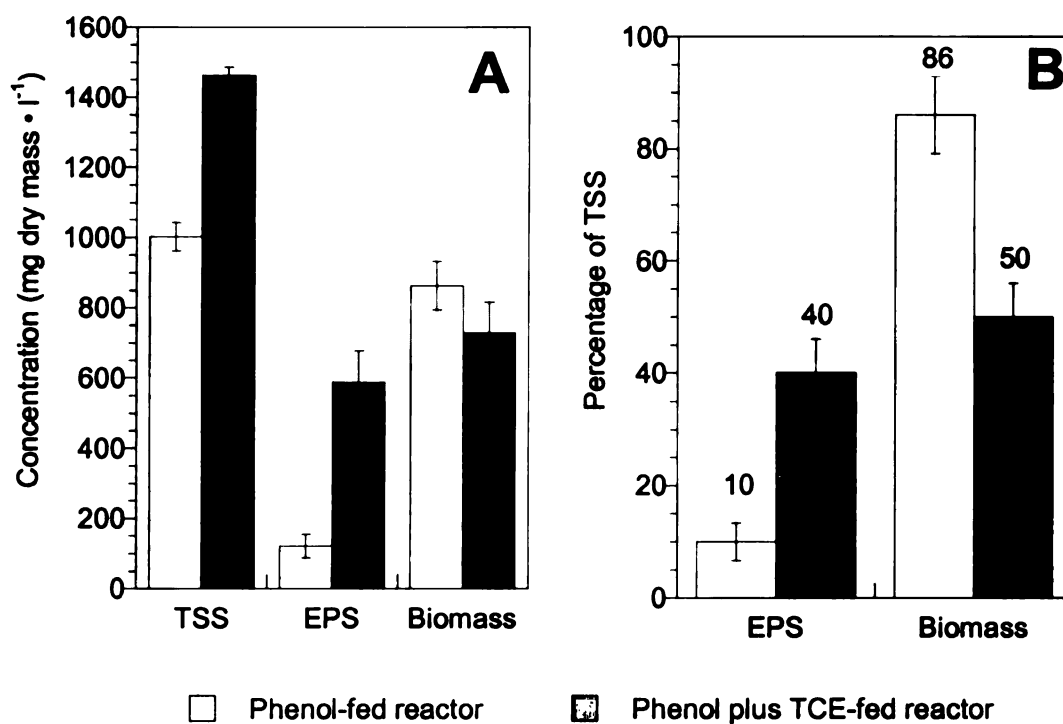


Figure 3.3. Fractionation of the TSS (A) and percentage of the fractions relative to the TSS (B). Values represent means \pm 95 % confidence intervals ($n=6$).

Table 3.1. Relative abundance of the EPS fraction in the phenol-fed and the phenol plus TCE-fed reactor. Values represent the percentage of the EPS relative to the TSS.

Day	Percentage of EPS	
	Phenol-fed reactor	Phenol plus TCE-fed reactor
42	8 %	6 %
63	10 %	30 %
90	10 %	43 %
119	9 %	46 %
151	10 %	49 %
173	12 %	44 %
350	8 %	41 %
689	11 %	45 %
800	11 %	40 %

EPS composition

To determine the composition of the EPS, large samples from each reactor were extracted with potassium hydroxide and purified by dialysis. Since we were not able to recover sufficient EPS from the phenol-fed reactor after dialysis we focused on the EPS composition of the phenol plus TCE-fed reactor. GC and GC-MS analysis revealed that this EPS was mainly composed of hexose sugars, i.e. rhamnose, fucose, arabinose, xylose, mannose, galactose, glucose; and one amino sugar, i.e, N-acetylglucosamine (Figure 3.4). Further evidence to support this identification was obtained by H^1 NMR analysis (Figure 3.5). Singlets between 1.2 and 1.5 ppm were assigned to the 6-deoxy groups of rhamnose, while signals between 5.0 and 5.5 ppm were assigned to the alpha linkages of rhamnose. Signals between 3.4 and 4.3 ppm were assigned to the remaining sugar protons. The two singlets between 2.0 and 2.2 ppm were assigned to the N-acetyl groups of N-acetylglucosamine while the signals between 4.7 and 4.9 ppm were assigned to the beta linkages. The most abundant sugar identified was rhamnose representing 56 % of all the carbohydrates identified, followed by mannose with 22 % (Figure 3.6).

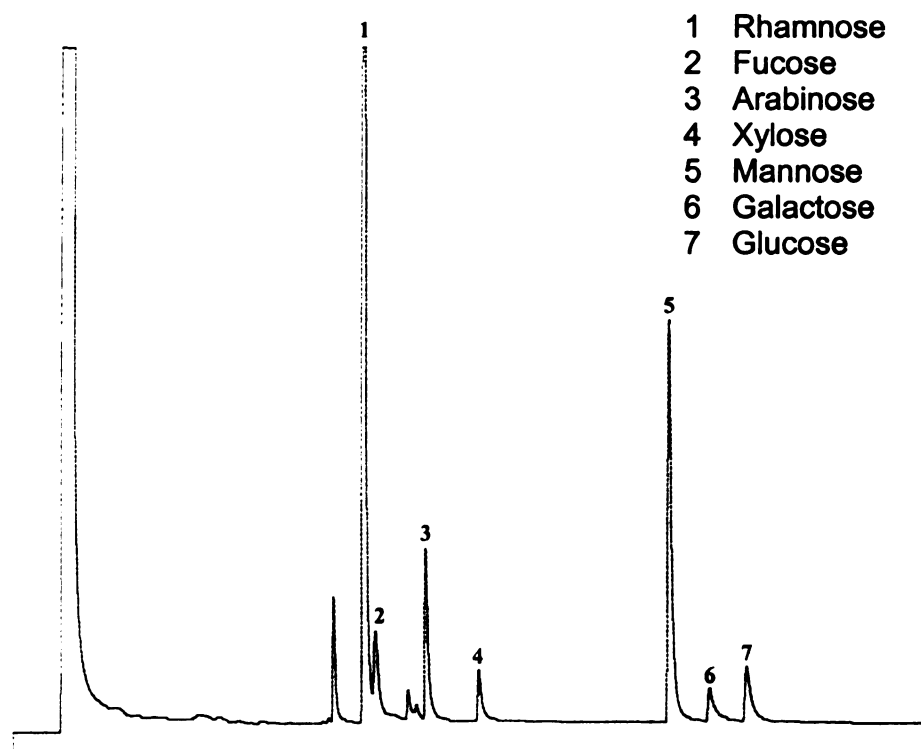


Figure 3.4. Gas chromatogram of alditol acetates from the phenol plus TCE-fed reactor purified EPS. The identities of the peaks were determined by coelution with standards and analysis of mass spectra. The peak before rhamnose is an unidentified compound. N-acetylglucosamine is not shown due to its long retention time.

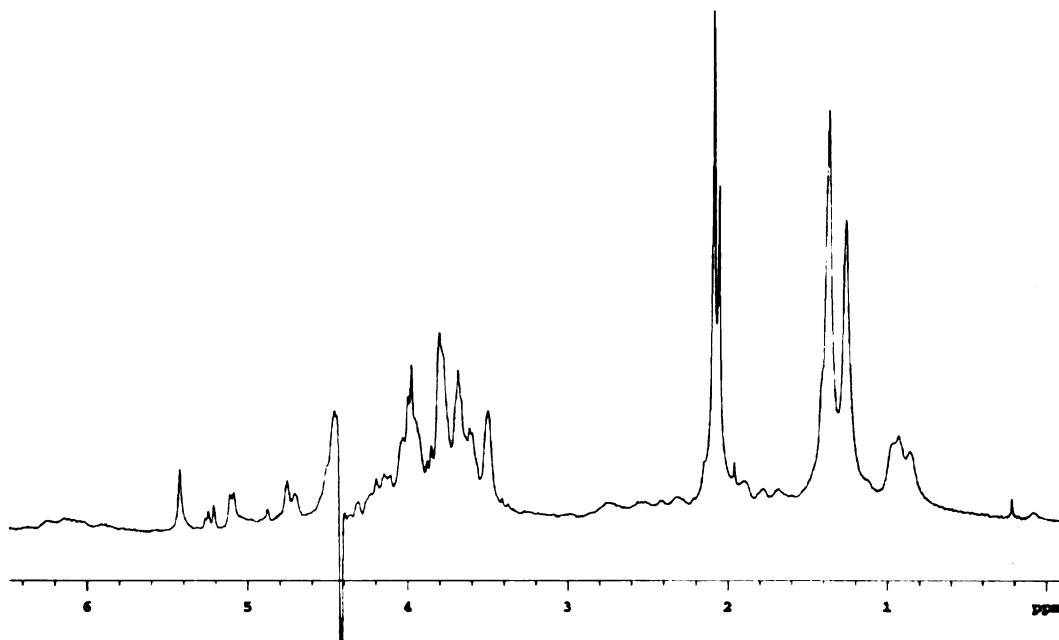


Figure 3.5. ¹H NMR spectrum of the extracellular polysaccharide. Signals characteristic of rhamnose include two singlets between 1.2 and 1.5 ppm that were assigned to the 6-deoxy groups and signals between 5.0 and 5.5 ppm that were assigned to the alpha linkages of rhamnose. The two singlets between 2.0 and 2.2 ppm correspond to N-acetyl groups of N-acetylglucosamine and the signals between 4.7 and 4.9 ppm correspond to beta linkages of N-acetylglucosamine. Signals between 3.4 and 4.3 ppm correspond to the remaining sugar protons. PPM, part per million.

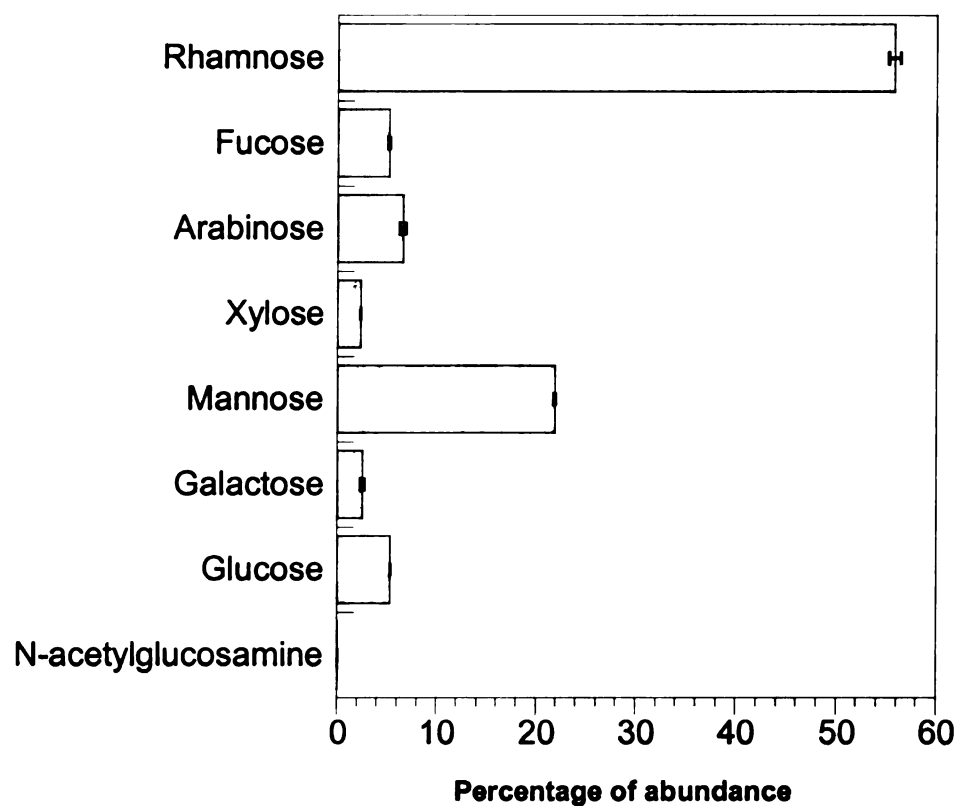


Figure 3.6. Composition of the EPS from the phenol plus TCE-fed reactor. Values represent averages \pm one standard deviation of triplicate injections.

Discussion

The majority of the studies that investigated the effects of TCE on cells have focused on cell viability, growth rates, toxicity and enzymatic activity and they suggest that TCE has detrimental effects on the cells that degrade it. However, studies in *Pseudomonas putida* suggest that TCE could induce its own degradation (Shingleton et al. 1998). This suggests that other responses might be induced by TCE. We observed an increase in the EPS content in the reactor that was exposed to TCE both by microscopy and solids fractionation (Figures 3.1-3.3, Table 3.1). EPS represented between 40-50 % of the TSS in the phenol plus TCE-fed reactor, while it represented between 8-12 % in the phenol fed reactor. Similar ranges in EPS values have been documented in activated sludge (10-15%) (Urbain et al. 1993) and biofilm reactors (40-80%) (Characklis and Cooksey 1983). Furthermore, Chang (1996) (Chang 1996) who evaluated the effects of increasing levels of TCE on the predecessors to these reactors, noted floc formation and persistence in a phenol plus TCE-fed reactor exposed to increasing amounts of TCE, but did not further study the observation. Together, these results suggest that TCE application could induce the formation of substantial amounts of EPS. Similar results were observed when *Pseudomonas aeruginosa* was exposed to ethanol (DeVault et al. 1990) or kanamycin (Drenkard and Ausubel 2002), since those compounds caused an increase in alginate production and the formation of biofilms. These authors propose that biofilm formation is the mechanism used by *Pseudomonas*

aeruginosa to reduce the diffusion of the antibiotics inside the cell, thus increasing its survival (Drenkard and Ausubel 2002).

Although there are several possible explanations for the accumulation of EPS in the TCE-fed reactor, a plausible one is that EPS is a protection mechanism against TCE or TCE induced toxicity. As has been proposed by various investigators, the toxicity of TCE or its metabolites are the major hurdles in aerobic TCE cometabolism (Alvarez-Cohen and McCarty 1991; Mars et al. 1996; Mars et al. 1998). The TCE epoxide, and some its derivatives are toxic to the TCE degraders and to other microbes (Alvarez-Cohen and McCarty 1991; Yeager et al. 2001). Thus, continuous exposure to TCE should favor microorganisms or communities with increased resistance to the toxic solvent. It is possible that EPS accumulation could be a mechanism to control toxicity by limiting the diffusion of the toxicant into the cells. Diffusion limitation by changes in membrane composition was the resistance mechanism observed in *Pseudomonas putida* DOT-T1 when exposed to high concentrations of toluene (Ramos et al. 1997). On the other hand, recent studies on toluene oxidizers suggest that EPS production could be a protective mechanism against the toxic effects of toluene (Putthividhya and Abriola 2002). Studies on *Flavobacterium* cells revealed that they transformed pentachlorophenol only when immobilized in polyurethane (O'Reilly and Crawford 1989). Furthermore, studies on a phenol degrading methanogenic consortium entrapped in agar beads revealed that immobilization resulted in a reduction in degradation rates, but increased resistance to phenol inhibition (Dwyer et al. 1986). It is possible that the EPS

produced by the microbial community causes the same effect that agar and polyurethane caused to immobilized cells; a reduction in the diffusion of inhibitory compound, TCE, inside the cells thereby limiting the toxic effects. If TCE does not penetrate the cell, the toxic metabolites will not be generated and TCE mediated toxicity will not occur. This type of protective mechanism could result in decreased phenol and TCE degradation rates, a phenomenon previously observed (Chapter 2) and that supports the proposed role of EPS. Additional research with pure cultures or simple communities is needed to determine if this hypothesis is correct and to rule out other alternatives such an opposite effect by retaining the toxic metabolites inside the cells.

The increase in EPS accumulation could have an effect on the structure of the microbial community. High amounts of EPS will reduce the diffusion of oxygen to inner layers, resulting in microaerobic or anaerobic conditions. Such conditions will foster the formation of anaerobic microbial communities in the interior of the flocs. For instance, sulfate reducing microorganisms have been observed in aerobic activated sludge systems suggesting that anaerobic areas within the flocs exist. Alternatively, facultative microorganisms such as denitrifiers could be enriched under anoxic conditions. Since ammonia oxidizers were present in these communities, nitrification is a feasible alternative (Chapter 5). Nevertheless, enrichment cultures for anaerobic microorganisms and the measurement of anaerobic intermediates are needed to determine if anaerobes or facultative microbes were present in the reactor communities.

Carbohydrate analysis of the EPS from the phenol plus TCE-fed reactor revealed that it was mainly composed of neutral sugars. Although we did not analyze the EPS for protein content it is likely that it is mainly carbohydrate because the only method that successfully extracted the EPS was solubilization with potassium hydroxide. This method is effective for the extraction of tightly bound EPS composed of neutral sugars, (Graber et al. 1988; Nielsen and Jahn 1999; Sutherland 2001; Liu and Fang 2002), although some proteins can be solubilized under these conditions.

The EPS was composed of rhamnose, mannose, glucose, galactose, arabinose, xylose and N-acetylglucosamine. These sugars are commonly found in the EPS of a variety of bacterial species and in anaerobic microbial communities (Veiner et al. 1995; Veiga et al. 1997). The most abundant carbohydrate was rhamnose representing 56 % of the carbohydrates identified. Rhamnose is a common component of the cell wall and capsule of many bacteria (Graber et al. 1988; Giraud and Naismith 2000). Studies in *Streptococcus mutans* and *Vibrio cholerae* revealed that mutations in some of rhamnose biosynthesis genes blocked the synthesis of cell wall polysaccharides and the cells were unable to colonize tissue and begin infections (Chiang and Mekalanos 1999; Yamashita et al. 1999). Furthermore, rhamnose is the third most abundant carbohydrate in methanogenic granules (Veiga et al. 1997). These observations suggest that rhamnose might be an important carbohydrate in aggregate and biofilm formation and could explain its high abundance in the EPS of the phenol plus TCE-fed reactor.

Marked differences in the spatial arrangement of bacteria in the two reactors were observed. While bacteria in the phenol-fed reactor formed cell aggregates with small amounts of EPS, the bacteria in the phenol plus TCE-fed reactor formed flocs with high amounts of EPS, and bacteria embedded along filaments that resembled a star form. Previous structural studies in aerobic biofilm communities revealed that biofilms are a discontinuous layer of bacteria with cell-free channel structures that allow the diffusion of oxygen and substrates (Lawrence et al. 1991; Massol-Deyá et al. 1995). If bacteria form a dense spherical structure, oxygen and substrates may be limiting in the inner layers. Thus, the formation of “star-like” aggregates could be a strategy that allows protection while maintaining some diffusion of oxygen and growth substrates to the inner layers of the filaments.

One of the most remarkable characteristics of bacteria is their ability to adapt to changes in their surrounding environment. In microbial communities, the adaptation process is far more complex and robust because of microbial interactions and metabolic diversity. In this study the long-term effect TCE application appears to be accumulation of EPS. This major shift in carbon flow is remarkable, and suggests that it might be beneficial. The reactor operated at lower but stable phenol and TCE degradation rates for two years, and hence it should be an ecologically successful adaptation.

References

Alvarez-Cohen, L. and P. L. McCarty. (1991). Product toxicity and cometabolic competitive-inhibition modeling of chloroform and trichloroethylene

- transformation by methanotrophic resting cells. *Appl. Environ. Microbiol.* **57**: 1031-1037.
- Bossier, P. and W. Verstrate.** (1996). Trigger for microbial aggregation in activated sludge. *Appl. Microbiol. Biotechnol.* **45**: 1-6.
- Cerantola, S., J. D. Bounery, C. Segonds, N. Marty and H. Montrozier.** (2000). Exopolysaccharide production by mucoid and non-mucoid strains of *Burkholderia cepacia*. *FEMS Microbiol. Lett.* **185**: 243-246.
- Chang, W.** (1996). Kinetics characterization of cometabolizing communities and adaptation to nongrowth substrate. Ph. D. dissertation. Michigan State University, East Lansing, MI.
- Characklis, W. G. and K. E. Cooksey.** (1983). Biofilms and microbial fouling. *Advances in Applied Microbiology* **29**: 93-138.
- Chiang, S. L. and J. J. Mekalanos.** (1999). *rfb* mutations in *Vibrio cholerae* do not affect surface production of toxin-coregulated pili but still inhibit intestinal colonization. *Infect. Immun.* **67**: 976-980.
- Costerton, J. W., P. S. Stewart and E. P. Greenberg.** (1999). Bacterial biofilms: a common cause of persistent infections. *Science* **284**: 1318-1322.
- Davey, M. E. and G. A. O'Toole.** (2000). Microbial biofilms: from ecology to molecular genetics. *Microb. Molec. Rev.* **64**: 847-867.
- De Vuyst, L., F. Vanderveken, S. Van de Ven and B. Degeest.** (1998). Production and isolation of exopolysaccharides from *Streptococcus thermophilus* grown in a milk medium and evidence for their growth-associated biosynthesis. *J. Appl. Microbiol.* **84**.
- Decho, A. W. and G. R. Lopez.** (1993). Exopolymer microenvironments of microbial flora: multiple and interactive effects on trophic relationships. *Limnol. Oceanogr.* **38**.
- Denner, E. B. M., S. Paukner, P. Kampfer, E. R. B. Moore, W. R. Abraham, H. J. Busse, G. Wanner and W. Lubitz.** (2001). *Sphingomonas pituitosa* sp nov., an exopolysaccharide-producing bacterium that secretes an unusual type of sphingan. *Int. J. Syst. Evol. Microbiol.* **51**: 827-841.
- DeVault, J. D., K. Kimbarra and A. M. Chakrabarty.** (1990). Pulmonary dehydration and infection in cystic fibrosis: evidence that ethanol activates alginate gene expression and induction of mucoidy in *Pseudomonas aeruginosa*. *Mol. Microbiol.* **4**: 737-745.

- Dignac, M. F., V. Urbain, D. Rybacki, A. Bruchet, D. Snidaro and P. Scribe.** (1998). Chemical description of extracellular polymers: implication on activated sludge floc structure. *Water Sci. Technol.* **38**: 45-53.
- Drenkard, E. and F. M. Ausubel.** (2002). *Pseudomonas* biofilm formation and antibiotic resistance are linked to phenotypic variation. *Nature* **416**: 740-743.
- Dwyer, D. F., M. L. Krumme, S. A. Boyd and J. M. Tiedje.** (1986). Kinetics of phenol biodegradation by an immobilized methanogenic consortium. *Appl. Environ. Microbiol.* **52**: 345-351.
- Flemming, H. C. and J. Wingender.** (2001). Relevance of microbial extracellular polymeric substances (EPSs). Part I: structural and ecological aspects. *Water Sci. Technol.* **43**: 1-8.
- Frolund, B., R. Palmgren, K. Keiding and P. H. Nielsen.** (1996). Extraction of extracellular polymers from activated sludge using a cation exchange resin. *Water Res.* **30**: 1749-1758.
- Gilber, P. and M. R. W. Brown.** (1995). Mechanisms of the protection of bacterial biofilms from antimicrobial agents. *In* Microbial biofilms. H. M. Lappin-Scott and J. W. Costerton. Cambridge, Cambridge University Press 118-130.
- Giraud, M. F. and J. H. Naismith.** (2000). The rhamnose pathway. *Curr. Opin. Struct. Biol.* **10**: 687-696.
- Graber, M., A. Morin, F. Duchiron and P. Monsan.** (1988). Microbial polysaccharides containing 6-deoxysugars. *Enzyme. Microb. Technol.* **10**: 198-206.
- Grobe, S., J. Wingender and H. G. Truper.** (1995). Characterization of mucoid *Pseudomonas Aeruginosa* strains isolated from technical water systems. *J. Appl. Bacteriol.* **79**: 94-102.
- Iwabuchi, N., M. Sunairi, H. Anzai, M. Nakajima and S. Harayama.** (2000). Relationships between colony morphotypes and oil tolerance in *Rhodococcus rhodochrous*. *Appl. Environ. Microbiol.* **66**: 5073-+.
- Kachlany, S. C., S. B. Levery, J. S. Kim, B. L. Reuhs, L. W. Lion and W. C. Ghiorse.** (2001). Structure and carbohydrate analysis of the exopolysaccharide capsule of *Pseudomonas putida* G7. *Environ. Microbiol.* **3**: 774-784.
- Kim, D. S., S. Thomas and H. S. Fogler.** (2000). Effects of pH and trace minerals on long-term starvation of *Leuconostoc mesenteroides*. *Appl. Environ. Microbiol.* **66**: 976-981.

- Lawrence, J. R., D. R. Korber, B. D. Hoyle, J. W. Costerton and D. E. Caldwell.** (1991). Optical sectioning of microbial biofilms. *J. Bacteriol.* **173**: 6558-6567.
- Lewis, D. L. and D. K. Gattie.** (1990). Effects of cellular aggregation on the ecology of microorganisms. *ASM news* **56**: 263-268.
- Li, D., H. and J. J. Ganzarczyk.** (1990). Structure of activated sludge flocs. *Biotechnol. Bioeng.* **35**: 57-56.
- Liao, B. Q., D. G. Allen, I. G. Droppo, G. G. Leppard and S. N. Liss.** (2001). Surface properties of sludge and their role in bioflocculation and settleability. *Water Res.* **35**: 339-350.
- Liu, H. and H. H. P. Fang.** (2002). Extraction of extracellular polymeric substances (EPS) of sludges. *J. Biotech.* **95**: 249-256.
- Mars, A. E., J. Houwing, J. Dolfing and D. B. Janssen.** (1996). Degradation of toluene and trichloroethylene by *Burkholderia cepacia* G4 in growth-limited fed-batch culture. *Appl. Environ. Microbiol.* **62**: 886-891.
- Mars, A. E., G. T. Prins, P. Wietzes, W. De Koning and D. B. Janssen.** (1998). Effect of trichloroethylene on the competitive behavior of toluene-degrading bacteria. *Appl. Environ. Microbiol.* **64**: 208-215.
- Massol-Deyá, A. A., J. Whallon, R. F. Hickey and J. M. Tiedje.** (1995). Channel structures in aerobic biofilms of fixed-film reactors treating contaminated groundwater. *Appl. Environ. Microbiol.* **61**: 769-777.
- Neu, T. R.** (1996). Significance of bacterial surface-active compounds in interaction of bacteria with interfaces. *Microb. Rev.* **60**.
- Nielsen, P. H., B. Frolund and K. Keiding.** (1996). Changes in the composition of extracellular polymeric substances in activated sludge during anaerobic storage. *Appl. Microbiol. Biotechnol.* **44**: 823-830.
- Nielsen, P. H. and A. Jahn.** (1999). Extraction of EPS. *In* Microbial extracellular polymeric substances: characterization, structure and function. J. Wingender, T. R. Neu and H. C. Flemming. Berlin, Springer-Verlag 49-72.
- O'Reilly, K. T. and R. L. Crawford.** (1989). Degradation of pentachlorophenol by polyurethane immobilized *Flavobacterium* cells. *Appl. Environ. Microbiol.* **55**: 2113-3118.
- Putthividhya, A. and L. M. Abriola.** (2002). Effects of substrate history on EPS production by toluene oxidizing bacteria. Abstract. International symposium on subsurface microbiology, Copenhagen, Denmark.

- Ramos, J. L., E. Duque, J. J. Rodríguez-Herva, P. Godoy, A. Haïdours, F. Reyes and A. Fernández-Barrero.** (1997). Mechanisms for solvent tolerance in bacteria. *J. Biol. Chem.* **272**: 3887-3890.
- Shingleton, J. T., B. M. Applegate, A. C. Nagel, P. R. Bienkowski and G. S. Saylor.** (1998). Induction of the *tod* operon by trichloroethylene in *Pseudomonas putida* TVA8. *Appl. Environ. Microbiol.* **64**: 5049-5052.
- Sponza, D. T.** (2002). Extracellular polymer substances and physicochemical properties of flocs in steady- and unsteady-state activated sludge systems. *Process Biochem.* **37**: 983-998.
- Stehr, G., S. Zorner, B. Bottcher and H. P. Koops.** (1995). Exopolymers - an ecological characteristic of a floc-attached, ammonia-oxidizing bacterium. *Microb. Ecol.* **30**: 115-126.
- Sutherland, I. W.** (2001). Exopolysaccharides in biofilms, flocs and related structures. *Water Sci. Technol.* **43**: 77-86.
- Urbain, V., J. C. Block and J. Manem.** (1993). Biofloculation in activated sludge: an analytical approach. *Water Res.* **27**: 829-838.
- Veiga, M. C., M. K. Jain, W.-M. Wu, R. I. Hollingsworth and J. G. Zeikus.** (1997). Composition and role of extracellular polymers in methanogenic granules. *Appl. Environ. Microbiol.* **62**: 403-407.
- Veiner, R., S. Langille and E. Quintero.** (1995). Structure, function and immunochemistry of bacterial exopolysaccharides. *J. Indust. Microb.* **15**: 339-346.
- Wang, Y. and R. I. Hollingsworth.** (1994). The structure of the O-antigenic chain of the lipopolysaccharide of *Rhizobium trifolii* 4s. *Carbohydr. Res.* **260**: 305-317.
- Watnick, P. and R. Kolter.** (2000). Biofilm, city of microbes. *J. Bacteriol.* **182**: 2675-2679.
- Wingender, J., T. R. Neu and H. C. Flemming.** (1999). What are bacterial extracellular polymeric substances. *In* Microbial extracellular polymeric substances: characterization, structure and function. J. Wingender, T. R. Neu and H. C. Flemming. Berlin, Springer-Verlag 1-19.
- Yamashita, Y., K. Tomihisa, Y. Nakano, Y. Shimazaki, T. Oho and T. Koga.** (1999). Recombination between *gtfB* and *gtfC* is required for survival of a dTDP-rhamnose synthesis-deficient mutant of *Streptococcus mutans* in the presence of sucrose. *Infect. Immun.* **67**: 3693-3697.

Yeager, C. M., P. J. Bottomley and D. J. Arp. (2001). Cytotoxicity associated with trichloroethylene oxidation in *Burholderia cepacia* G4. Appl. Environ. Microbiol. 67: 2107-2115.

CHAPTER 4

CHARACTERIZATION OF THE CULTIVABLE MEMBERS FROM PHENOL AND PHENOL PLUS TRICHLOROETHENE-FED REACTOR COMMUNITIES, AND THEIR DENSITIES OVER 2 YEARS OF REACTOR OPERATION.

Introduction

The functional dissection of microbial communities has been a major challenge for microbial ecologists. Assignment of functions to different microbial groups, and their enumeration are necessary steps to understand and predict the effects of perturbations on community function and stability. From an applied perspective this knowledge will help improve the design and operation of biological waste treatment processes. Surveys by 16S rDNA cloning and sequencing have revealed that communities in nature are very diverse, and that the microbes in culture represent a minor fraction of the microbial world (Hugenholtz et al. 1998). In many ecosystems the so called “non-cultivable microorganisms” are numerically abundant and thought to be important and perhaps necessary for community function. Isolation and physiological characterization of microorganisms remains the main means to understand their role in microbial communities. For instance, 16S rDNA analysis of aerobic sludge revealed that wastewater communities are very diverse, but allowed only limited inferences about the possible roles of some of the community members (Bond et al. 1995; Bond et al. 1999; Juretschko et al. 2002). Physiological

analyses of pure cultures, in combination with perturbation experiments, can aid in determining the function of the different microbes in the community.

Trichlorethene (TCE) is an industrial chlorinated solvent that, due to inappropriate management and disposal, is a frequent contaminant in soil and groundwater (ATSDR 1994). Aromatic compounds such as phenol and toluene have been successfully used to stimulate the degradation of TCE, since aromatic oxygenases fortuitously oxidize TCE in a process known as cometabolism (Nelson et al. 1987; Wackett and Gibson 1988; Hopkins et al. 1993a). The cometabolism of TCE produces an unstable epoxide that yields non-toxic products such as formate and glyoxylate (Li and Wackett 1992; Newman and Wackett 1997b). Although the epoxide lasts ~ 20 sec inside the cell, some of it reacts with the catalytic enzyme and DNA reducing degradation rates or killing the TCE degraders. Based on these results, several investigators suggest that field stimulation of TCE degradation by aromatic compounds would eventually result in a takeover of the community by TCE inactive populations that metabolize the primary substrate only (Mars et al. 1996; Fries et al. 1997a; Mars et al. 1998). On the other hand, toxicity studies on a derivative of *Ralstonia eutropha* JMP 134 revealed that this microorganism can resist high doses of TCE without a decrease in activity, suggesting that adaptations to TCE toxicity exist in nature (Ayoubi and Harker 1998).

Studies in a field site where phenol and toluene were used to stimulate TCE cometabolism, and on phenol-fed reactors suggest that the microbial communities of these two ecosystems are diverse, and the dominant members

of the community can be recovered in culture (Fries et al. 1997b; Watanabe et al. 1998). The purpose of this work was to isolate, characterize and enumerate the cultivable members of two sequencing batch reactors (SBR), one fed phenol and the other fed phenol and TCE, for more than 2 years. Although communities that degrade phenol and cometabolize TCE have been studied previously, the SBR system used in this study has been exposed to a TCE dose 10 times higher than previous studies (Hopkins et al. 1993a; Hopkins et al. 1993b; Fries et al. 1997b) and has established low but stable degradation rates (Chapter 2). Therefore, the effects of long-term TCE application on the abundance of TCE degraders can be determined. The objectives of this work were: (i) to determine the cultivable diversity present in these reactor communities; (ii) elucidate if the isolates degrade phenol and TCE, and the diversity of the phenol hydroxylases among them; and (iii) determine the abundance of selected TCE active and inactive populations over the 2 years of exposure.

Materials and Methods

Pure culture isolation and characterization

Reactor samples (10 ml) were aseptically collected from each reactor at day 340 of operation. Samples were vortexed for 1 min, homogenized by passing the sample through a syringe with a gauge 30 needle, before being serially diluted using sterile mineral medium (described in Chapter 2). An aliquot from each dilution was plated on R2A agar (Difco, Detroit, Mich.) and the plates were incubated for 3 weeks at 25° C. Colonies representing the different

morphologies on the plates were selected and further purified by repetitive streaking on fresh medium. Additionally, enrichments for ammonia oxidizers were established from samples taken after 900 days of operation using mineral medium with 0.01 % phenol red as an indicator (Chapter 2). The motivation to attempt to isolate this group of bacteria was the observation of structures that resembled ammonia oxidizing bacteria from transmission electron micrographs of the community (data not shown). Enrichments were transferred several times until pure cultures were obtained by direct plating on mineral medium with 0.01 % phenol red, and 15 % w/v agar. Genomic fingerprints from each isolate were generated using BOX-PCR as described previously (Rademaker et al. 1998), and were analyzed using GelCompar 4.5 (Applied Maths, Kortrijk, Belgium). Isolates with identical fingerprints were considered the same strain, and one representative was kept for further analysis.

The isolates were tested for phenol degradation by inoculating single colonies into 20 ml vials containing a mix of mineral medium and phenol at 50 and 10 mg/l; and at 10 mg/l with 1X Wolin Vitamins (Wolin et al. 1963). Vials were sealed with Teflon caps and aluminum crimp seals before being incubated for 2 weeks at 25° C on a rotary shaker. An aliquot (1 ml) was removed from each vial to measure the remaining phenol concentration by HPLC with a Hibar RP-18 column at a flow rate of 1.5 ml/min, an eluent of water-acetonitrile-phosphoric acid (66:33:0.1), and a UV detector set to 218 nm. Isolates that removed more than 15% of the initial phenol concentration were considered phenol degraders and tested for TCE degradation. The 15% cutoff was

determined based on abiotic losses of phenol from vials without cells or with killed cells. For TCE degradation tests single colonies were inoculated in phenol medium at the appropriate concentration, and the vials were amended with TCE to a final concentration of 1 mg/l. Vials were sealed and incubated as described above. The amount of TCE removed was quantified by gas chromatography (GC) as described previously (Chapter 2).

DNA isolation and purification

One colony from each isolate was inoculated in 5 ml of 0.20X nutrient broth (Difco) and was incubated at 30° C until sufficient turbidity was observed. The cell pellet used for DNA extraction was obtained by centrifugation of a 2 ml aliquot at 12,000 x g, followed by supernatant removal. Nucleic acids were extracted using freeze-thaw cycles, enzymatic digestions and phenol chloroform purification as described previously (Chapter 2), and were stored at -20° C until use.

16S rDNA and phenol hydroxylase sequencing, and phylogenetic analyses.

The 16S rDNA gene from each isolate was amplified with primers 8F (5'-AGAGTTTGATCMTGGCTCAG-3' where M stands for A or C) (Giovannoni 1991), and 1522R (5'-ACGGGCGGTGTGTACA-3') (Amman et al. 1995) using the same reaction conditions and cycles described previously (Chapter 2). The amplicon was checked for purity by separation in a 1 % agarose gel followed by primer and nucleotide removal using a Qiaquick PCR purification kit (Qiagen,

Chatsworth, Calif.). Partial 16S rDNA sequences were obtained using the dye terminator method at the Michigan State University DNA sequencing facility using primers 8F and 787R (5'-TACCAGGGTATCTAAT-3'), modified from a previously published primer (Amman et al. 1995). For selected isolates, nearly complete 16S rDNA sequences were obtained by additional sequencing using primers 1522R and 533F (5'-CAGCAGCCGCGGTAA-3') (Rhodes et al. 1998).

Consensus 16S rDNA sequences generated from the assembly of different sequence reads, were aligned against the most similar sequences in the Ribosomal Database Project II (RDP-II) release 8.0 database (Maidak et al. 2001), using the fast align procedure of the ARB software package (Strunk and Ludwig 1995). Sequences were also compared against the GenBank database from the National Center for Biotechnology Information (NCBI) using the Basic Local Alignment Search Tool (BLAST) (Altschul et al. 1990). Sequences with high similarity scores that were not present in the RDP-II database were retrieved, aligned as described above, and included in the phylogeny. Alignments were corrected manually by taking into account primary and secondary structure considerations, and ambiguously aligned regions were removed from the analysis. Phylogenetic trees were generated using maximum likelihood with the fastDNAmI program (Olsen et al. 1994). Bootstrap values were generated from 100 replicate trees. Sequence similarities were calculated using the ARB software package.

The isolates were screened for phenol hydroxylase genes using PCR primers that target conserved regions of the alpha subunit of the multicomponent

phenol hydroxylase gene family (Futamata et al. 2001). All amplifications were carried out as described previously (Futamata et al. 2001) in a GeneAmp 9600 thermal cycler (Perking Elmer Biosystems, Norwalk, CT). Isolates that generated a band of the correct size were sequenced as described above with the modification that the PCR products were gel purified with a QIAquick gel extraction kit (Qiagen, Chatsworth, Calif.). The consensus nucleotide sequences were translated to amino acids using the program BioEdit (Hall 1999), and were aligned against all the phenol hydroxylase sequences available in the GenBank database using the alignment program CLUSTALX (Thompson et al. 1997). Alignments were corrected manually and unambiguously aligned positions were used for the analysis. Phylogenetic trees were constructed using protein maximum likelihood with the program PROTML from the Phylogeny inference package (PHYLP) version 3.6a (J. Felsenstein, Department of Genetics, University of Washington, Seattle). Bootstrap values were generated from 100 replicate trees using SEQBOOT, while sequence identities were calculated using PROTDIST, both from the PHYLP package.

***In-silico* generation of terminal restriction fragments and community comparisons**

The 16S rDNA sequences from each isolate were used to generate *in-silico* terminal restriction restriction fragments (T-RFs) for two enzymes, *CfoI* and *HaeIII*. These computer generated T-RFs were compared against the T-RFLPs previously generated from the reactor samples (Chapter 2) to determine what fraction of the community could be accounted for by the isolates. Isolate T-RFs

that were within 3 bp from any T-RF in the community, were considered a match to the community.

SYBR green quantitative PCR

The abundance of selected isolates was quantified using the real-time PCR method based on the SYBR green I chemistry (Rantakokko-Jalava and Jalava 2001; Collantes-Fernández et al. 2002; De Preter et al. 2002; Dhar et al. 2002). The method monitors the increase in fluorescence of the DNA binding dye SYBR green I during the PCR cycles, as a measurement of the PCR product generated. The cycle number when the fluorescence crosses a threshold (C_T), calculated using a reference dye, is proportional to the initial amount of template (Grüntzig et al. 2001). This method allows the quantitation of the product in the linear range of the PCR reaction, thus avoiding the problems of terminal cycle quantitation.

Primers specific for the 16S rDNA of each isolate were initially designed using the probe design function of the ARB software package and visual comparisons against aligned sequences (Table 4.1). The primers were tested using the Primer Express software package (Perkin Elmer Applied Biosystems, Foster City, CA) to determine if they follow the annealing temperatures, distances between primers and GC contents suggested by the manufacturer. All the primers were aligned against all the sequences of the isolates using the CLUSTALX program to determine their specificity *in-silico* and the distribution and number of mismatches against all the sequences. Primers with more than

five mismatches against all isolate sequences, and with mismatches close to the 3' end of the primer were selected for further testing. The primers were also tested for specificity against the GenBank database using BLAST searches, and using the check probe function of the RDP-II (Maidak et al. 2001). To determine if the primers were specific in the presence of non-target DNA, mixtures containing 2.0 ng of different non-target DNAs were prepared and added to individual PCR reactions. Each mixture consisted of DNA from all the phylogenetically similar isolates. To improve the specificity of the primers different magnesium chloride concentrations were tested until non-specific products were not detected. The reaction mixture, prepared using the SYBR green core reagent kit (Perking Elmer Applied Biosystems), consisted of 1X SYBR green PCR buffer, 0.2 mM dNTPs (1:1:1:1 mix), 0.005 U/ μ l AmpErase UNG, 0.1 U/ μ l Amplitaq gold Taq polymerase and 150 nM of each primer in a total volume of 30 μ l. All reactions were carried out in a 7700 Sequence Detector (Perking Elmer Applied Biosystems), with the cycling conditions recommended by the manufacturer.

Calibration curves based on total cells were constructed to correct for differences in 16S rDNA operon copy number in different microorganisms. Cells from early to mid exponential phase cultures were harvested and serially diluted in both phosphate buffered saline and 0.05 N NaOH. The PBS dilutions were plated on R2A agar to determine total cell counts, while dilutions in NaOH were lysed for 20 min at 99° C in a thermal cycler (model 9600, Perking Elmer Applied Biosystems), and kept on ice until use. Duplicate PCR reactions were prepared

from each cell dilution lysate, and calibration curves were generated using the viable counts. The abundance of each isolate during the 2 years of reactor operation was determined from previously extracted community DNA (Chapter 2) by preparing duplicate PCR reactions for two different concentrations (20 and 2 ng) of community DNA. Means and standard deviation for each sample were determined after conversion of C_T values to cell values using the appropriate calibration curves.

An estimate of the total bacterial abundance of each sample was determined with the same procedure described above, but using bacterial primers 1108F (5'-ATGGYTGTCGTCAGCTCGTG-3') (Amman et al. 1995) and 1123R-b (5'-GGGTTGCGCTCGTTGC-3') (Wilmotte et al. 1993), and PCR conditions described previously (Riley-Buckley 2001). *Pseudomonas stutzeri* JM300 was used for the standard curve.

The reproducibility of the SYBR green methodology was tested by quantifying the abundance of a reactor isolate and total bacteria on replicate samples from each reactor. Duplicate PCR reactions were prepared from DNA from each of eight independent samples from each reactor obtained previously (Chapter 2).

Table 4.1. Primers and magnesium chloride concentrations used for SYBR green quantitative PCR of selected isolates. β proteo, beta *Proteobacteria*.

Target organisms	Genera	Primer name	Primer sequence (5'-3')	MgCl ₂ concentration (mM)
SBR-P10, T15	Unidentified β proteo	166F	GGCCTCACGCGTTTGAG	1.9
		434R	TGAGCTCCCTGTATTAGAGAG	
SBR-P16, T10	<i>Sphingomonas</i> sp.	562F	AAGACTGCATCGTCGAATC	1.5
		685R	ACCTCAGCGTCAATACCGGT	
SBR-T23	<i>Phenylobacterium</i> sp.	472F	CGCGTAGGCGGACAGTTTAGT	1.8
		552R	ACCTCTCCGAACTCAAGACAG	
SBR-T9	<i>Pseudomonas</i> sp.	539F	GCGTAGGTGGTTTGGTAAGATG	1.8
		620R	CGTACTCTAGTCAGGCAGTTATGG	
SBR-T14, P1	<i>Microbacterium</i> sp.	71F	CGAGCTTGCTCTGTGGGAT	2
		195R	CAGACCATGCGATCACGTCA	
SBR-P24, T26	<i>Nitrosomonas</i> sp.	428F	AGCTATGATTTATGACGGTACCGAC	1.5
		713R	GTCAGTGTCACCCAGGAGCT	
SBR-T7, P21	<i>Acinetobacter</i> sp.	179F	TGCGCTAAATGATGAGCCTAAG	2
		426R	GTA CTAGTAGCCTCCTCCTCGCTT	
SBR-P13	<i>Flexibacter</i> sp.	144F	AAAGATTTATCACCTTGAGATGGCTGT	2
		408F	TTGACCTAGAAAGGCCCTTTT	
SBR-T20	Unidentified β proteo	62F	GGTAACAGGTCTTCGGATGCT	1.8
		486R	CTTATTCCTACGGTACCGTCATGATC	
SBR-T4	<i>Variovorax</i> sp.	423F	ACGGAACGAAACGGCCTTT	1.8
		635R	TCCAGCAATGCAGTCACAGATG	
SBR-T2	<i>Burkholderia</i> sp.	425F	CGGAAAGAAATCCTTGGCTCTAAT	2
		649R	CCCTCTGCCATACTCTAGCCTG	
SBR-T1, P22	<i>Rhizobium</i> sp.	58F	GCATCCCTTCGGGGTGAGT	1.5
		157R	GGCACATACGGTATTAGCACACG	
SBR-T16	<i>Bacillus</i> sp.	155F	GGTGGCTTTTGCTACCACTTACA	1.5
		424R	CGCCCTATTTGAATGTCG	

Results

Strain isolation and identification.

A total of 73 isolates was obtained from both reactors by direct plating on R2A medium. Fifty isolates with different BOX-PCR fingerprints were retained; 24 came from the phenol-fed reactor (SBR-P) and 26 from the phenol plus TCE-fed reactor (SBR-T). To determine if these isolates matched any of the T-RFLP fragments generated previously (Chapter 2), the T-RFs of each isolate generated *in-silico* from 16S rDNA sequences with *Hae*III and *Cfo*I restriction enzymes were compared against the community T-RFLPs. All the isolates matched the community T-RFs with at least one restriction enzyme, and the majority matched with two (Table 4.2). Analysis of the collection with *Hae*III restriction enzyme yielded five isolates that did not match any peak in the community database, while *Cfo*I yielded nine isolates that did not match any community peak. Interestingly, eight isolates had a *Cfo*I T-RF that matched a 66 bp community fragment while another seven matched a 206 bp fragment. These T-RFs were among the most abundant T-RFs in the community T-RFLPs at different times (Chapter 2).

Comparisons between the T-RFs of the isolates and the community at the sampling day revealed that the isolates represent at least 37 % of all the peaks in the community (Table 4.3). The isolates from the phenol-fed reactor represented 47 and 37 % of all the peaks generated with *Hae*III and *Cfo*I respectively. In the phenol plus TCE-fed reactor the isolates' T-RFs represented 43 % of all the peaks on the sampling day for the two restriction enzymes.

Table 4.2. Assignment of isolate T-RFs to community T-RFLPs. Isolate names in bold, indicate strains that T-RFs from both enzymes matched a community T-RF. NR, no restriction site. NM, no match with community T-RFLPs using a ± 3 bp window.

Isolate name	T-RF <i>Haelll</i>	Match with Community	T-RF <i>Cfol</i>	Match with Community
SBR-P1	229	228	144	142
SBR-P2	193	194	341	NM
SBR-P3	225	225	61	60
SBR-P4	230	228	581	580
SBR-P5	193	194	341	NM
SBR-P6	245	NM	84	NM
SBR-P7	243	NM	64	63
SBR-P8	199	199	66	66
SBR-P9	229	228	143	142
SBR-P10	198	199	66	66
SBR-P11	39	38	176	176
SBR-P12	67	66	441	444
SBR-P13	328	330	NR	NM
SBR-P14	199	199	206	206
SBR-P15	293	291	81	NM
SBR-P16	295	296	81	NM
SBR-P17	190	189	60	60
SBR-P18	309	307	240	237
SBR-P19	165	166	580	580
SBR-P20	39	38	176	176
SBR-P21	252	255	206	206
SBR-P22	192	194	340	NM
SBR-P23	201	199	66	66
SBR-P24	78	77	207	206
SBR-T1	192	194	340	NM
SBR-T2	203	205	208	206
SBR-T3	192	194	342	345
SBR-T4	218	218	66	66
SBR-T5	260	258	214	215
SBR-T6	200	199	65	66
SBR-T7	254	255	208	206
SBR-T8	219	218	229	232
SBR-T9	39	38	206	206
SBR-T10	293	291	83	NM
SBR-T11	68	66	58	58
SBR-T12	199	199	68	66
SBR-T13	226	225	342	345
SBR-T14	233	235	148	147
SBR-T15	199	199	68	66
SBR-T16	310	308	239	237
SBR-T17	39	38	176	176
SBR-T18	194	194	345	345
SBR-T19	225	225	62	62
SBR-T20	218	218	204	204
SBR-T21	182	NM	146	147
SBR-T22	312	NM	581	580
SBR-T23	38	38	60	60
SBR-T24	244	NM	84	NM
SBR-T25	201	199	68	66
SBR-T26	77	77	207	206

Moreover, the isolates' T-RFs were compared against the total number of peaks detected during the 800 days of operation, and the phenol-fed reactor isolates represented only 32 and 16 % of the *Haelll* and *Cfol* community T-RFs respectively, while the phenol plus TCE-fed reactor isolates represented 30 and 24 % of the T-RFs for the same enzymes. Analyses of the T-RFs from the two collections revealed that all the isolates obtained represented 60 and 47 % of all the *Haelll* and *Cfol* fragments for the sampling day while they represented 41 and 27 % of peaks observed for all the days. These results indicate that the sampling day was a factor determining the success of isolation approaches in recovering the diversity in the community, but that isolates like many of these strains were present throughout the sampling period.

Collection	<i>n</i>	% of <i>Haelll</i> TRFs that match the community		% of <i>Cfol</i> TRFs that match the community	
		Sampling day	All days	Sampling day	All days
Phenol-fed reactor	24	47	32	37	16
Phenol plus TCE-fed reactor	26	43	30	43	24
All isolates	50	60	41	47	27

Table 4.3. Percentages of community T-RFs that matched the isolates T-RFs. *n*, number of isolates.

Phylogeny of the isolated populations

The phylogenetic placement of all the isolates was performed by partial sequencing of the 16S rDNA and phylogenetic analysis. Sequence similarities among all the isolates revealed that nine different isolates from the phenol-fed reactor had isolates with identical sequences in the phenol plus TCE-fed reactor.

For phylogenetic analysis, the isolates were grouped in the following bacterial phyla and classes according to the taxonomic outline of the Bergey's Manual of Systematic Bacteriology (Garrrity et al. 2001): *Proteobacteria* (alpha, beta and gamma classes), *Deinococcus-Thermus*, *Firmicutes* (Low G+C gram positives), *Actinobacteria* (High G+C gram positives) and *Bacteroidetes*. Assignment of the isolates to operational taxonomic units (OTUs) using a 97 % similarity cutoff (Stackebrandt and Goebel 1994; Juretschko et al. 2002) resulted in 32 different OTUs. The predominant phylum was the *Proteobacteria* representing 60 % of all the OTUs from the two reactors, followed by *Actinobacteria* (15 %), *Firmicutes* (13 %), *Bacteroidetes* (9 %) and *Deinococcus-Thermus* (4 %) (Figure 4.1). Within the *Proteobacteria*, the beta class (β -*Proteobacteria*) was the most dominant with 25 % of all the isolates, followed by the alpha (α -*Proteobacteria*) and gamma (γ -*Proteobacteria*) classes with 22 and 13 % respectively.

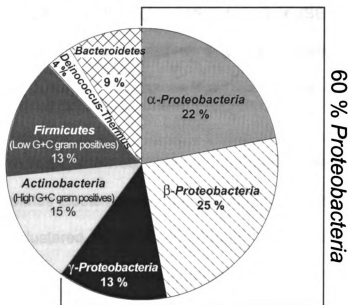


Figure 4.1. OTU composition of the isolate collection from the two reactors. An OTU was defined as one or more sequences with more than 97 % sequence similarity.

Thirteen isolates belonged to the α -*Proteobacteria* class, and were distributed among six different genera (Figure 4.2). Two of the isolates (SBR-P5, T3) clustered with *Afipia* genosp 7, a human pathogen previously isolated from hospital water supplies (La Scola et al. 2000). Isolates SBR-P2, T18 clustered with *Bosea thiooxidans*, a group of heterotrophic organisms that could oxidize thiosulfate to sulfate (Stubner et al. 1998). One isolate clustered with *Phenylobacterium immobile* (SBR-T23), a member of a group with an extremely limited nutritional spectrum, that degrades the poly-aromatic herbicide chloridazon (Eberspacher 2002). The bacterial family with the highest representation within the α -*Proteobacteria* class was the *Rhizobiaceae* with five isolates. One isolate clustered with *Rhizobium giardinii* (SBR-T13), two clustered with *Mesorhizobium* (SBR-P3, T19) and two more isolates had no specific affiliation based on the bootstrap values (SBR-T1, P22). Finally, three of the isolates clustered within the *Sphingomonas* genus (SBR-T10, P16 and P15), in which some of the representatives degrade aromatic pollutants and generate extracellular polymeric substances (Fredrickson et al. 1998; Denner et al. 2001).

A total of 12 isolates clustered within the β -*Proteobacteria* class (Figure 4.3). Two of the isolates clustered with *Nitrosomonas eutropha* str. C-9 (SBR-P24, T26), and one clustered within the *Burkholderia* family (SBR-T2), a group of microbes with some members known to degrade aromatic compounds and TCE (Folsom et al. 1990). The remaining isolates appear to belong to the metabolically diverse *Comamonadaceae* family, with the exception of one isolate

that clustered with the *Variovorax paradoxus* group (SBR-T4); their specific identities could not be resolved.

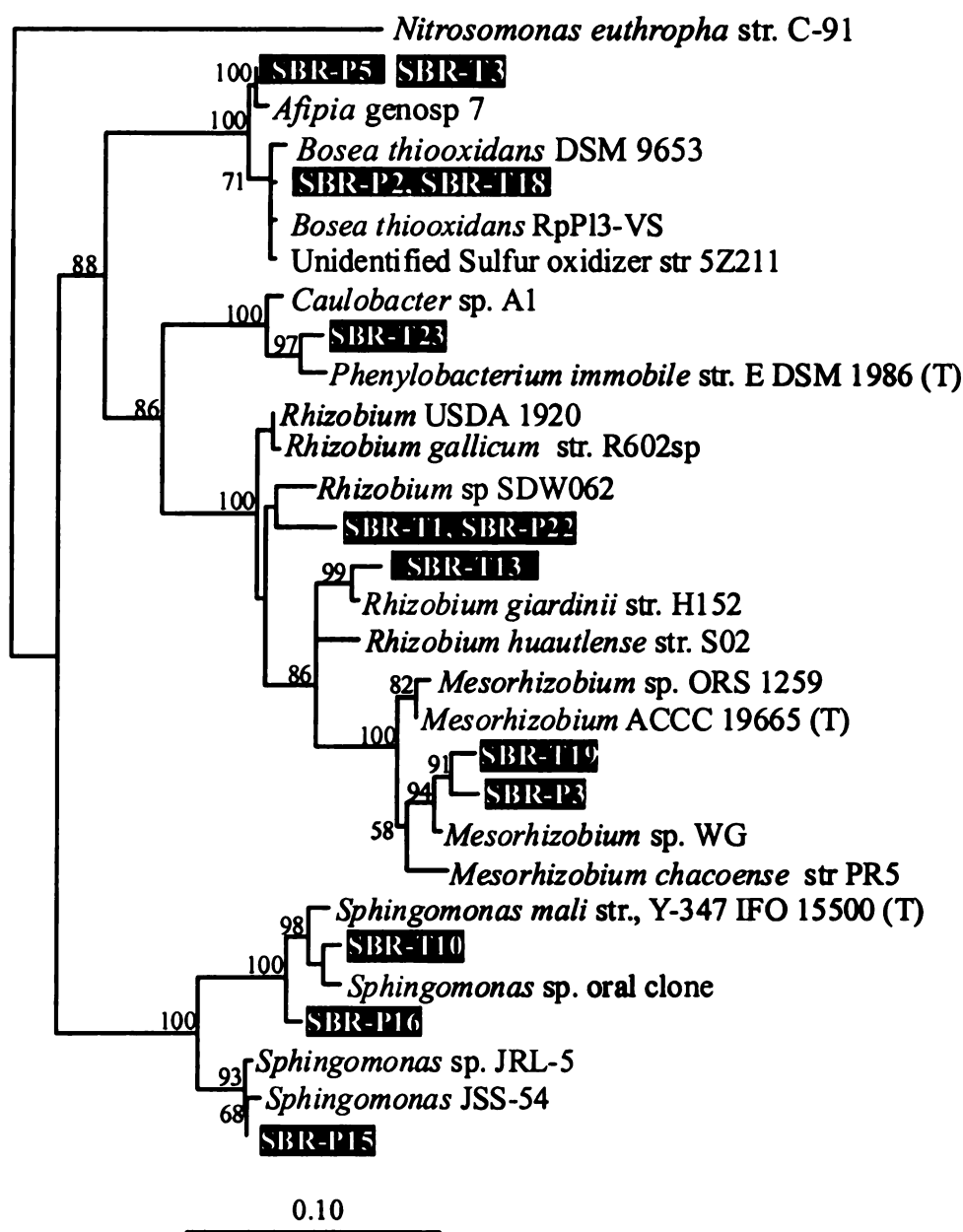


Figure 4.2. Phylogenetic tree of 16S rDNA sequences of isolates that belonged to the α -Proteobacteria class. The tree was constructed from 605 unambiguously aligned positions using the maximum-likelihood method, and was rooted using *Nitrosomonas eutropha*. Numbers at nodes represent the percentage of 100 bootstraps. The nodes without bootstraps values represent either nodes with bootstrap values below 50 %, or inconsistent branch order when compared against the consensus tree. The scale bar represents the number of substitutions per nucleotide position. T, type strain.

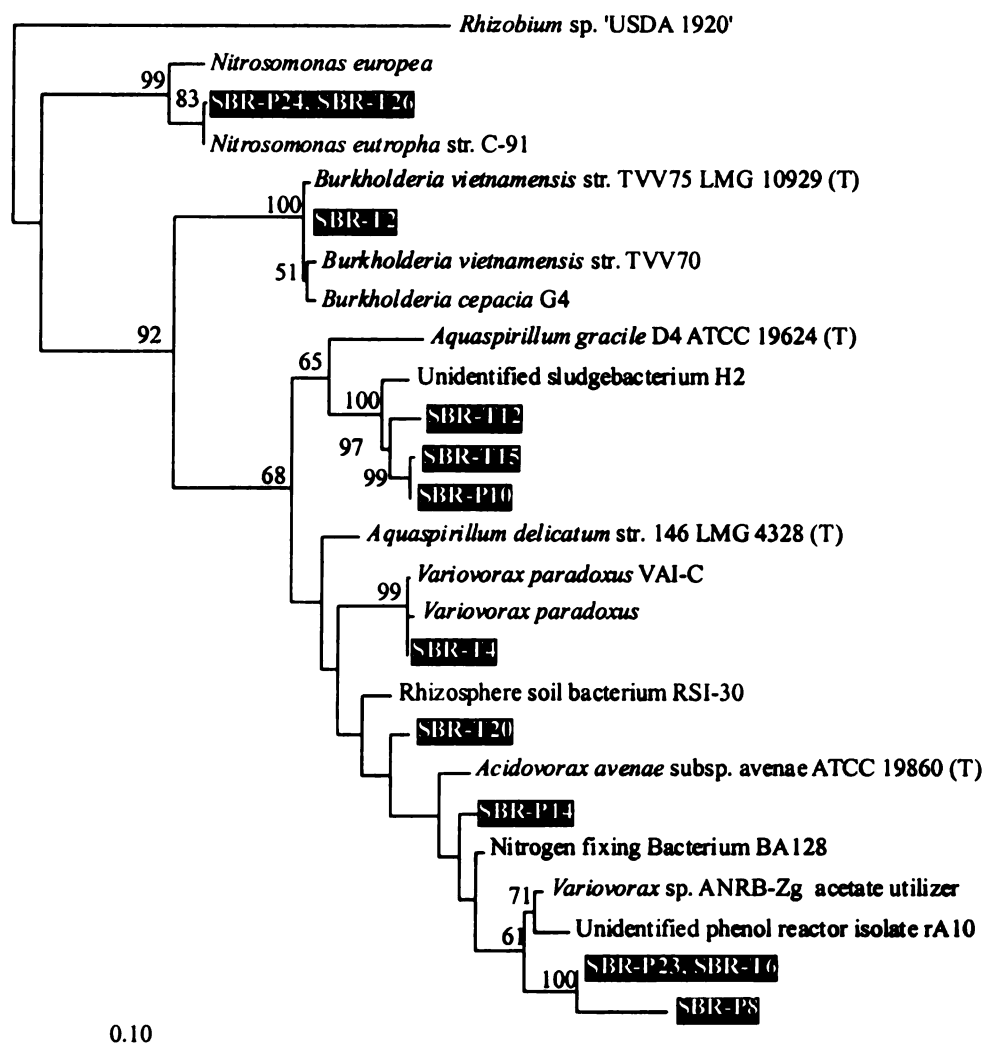


Figure 4.3. Phylogenetic tree of 16S rDNA sequences of isolates that belonged to the β -Proteobacteria class. The tree was constructed from 677 unambiguously aligned positions using the maximum-likelihood method, and was rooted using *Rhizobium* sp. Numbers at nodes represent the percentage of 100 bootstraps. The nodes without bootstraps values represent either nodes with bootstrap values below 50 %, or inconsistent branch order when compared against the consensus tree. The scale bar represents the number of substitutions per nucleotide position. T, type strain.

Isolates SBR-T12, T15 and P10 clustered with an uncultured sludge bacterium and *Aquaspirillum gracile*, while isolates SBR-T20 and P14 were nested within other sequences without forming a cluster. Finally, isolates SBR-P23, T6 and P8 formed a single cluster where the closest known relatives were an unidentified phenol reactor isolate (Watanabe et al. 1998) and an acetate user that was described as a *Variovorax* sp.

Two isolates belonged to the *Deinococcus-Thermus* phylum (SBR-P6 and T24) with 99 % sequence similarity to *Deinococcus radiopugnans* (Figure 4.4), a radiation resistant microorganism. Six isolates grouped with the γ -*Proteobacteria* class (Figure 4.4). Two isolates were nested between *Thermomonas haemolytica* and an unidentified denitrifying iron oxidizer (SBR-T16 and P11), while another one clustered near *Xanthomonas* (SBR-P20) with 89 % sequence similarity. An additional isolate clustered within the *Pseudomonadaceae* family (SR-T9) and two isolates clustered with members of the *Acinetobacter* genus (SBR-T7 and P21). Finally, three isolates clustered with members of the *Bacteroidetes* phylum. One isolate clustered with *Flavobacterium ferrugineum* and its sequence was 93 % similar (SBR-T15), while SBR-P13 was nested between the *Flexibacter* and *Flavobacter* genera and its sequence was 92 % similar to *Flexibacter filiformis*. The closest known organism to isolate SBR-P7 was *Dyadobacter fermentens* although they were only 86 % similar in sequence.

The *Firmicutes* phylum (High G+C gram positives) represented five isolates that belonged to *Bacillaceae* family (Figure 4.5). One of the isolates

(SBR-T8) formed a defined cluster with *Brevibacillus* while the other four were affiliated with different *Bacillus* species. Six isolates belonged to the *Actinobacteria* phylum, clustering with *Rhodococcus* (SBR-P12), *Pseudonocardia* (SBR-T11) and *Microbacterium* (SBR-T14, P1 and P9).

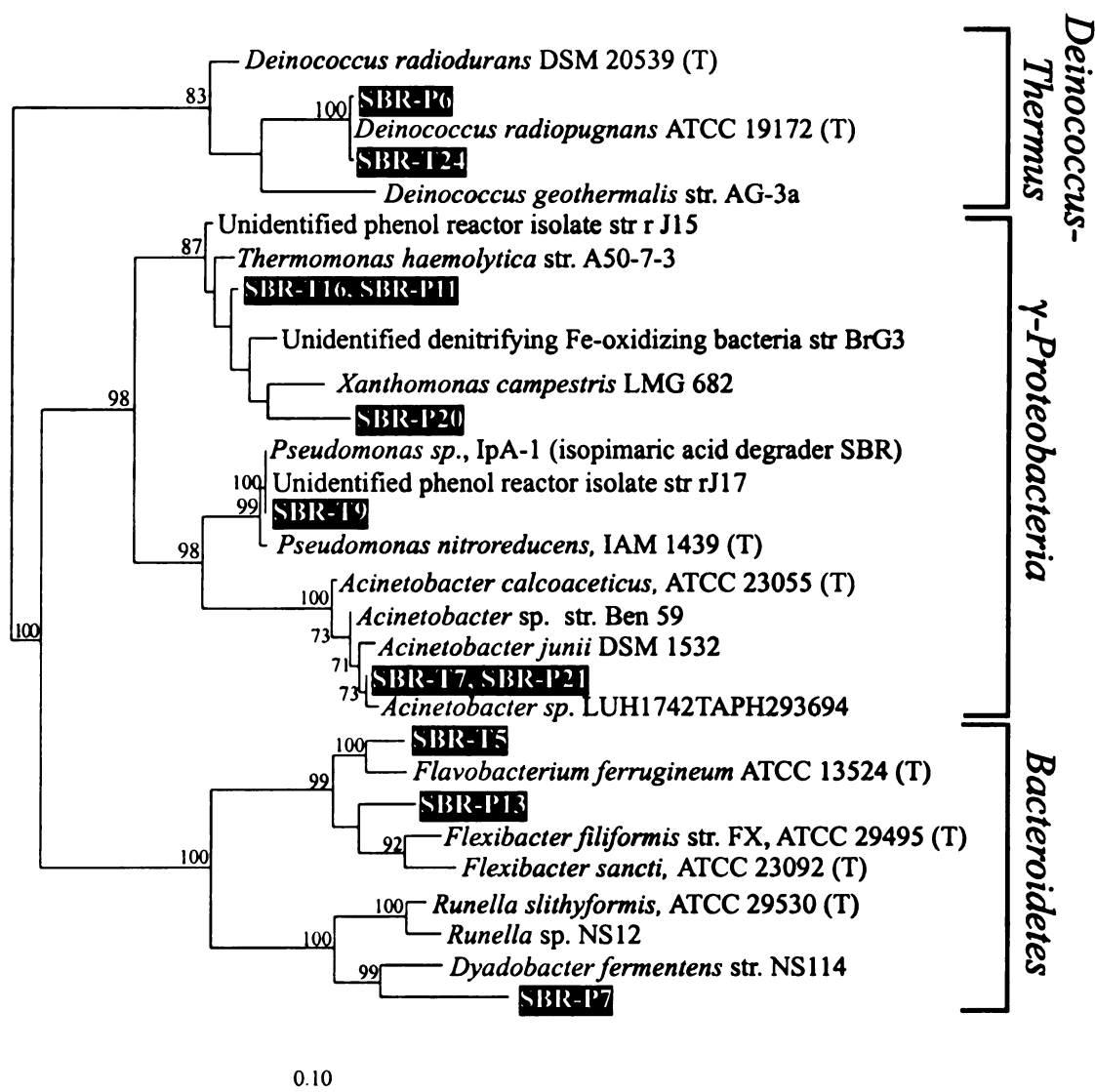


Figure 4.4. Phylogenetic tree of 16S rDNA sequences of isolates that belonged to the *Deinococcus-Thermus* phylum, γ -*Proteobacteria* class, and *Bacteroidetes* phylum. The tree was constructed from 659 unambiguously aligned positions using the maximum-likelihood method. Numbers at nodes represent the percentage of 100 bootstraps. The nodes without bootstraps values represent either nodes with bootstrap values below 50 %, or inconsistent branch order when compared against the consensus tree. The scale bar represents the number of substitutions per nucleotide position. T, type strain.

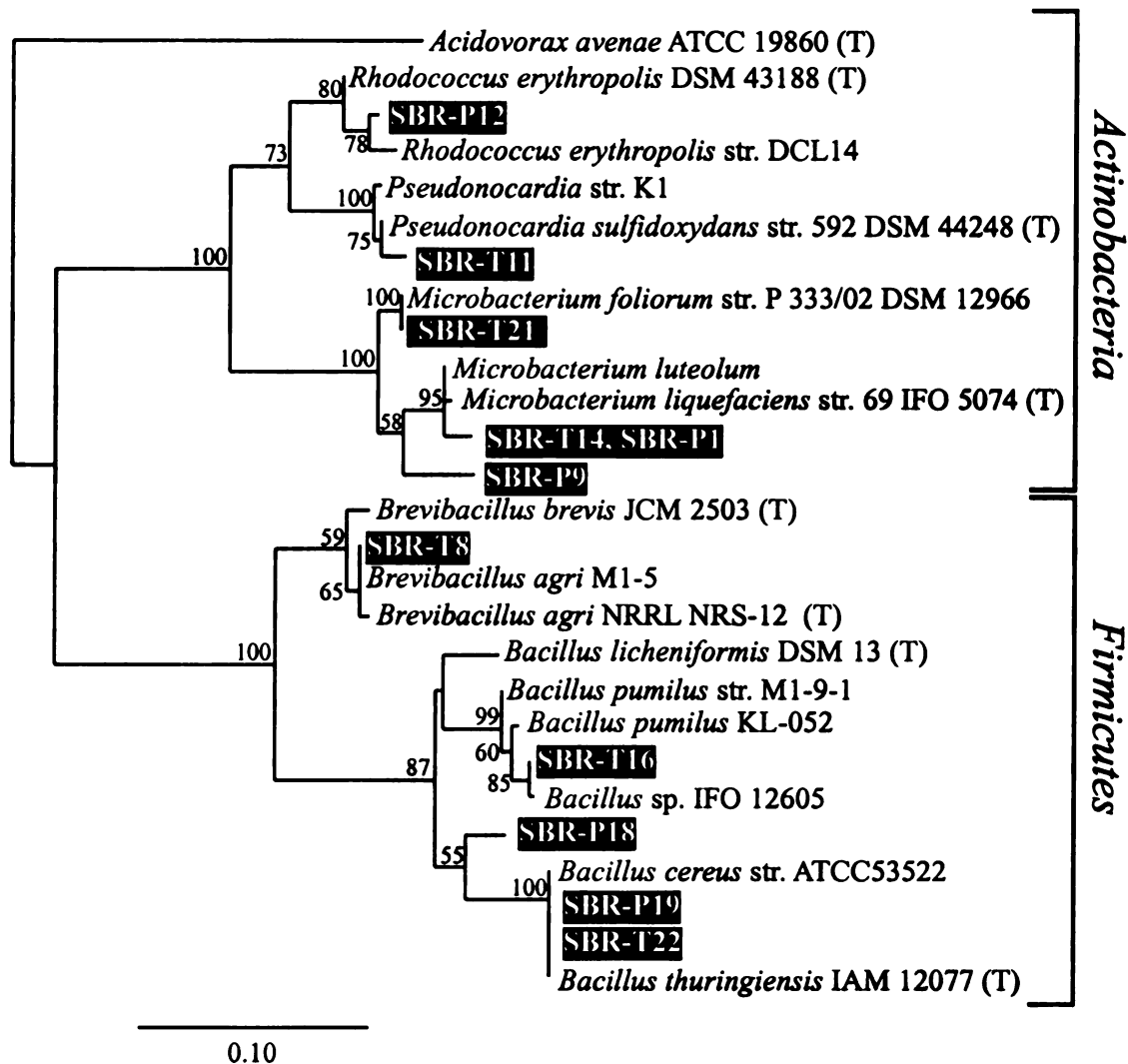


Figure 4.5. Phylogenetic tree of 16S rDNA sequences of isolates that belonged to *Actinobacteria* and *Firmicutes* phyla. The tree was constructed from 449 unambiguously aligned positions using the maximum-likelihood method, and was rooted using *Acidovorax avenae*. Numbers at nodes represent the percentage of 100 bootstraps. The nodes without bootstraps values represent either nodes with bootstrap values below 50 %, or inconsistent branch order when compared against the consensus tree. The scale bar represents the number of substitutions per nucleotide position. T, type strain.

Degradative characterization.

The isolates were tested for growth on phenol as the sole carbon source at different concentrations in order to minimize the inhibitory effects noted by Fries et al. (1997a). Twenty eight percent of the isolates tested degraded phenol under the conditions tested (Table 4.4). Five isolates degraded 100% of the phenol when tested at 50 mg/l, one isolate from the phenol-fed reactor (SBR-P12) and four from the phenol plus TCE-fed reactor (SBR-T2, T4, T11 and T20). Six additional isolates degraded phenol at 10 mg/l; three from the phenol-fed (SBR-P3, P5 and P18) and three from the phenol plus TCE-fed (SBR-T16, T19, T23) reactor. Supplementation of the 10 mg/l phenol medium with vitamins allowed three additional isolates to degrade 93-100 % of the phenol in the vial (SBR-P10, T12 and T15). These isolates were also able to grow on 50 mg/l phenol if vitamins were provided.

The 14 isolates that degraded phenol and the two ammonia oxidizers were tested for TCE cometabolism by re-inoculating them in fresh medium with 1 mg/l TCE. Five isolates removed 100 % of the TCE, one from the phenol-fed reactor (SBR-P11), and four from the phenol plus TCE-fed reactor (SBR-T2, T4, T15 and T20). One isolate from the phenol plus TCE-fed reactor removed 80 % of the TCE (SBR-T12) and two other isolates removed 19 and 17 % respectively (SBR-P3 and SBR-T18). The remaining phenol degrading isolates and the ammonia oxidizers did not remove significant amounts of TCE (0-5 %) under the conditions tested.

Table 4.4 Phenol and TCE degrading properties of the reactor isolates. Values represent percentage of removal. For the TCE degradation test fresh phenol medium at the appropriate concentration and TCE were mixed simultaneously. SBR-P, phenol-fed reactor; SBR-T, phenol plus TCE-fed reactor. NT, not tested. WV, Wolin's vitamins.

Name	Phenol 50 mg/l	Phenol 10 mg/l	Phenol 10 mg/l WV	TCE 1 mg/l
SBR-P1	9 %	5 %	7 %	NT
SBR-P2	5 %	0 %	2 %	NT
SBR-P3	0 %	17 %	0 %	19 %
SBR-P4	3 %	0 %	3 %	NT
SBR-P5	3 %	20 %	0 %	5 %
SBR-P6	11 %	5 %	4 %	NT
SBR-P7	8 %	13 %	0 %	NT
SBR-P8	4 %	0 %	3 %	NT
SBR-P9	7 %	0 %	2 %	NT
SBR-P10	8 %	12 %	100 %	100 %
SBR-P11	9 %	13 %	8 %	NT
SBR-P12	100 %	NT	NT	0 %
SBR-P13	9 %	9 %	4 %	NT
SBR-P14	1 %	9 %	0 %	NT
SBR-P15	1 %	6 %	4 %	NT
SBR-P16	0 %	4 %	5 %	NT
SBR-P17	0 %	14 %	12 %	NT
SBR-P18	6 %	16 %	NT	0 %
SBR-P19	8 %	5 %	8 %	NT
SBR-P20	0 %	7 %	9 %	NT
SBR-P21	7 %	9 %	0 %	NT
SBR-P22	8 %	4 %	0 %	NT
SBR-P23	6 %	5 %	8 %	NT
SBR-P24	NT	NT	NT	0 %
SBR-T1	2 %	7 %	10 %	NT
SBR-T2	100 %	NT	NT	100 %
SBR-T3	2 %	6 %	5 %	NT
SBR-T4	100 %	NT	NT	100 %
SBR-T5	5 %	0 %	0 %	NT
SBR-T6	8 %	9 %	5 %	NT
SBR-T7	3 %	1 %	4 %	NT
SBR-T8	7 %	9 %	9 %	NT
SBR-T9	5 %	4 %	5 %	NT
SBR-T10	8 %	11 %	0 %	NT
SBR-T11	100 %	NT	NT	0 %
SBR-T12	7 %	11 %	93 %	80 %
SBR-T13	1 %	8 %	5 %	NT
SBR-T14	8 %	7 %	9 %	NT
SBR-T15	7 %	10 %	100 %	100 %
SBR-T16	7 %	19 %	4 %	2 %
SBR-T17	6 %	4 %	7 %	NT
SBR-T18	0 %	10 %	6 %	NT
SBR-T19	5 %	16 %	12 %	17 %
SBR-T20	100 %	NT	NT	100 %
SBR-T21	3 %	7 %	5 %	NT
SBR-T22	8 %	0 %	3 %	NT
SBR-T23	1 %	16 %	0 %	2 %
SBR-T24	0 %	8 %	5 %	NT
SBR-T25	5 %	3 %	0 %	NT
SNR-T26	NT	NT	NT	0 %

DNA from all the isolates was tested with primers that target conserved regions of the phenol hydroxylase gene to determine which strains carry similar genes. From the 50 isolates tested six produced a band of the correct size (SBR-T2, P10, T15, T20, T12 and T4), although some non-specific amplification was observed. Sequencing of the bands and GenBank searches using BLAST revealed that there was high sequence variability among the isolates. The amino acid identities of the phenol hydroxylases among the isolates were from 72 to 100 %, and isolates SBR-P10 and SBR-T15 had identical sequences. All the phenol hydroxylase sequences from the isolates contained regions resembling the conserved dinuclear iron binding domains typically found in monooxygenase enzymes (Fox et al. 1993). Furthermore, the spacing between these motifs was 94 amino acids, a value that is within the average for toluene oxygenases further supporting that these sequences belong to the oxygenase family (Johnson and Olsen, 1995). Phylogenetic analysis of the amino acid sequences shows that the isolates were distributed among different known phenol and toluene oxygenases (Figure 4.6). The phenol hydroxylase of SBR-T2 (*Burkholderia* sp.) was 100 % identical to the toluene ortho-monooxygenase (TOM) of *Burkholderia cepacia* G4. The sequences from the isolates SBR-T15 and P10 formed a distinct cluster that was 90 % similar to TOM of *Burkholderia cepacia* G4 and 92 % similar to the phenol hydroxylase of *Comamonas testosteroni* strains R5 and R2. The phenol hydroxylase of isolate SBR-T20 clustered with the toluene/benzene-2 monooxygenase of *Burkholderia* sp. str. JS 150, with 94 % amino acid identity. Interestingly, the phenol hydroxylase from

isolate SBR-T12 forms a deep clade and was 82 % identical to the phenol hydroxylase of *Comamonas* E6, although the 16S rDNA sequence of SBR-T12 was 98 % similar to SBRT15 and P20. Finally, the phenol hydroxylase of isolate SBR-T4 (*Variovorax* sp.) clustered with the phenol hydroxylase of a *Variovorax* sp isolated from a TCE contaminated site in Japan.

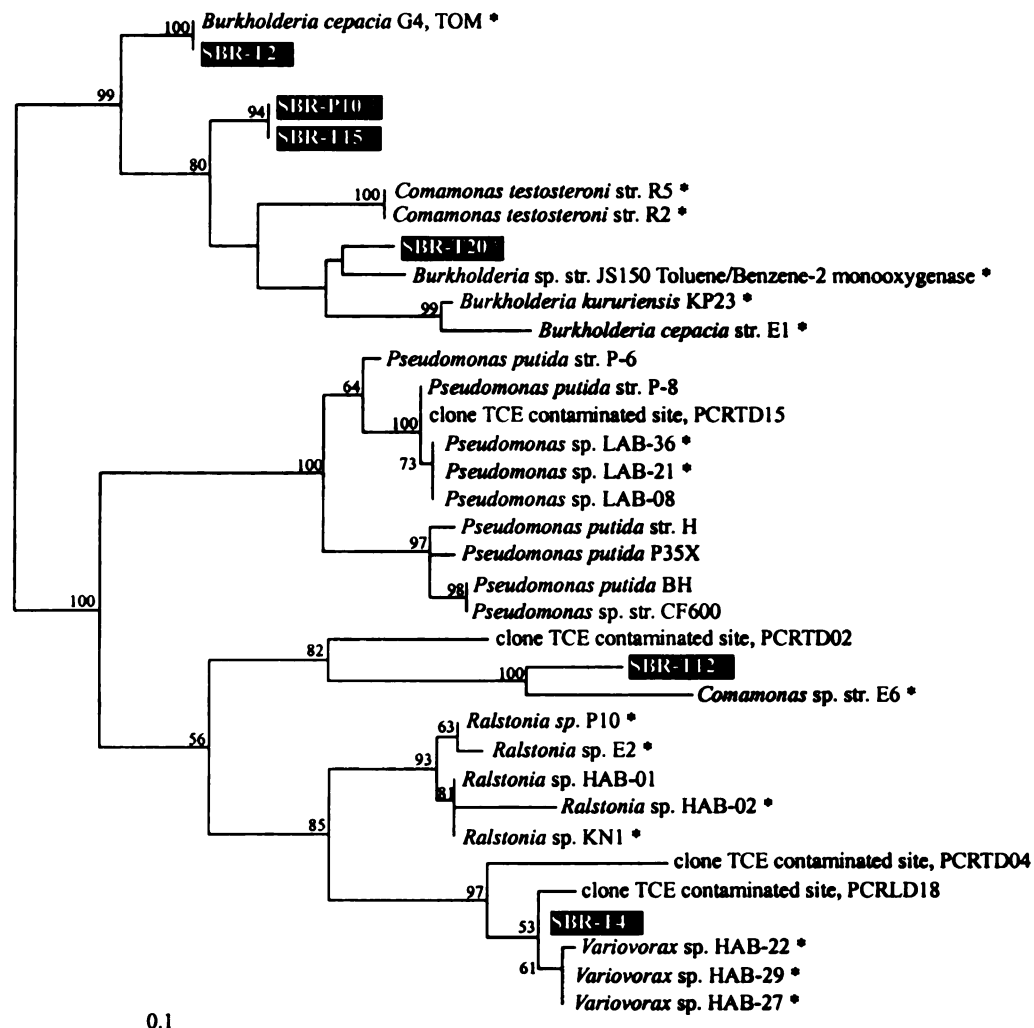


Figure 4.6. Unrooted phylogenetic tree of the phenol hydroxylase amino acid sequences of the isolates. The tree was constructed using 169 aligned amino acids, between positions 83 and 252 of *Pseudomonas* sp. CF600 *dmpN* gene, using the protein maximum-likelihood method. Numbers at nodes represent the percentage of 100 bootstraps. The nodes without bootstraps values represent either nodes with bootstrap values below 50 %, or inconsistent branch order when compared against the consensus tree. The scale bar represents the number of substitutions per amino acid position. The asterisk indicates strains that degrade TCE.

Primer design and specificity.

A total of 13 isolates were selected to design primers for quantitative PCR (Table 4.1). The isolates consist of two major groups: phenol degraders and non-phenol degraders. The phenol degraders were selected based on the presence of phenol hydroxylase genes and the T-RF matches against the community T-RFLPs. The non-phenol degraders were selected because either they represent genera known to degrade aromatics, or by their flocculation characteristics on rich medium. The specificity of the primers was tested using the reactor isolates because they represent a diverse collection (Figures 4.2-4.5). To obtain maximum specificity, MgCl_2 concentrations were adjusted since changes in the annealing temperature did not increase the specificity. Melting curve analysis was used to evaluate the specificity of the primers, since non-specific products will have different melting curves due to differences in size, AT/GC ratio and sequence of the amplicon (Ririe et al. 1997). Magnesium chloride concentrations between 1.5-2.0 mM resulted in PCR products of the correct melting temperature and the disappearance of non-specific products (Figure 4.7).

Sensitivity and reproducibility

The sensitivity of the SYBR green PCR assay was evaluated by using lysed 10-fold serial dilutions of bacterial cultures as template for the reactions (Figure 4.8). A decrease in the number of cycles needed for the fluorescence to cross the threshold (C_T) was inversely proportional the initial template concentration. A linear response between C_T and the log of total cells was

observed over five orders of magnitude ranging from 1.1 cell to 1.6×10^5 cells ($r^2 = 0.999$). Similar results were observed when the universal primers 1108F and 1123b were used with *Pseudomonas stutzeri* JM300, although the reaction was less sensitive (two fold) due to fluorescence in the no template negative controls.

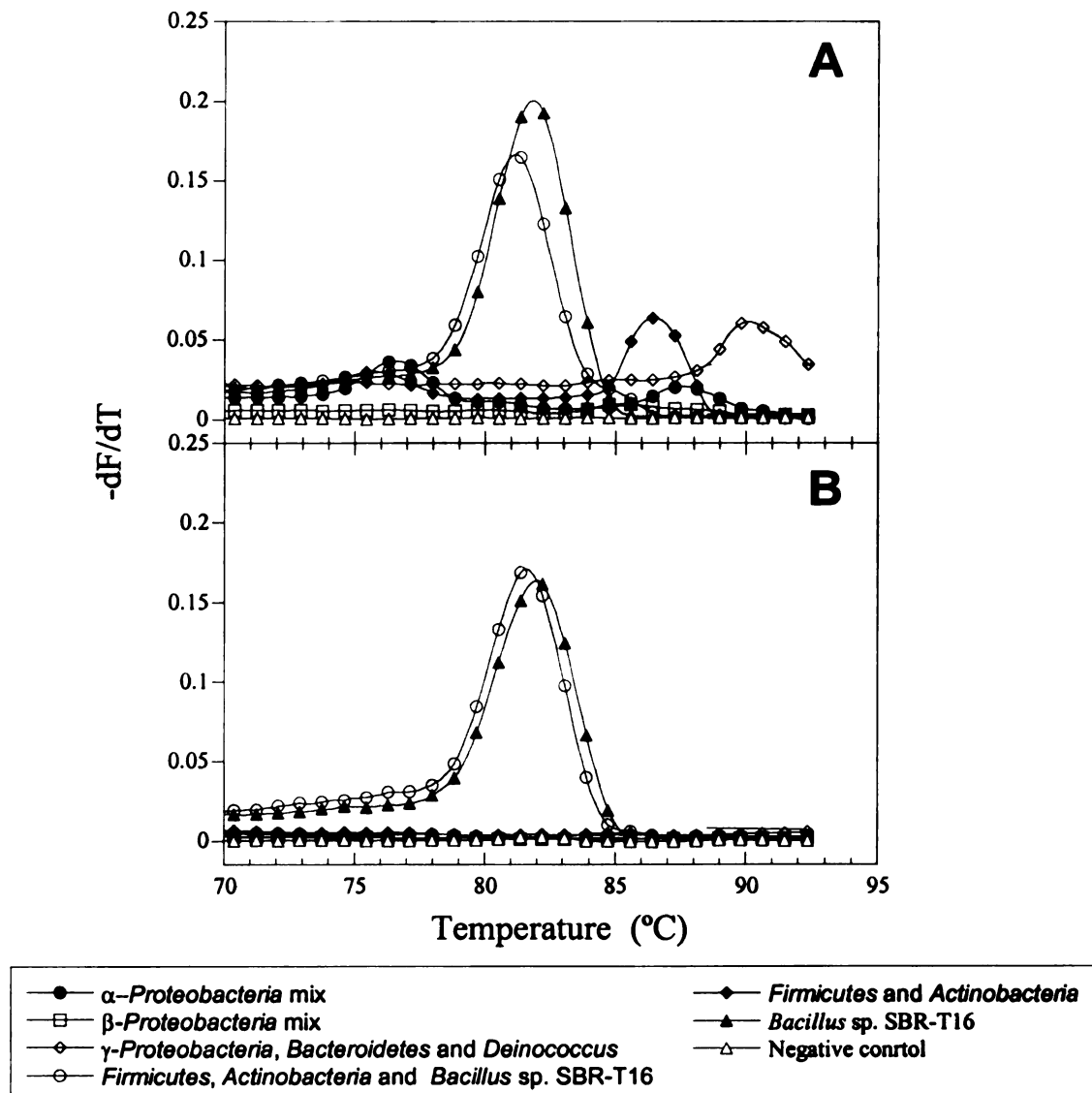


Figure 4.7. Specificity of the SYBR green PCR reaction at 1.8 (A), and 1.5 (B), mM MgCl_2 using melting peak analysis. $-dF/dT$, negative derivative of fluorescence with respect to temperature. Data points shown represent every tenth measurement.

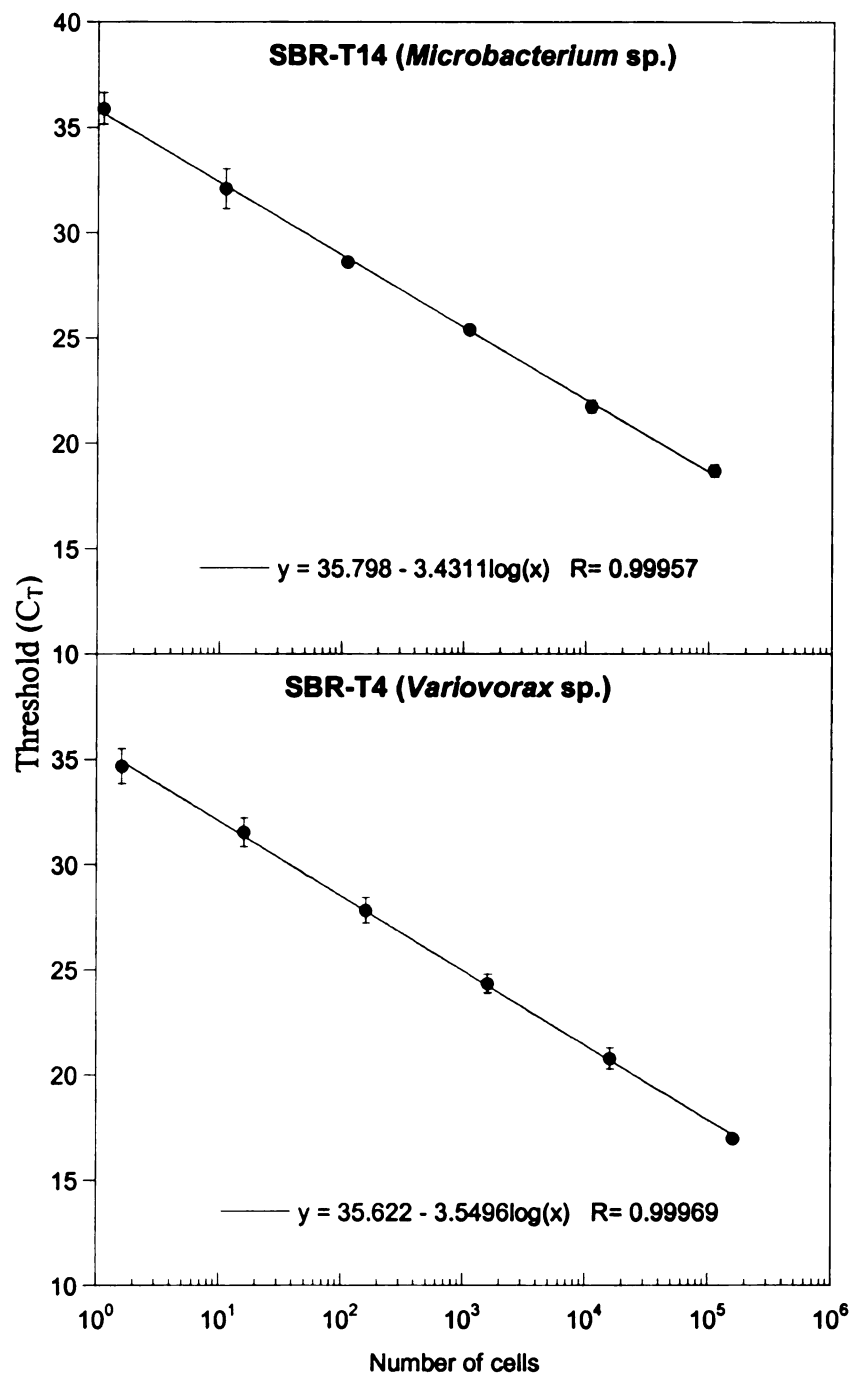


Figure 4.8. SYBR green I real time PCR calibration curves using cell lysates as template. Values represent averages of duplicate reactions \pm one standard deviation. C_T , cycle at which the fluorescence crosses an arbitrary threshold determined using a reference dye.

This problem has been observed before (Corless et al. 2000; Riley-Buckley 2001; Nadkarni et al. 2002) and two possible explanations have been suggested: primer dimer formation or contamination in the PCR master mix. Melting curve analysis of the negative controls resulted in PCR products with high melting temperatures (80-82° C) which suggest that signals detected were caused by contamination. Since the C_T of the negative reactions was between 33-35 cycles, any test sample with a C_T in this range was disregarded. Only test samples with a C_T below 28 were used for further analysis in order to avoid false positives.

The reproducibility of the SYBR green PCR method was tested by quantifying total bacteria abundance and SBR-T12, P10 and T15 abundance in eight replicate samples from each reactor. Quantifications were reproducible with 95 % confidence intervals within the same order of magnitude (Figure 4.9). Values for the bacterial primers were $3.2 \times 10^7 \pm 7.15 \times 10^6$ and $6.48 \times 10^7 \pm 1.84 \times 10^7$ cells $\times \mu\text{g}^{-1}$ of community DNA for the phenol and phenol plus TCE-fed reactors respectively. For the SBR-P10 and T15 primers values were $3.29 \times 10^6 \pm 7.02 \times 10^5$ and $5.26 \times 10^6 \pm 1.48 \times 10^6$ for the phenol and the phenol plus TCE-fed reactors respectively.

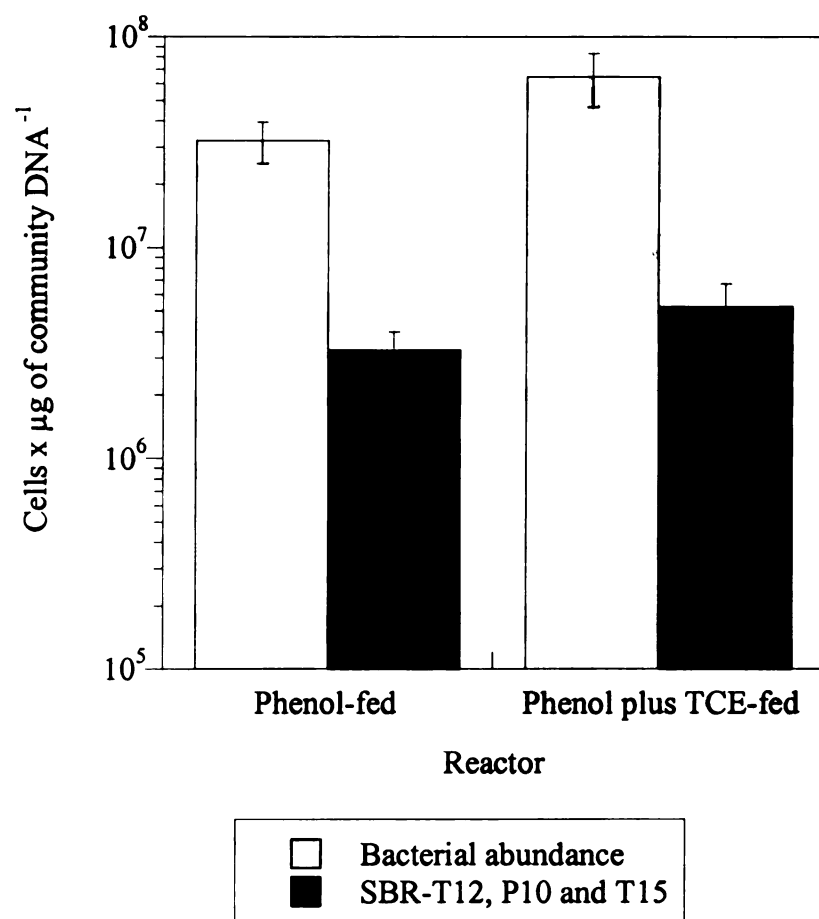


Figure 4.9. Reproducibility of SYBR green I real time PCR. Two different primer sets were used for the test. Values represent averages $\pm 95\%$ confidence intervals ($n = 8$).

Bacterial abundances.

Changes in total bacterial abundance were observed in the phenol-fed reactor during the 810 days of operation (Figure 4.10). The initial bacterial density in the phenol-fed reactor increased from 3.39×10^6 to 1.55×10^8 bacterial cells $\times \mu\text{g}$ of community DNA⁻¹ after 127 days of operation. Then, the bacterial cell density decreased 100 fold at day 198 and returned to similar levels 28 days later maintaining an average of 3.91×10^7 bacterial cells $\times \mu\text{g}$ of community DNA⁻¹ during 341 days of operation. Finally, there was a nearly one fold increase in abundance when the bacterial densities reached 1.0×10^8 bacterial cells $\times \mu\text{g}$ of community DNA⁻¹ during days 630-729.

In the phenol plus TCE-fed reactor the bacterial dynamics was relatively stable compared with the phenol-fed reactor (Figure 4.11). The initial density was 4.79×10^6 cells $\times \mu\text{g}$ of community DNA⁻¹ and reached a maximum of 7.06×10^7 cells $\times \mu\text{g}$ of community DNA⁻¹ after 127 days of operation. Bacterial densities then stabilized with minor sporadic increases averaging 2.69×10^7 cells $\times \mu\text{g}$ of community DNA⁻¹ during the remaining 584 days of operation.

Analysis of a selected group of phenol, and phenol plus TCE degraders revealed that an unidentified group of *β-Proteobacteria* isolates (SBR-T12, P10 and T15) were the most abundant population among the isolates evaluated in the phenol-fed reactor (Figures 4.10-4.13). The abundance of this phylogenetic group ranged from 4.0×10^4 to 1.64×10^7 cells $\times \mu\text{g}$ of community DNA⁻¹, with changes in abundance that correlated with changes in total bacterial densities ($R^2 = 0.90$). In contrast, the abundance of the phenol degrader

Phenylobacterium sp. SBR-T23, and the phenol/TCE degraders *Variovorax* sp. SBR-T4 and SBR T-20 was between 10 to 100 fold lower than the abundance of the unidentified β -*Proteobacteria* isolates (SBR-T12, P10 and T15). The ranking order of the remaining isolates, from most to least abundant, during the first 500 days of operation was SBR-T20 > *Variovorax* sp., SBR-T4 > *Phenylobacter* sp. SBR-T23, and their dynamics correlated with the bacterial dynamics during the first 500 days of operation. In contrast, the dynamics during the last 300 days of operation were variable, with *Phenylobacter* sp. SBR-T23 and unidentified SBR-T20 isolates having an opposite trend to *Variovorax* sp. SBR-T4 and the unidentified β *Proteobacteria* group (SBR-T12, P10 and T15).

In the phenol plus TCE-fed reactor the unidentified β -*Proteobacteria* group (SBR-T12, P10 and T15) was the predominant cultivable population (Figure 4.11). During the first 50 days, the cell density of the unidentified β -*Proteobacteria* group decreased from 7.8×10^5 to 4.2×10^4 cells x μg of community DNA⁻¹, and returned back to cell densities that were between 10^6 - 10^7 cells x μg of community DNA⁻¹ during the remaining 684 days. The cell densities of the other phenol and phenol plus TCE degrading populations were at least 100 fold lower than the dominant group. The dynamics of *Variovorax* sp. SBR-T4 and *Phenylobacter* sp. SBR-T23 were very similar to the dynamics of the most abundant group with abundances between 10^3 to 10^4 cells x μg of community DNA⁻¹. These values represent approximately a 10 fold increase compared to the values observed in phenol-fed reactor. In contrast, SBR-T20 was less abundant in phenol-fed reactor with values between 10^1 - 10^2 cells x μg

of community DNA⁻¹ with the exception of two conspicuous increases at days 240 and 541 reaching maximum levels of 5.3×10^2 and 3.2×10^3 cells x μg of community DNA⁻¹, respectively. The ranking order, from most to least abundant, in the phenol plus TCE-fed reactor was unidentified β *Proteobacteria* group (SBR-T12, P10 and T15) > *Variovorax* SBR-T4 and *Phenylobacter* SBR-T23 > SBR-T20. Although *Burkholderia* SBR-T2 was isolated from this reactor, it was detected only on the day of isolation.

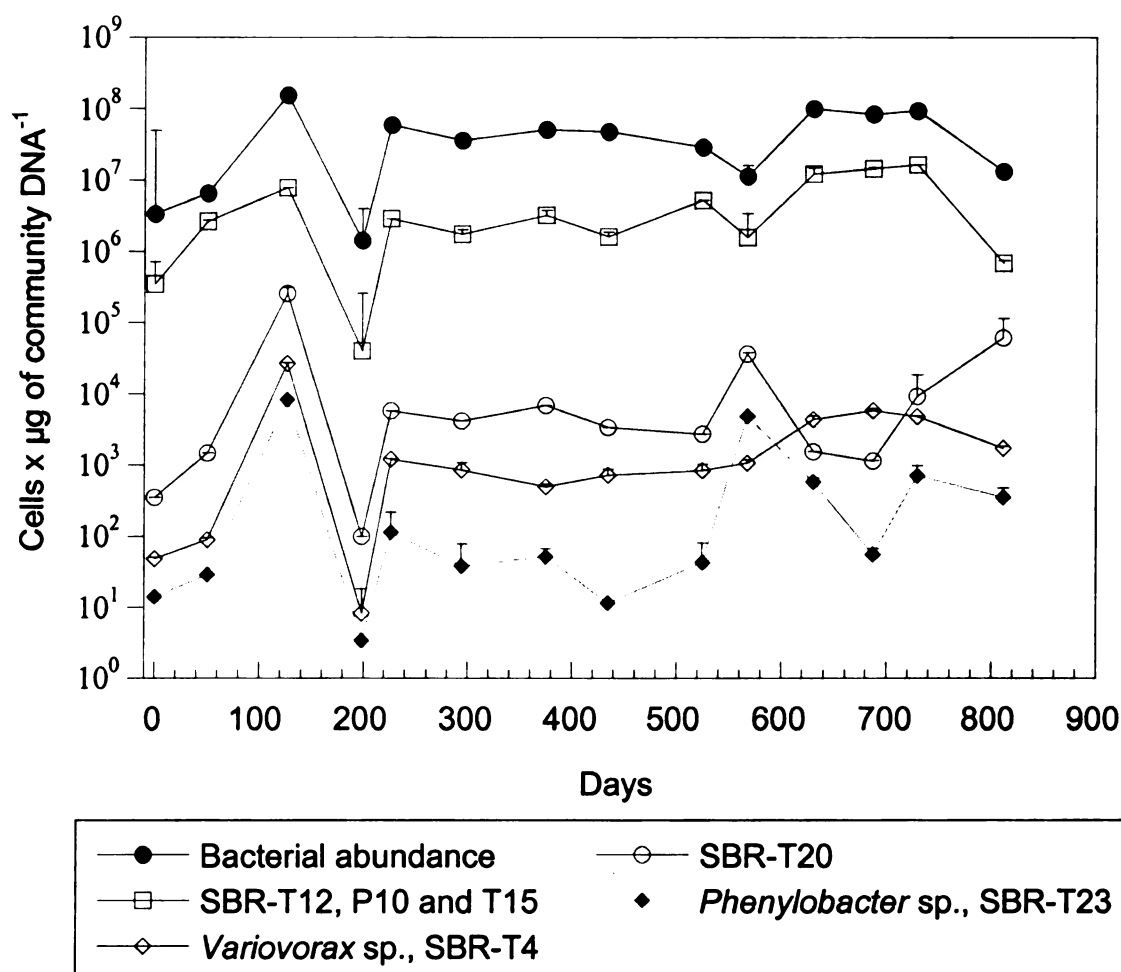


Figure 4.10. Abundance of phenol degraders in the phenol-fed reactor. Values represent averages \pm one standard deviation from duplicate reactions.

In the phenol plus TCE-fed reactor the unidentified β -*Proteobacteria* group (SBR-T12, P10 and T15) was the predominant cultivable population (Figure 4.11). During the first 50 days the cell density of the unidentified β -*Proteobacteria* group decreased from 7.8×10^5 to 4.2×10^4 cells $\times \mu\text{g}$ of community DNA⁻¹, and returned back to cell densities that were between 10^6 - 10^7 cells $\times \mu\text{g}$ of community DNA⁻¹ during the remaining 684 days. The cell densities of the other phenol and phenol plus TCE degrading populations were at least 100 fold lower than the dominant group. The dynamics of *Variovorax* sp. SBR-T4 and *Phenylobacter* sp. SBR-T23 were very similar to the dynamics of the most abundant group in the reactors with abundances between 10^3 to 10^4 cells $\times \mu\text{g}$ of community DNA⁻¹. These values represent approximately a 10 fold increase compared to the values observed in the phenol-fed reactor. In contrast, SBR-T20 was less abundant in the phenol-fed reactor with values between 10^1 - 10^2 cells $\times \mu\text{g}$ of community DNA⁻¹ with the exception of two conspicuous increases at days 240 and 541 reaching maximum levels of 5.3×10^2 and 3.2×10^3 cells $\times \mu\text{g}$ of community DNA⁻¹ respectively. The ranking order, from most to least abundant, in the phenol plus TCE-fed reactor was unidentified β -*Proteobacteria* group (SBR-T12, P10 and T15); *Variovorax* sp. SBR-T4 and *Phenylobacter* sp. SBR-T23; and SBR-T20. Although *Burkholderia* sp. SBR-T2 was isolated from this reactor, it was detected only on the day of isolation.

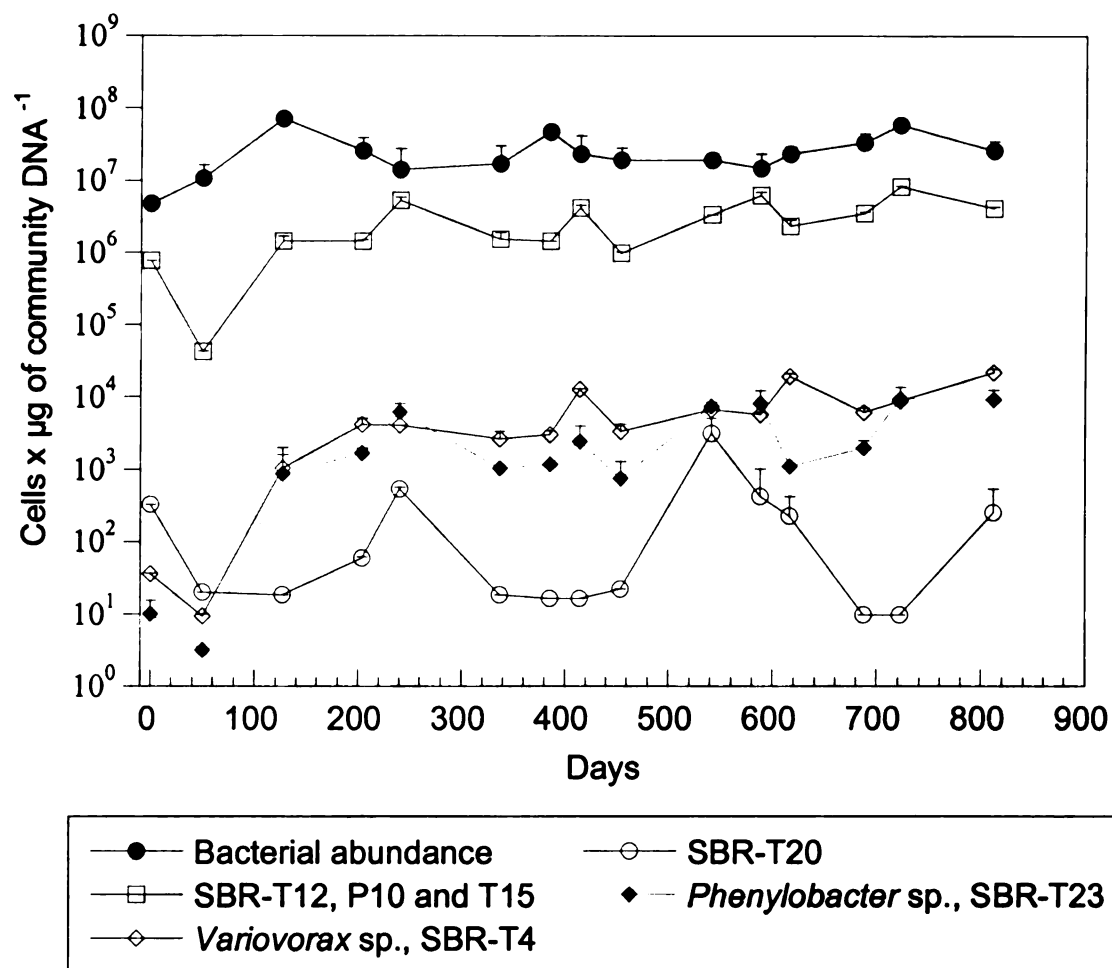


Figure 4.11. Abundance of phenol degraders in the phenol plus TCE-fed reactor. Values represent averages \pm one standard deviation from duplicate reactions.

The abundances of several non-phenol degrading populations were also examined in the two reactors. The non-phenol degrading populations were generally below 10^3 cells x μg of community DNA⁻¹ in the phenol-fed reactor with a few exceptions (Figure 4.12). At day 127 the abundance of all the isolates increased, with *Flexibacter* sp. SBR-P13 the most abundant with 1.1×10^5 cells x μg of community DNA⁻¹. Furthermore, *Flexibacter* sp. SBR-P13 was also the most abundant non-phenol degrader at days 226 and 811 with 3.3×10^3 and 4.5×10^4 cells x μg of community DNA⁻¹. On day 567 the abundance of all the non-phenol degrading isolates increased with *Nitrosomonas* sp. SBR-P24 the predominant with 3.3×10^3 cells x μg of community DNA⁻¹, an increase between 10 to 100 fold.

In the phenol plus TCE-fed reactor the abundance of the non-phenol degrading populations was dynamic (Figure 4.13). For instance, the abundance of *Microbacterium* sp. SBR-T14 increased from below 10 cells to 1.6×10^3 cells x μg of community DNA⁻¹ after 385 days of operation, and oscillated afterwards in the range of 10^2 to 10^3 cells x μg of community DNA⁻¹. The isolates *Nitrosomonas* sp. SBR-P24, *Acinetobacter* sp. SBR-T7 and *Pseudomonas* sp. SBR-T9 had abundances higher than 10^3 cells x μg of community DNA⁻¹ at particular days of operation, however there was no clear trend over the 800 days of operation. Finally, the isolates *Rhizobium* sp. SBR-T1 and *Bacillus* sp. SBR-T16 were not detected.

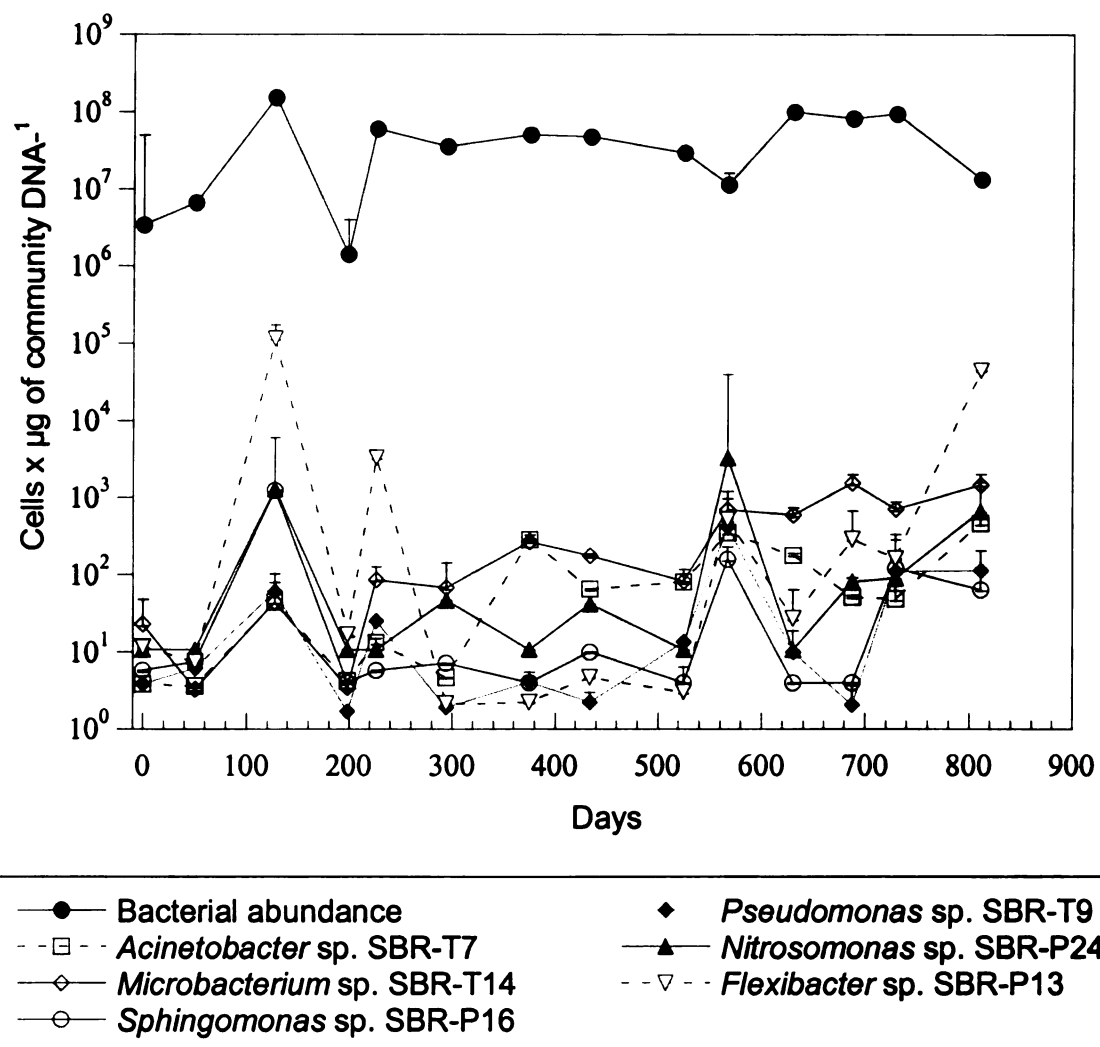


Figure 4.12. Abundance of non-phenol degraders in the phenol-fed reactor. Values represent averages \pm one standard deviation from duplicate reactions.

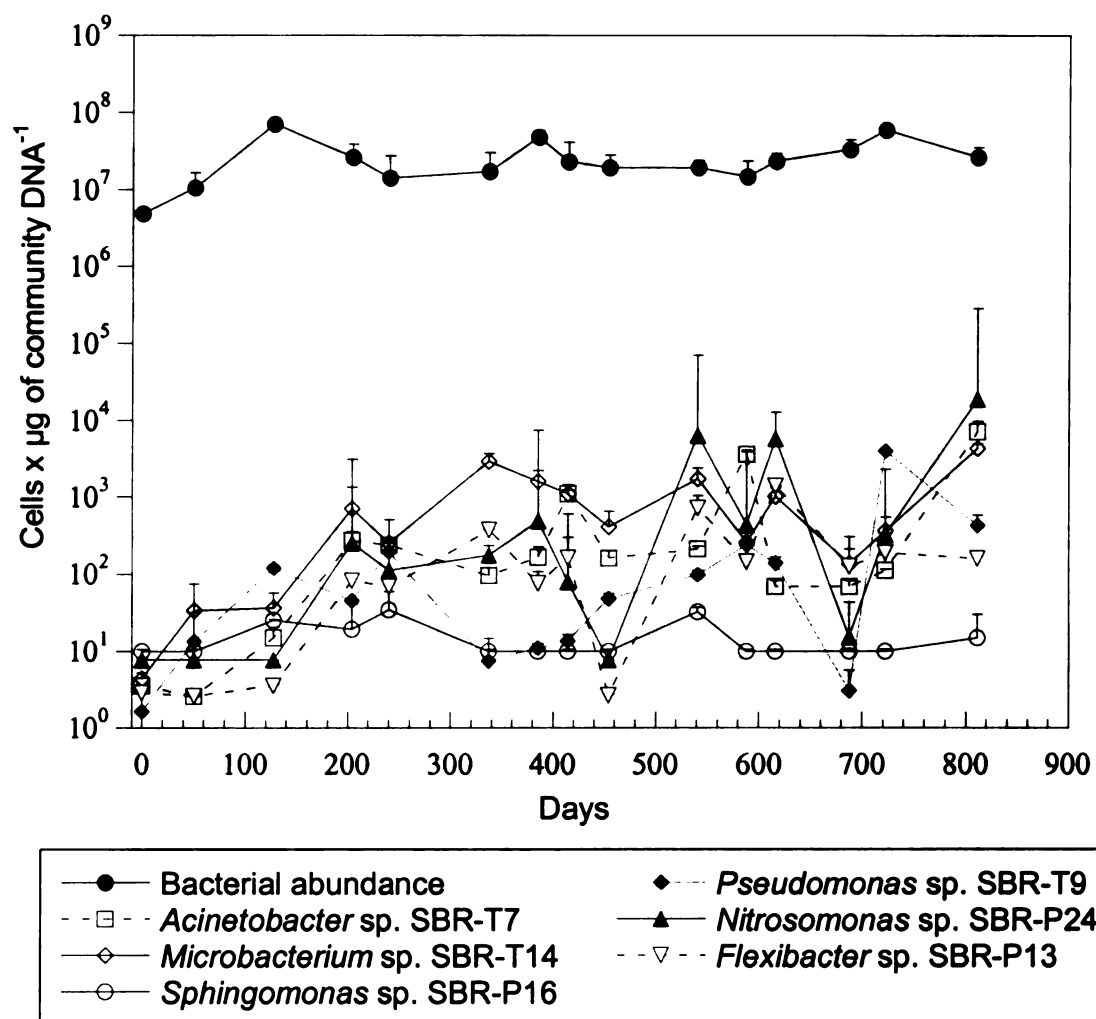


Figure 4.13. Abundance of non-phenol degraders in the phenol plus TCE-fed reactor. Values represent averages \pm one standard deviation from duplicate reactions.

Additional phylogenetic analysis of the dominant populations

In an attempt to clarify the phylogenetic identity of the most abundant group of microorganisms, nearly complete 16S rDNA sequences for SBR-T12, P10 and T15 were used for alignment and phylogeny. Analysis of 1336 unambiguously aligned positions revealed that this group of isolates belongs to the *Comamonadaceae* family of the β -*Proteobacteria* (Figure 4.14). The isolates formed a cluster where the closest relative was a clone from activated sludge and the sequence similarities among them were between 98.4 and 99.3 % (Table 4.5). The closest cultivable relatives to the isolated strains were an unidentified phenol reactor isolate (strain rM9) and *Aquaspirillum gracile*; with sequence similarities of 96.3 and 95.6 %, respectively. Different from *Aquaspirillum gracile* that has a helical morphology; SBR-T12, P10 and T15 are rods of small size and diameter. These isolates form aggregates when grown in mineral medium supplemented with phenol.

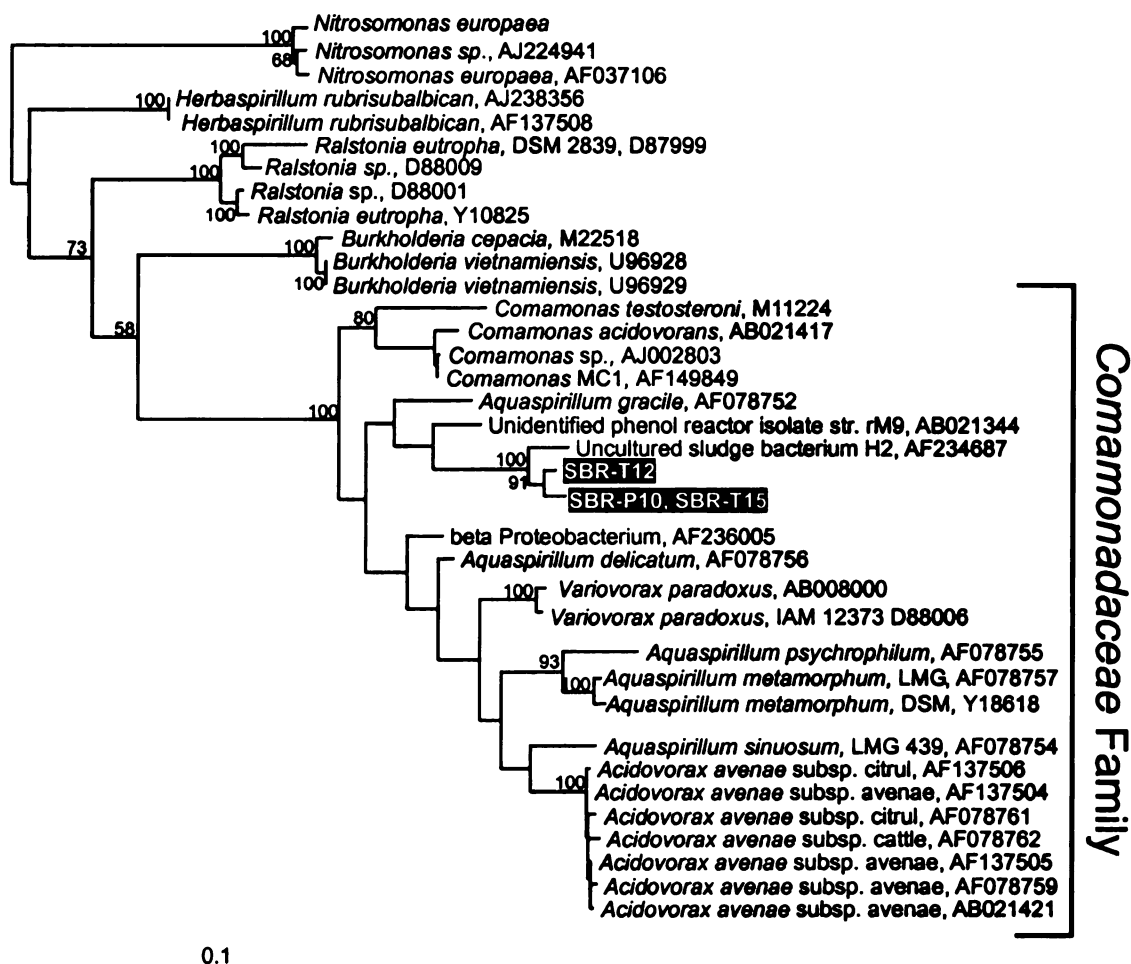


Figure 4.14. Phylogenetic tree of 16S rDNA sequences of the unidentified β Proteobacteria group. The tree was constructed from 1336 unambiguously aligned positions using the maximum-likelihood method, and was rooted using *Nitrosomonas europaea*. Numbers at nodes represent the percentage of 100 bootstraps. The nodes without bootstraps values represent either nodes with bootstrap values below 50 %, or inconsistent branch order when compared against the consensus tree. The scale bar represents the number of substitutions per nucleotide position.

Table 4.5. Sequence similarity values of selected sequences from Figure 4.14

Name	1	2	3	4	5	6	7	8	9
1 <i>Comamonas</i> sp.	100.0%								
2 <i>Comamonas</i> MC1	99.9%	100.0%							
3 <i>Aquaspirillum gracile</i>	95.5%	95.5%	100.0%						
4 Unidentified phenol reactor isolate str. rM9	95.4%	95.4%	96.2%	100.0%					
5 Uncultured sludge bacterium H2	94.2%	94.1%	95.5%	96.0%	100.0%				
6 SBR-T12	94.0%	93.9%	95.7%	96.3%	98.5%	100.0%			
7 SBR-P10, SBR-T15	93.8%	93.7%	95.6%	96.3%	98.4%	99.3%	100.0%		
8 Unidentified beta proteobacterium	96.1%	96.1%	96.0%	96.3%	95.4%	95.2%	94.9%	100.0%	
9 <i>Aquaspirillum delicatum</i>	95.8%	95.7%	95.8%	96.1%	95.6%	95.4%	95.1%	98.3%	100.0%

Discussion

Direct isolation on R2A medium resulted in 50 isolates that represented 47 % of all the T-RFs on the sampling day and 27 % when the results were compared against all days. These results suggest that although spatial variability plays a role in the success of isolation strategies, plating on R2A medium was an effective way of recovering a significant fraction of the community. This medium was previously used to isolate phenol and toluene-degrading bacteria from groundwater (Fries et al. 1997b), and from activated sludge (Kämpfer et al. 1996) with similar success suggesting that it meets the nutritional requirements of a variety of microorganisms.

Sequence analysis of the cultivable members of the microbial communities revealed that reactors were comprised by members of the *Proteobacteria* (α , β and γ classes), *Deinococcus-Thermus*, *Bacteroidetes*, *Firmicutes* (low G+C, gram positive bacteria) and *Actinobacteria* (high G+C gram positives) (Figure 4.1). The predominant phylum was the *Proteobacteria*, representing 60 % of all the isolates obtained, while the β -*Proteobacteria* class was predominant among the *Proteobacteria* phylum with 25% of the total. Although these results were affected by cultivation biases, several reports using fluorescent *in-situ* hybridization suggest that the *Proteobacteria* phylum is the most abundant group in activated sludge representing 50-80% of the bacteria detected (Wagner et al. 1993; Kämpfer et al. 1996; Bond et al. 1999; Juretschko et al. 2002). Furthermore, studies on TCE contaminated aquifers (Fries et al. 1997a; Fries et al. 1997b; Futamata et al. 2001), and on phenol-digesting sludge (Watanabe et

al. 1999) revealed that a major proportion of the isolates from these systems belonged to the β -*Proteobacteria* class, and were among the predominant populations as determined by MPN and quantitative PCR analyses. In the reactors studied herein, the best phenol and TCE degraders were in the β -*Proteobacteria* class. These findings suggest that the β -*Proteobacteria* class is an important group of microbes for the degradation of both phenol and the cometabolism of TCE.

Despite the fact that the reactors were exposed to phenol for at least one year before the isolations, only 28 % of the isolates degraded phenol under the different conditions tested. *Acinetobacter*, *Bacillus*, *Sphingomonas* and *Pseudomonas* were among the taxa isolated from the reactors that did not degrade phenol, but members of these genera have been shown to degrade xenobiotics in other studies (Ehrt et al. 1995; Kim and Oriel 1995; Fredrickson et al. 1998; Heinaru et al. 2000). Hence, either these strains lacked the ability to grow on phenol or the assay conditions used were not suited for these microbes. Without the appropriate cofactors or vitamins available in the community, some microbes may not be able to metabolize phenol. This was the case for isolates SBR-T12, P10 and T15 that degraded phenol only when vitamins were added. Secretion or leakage of cofactors from phenol degrading microorganisms could allow non-phenol degrading phenotypes to exist. Cross feeding of metabolites was the phenomenon that allowed the coexistence of the benzyl alcohol degraders *Acinetobacter* sp. C6 and *Pseudomonas putida* R1 to grow on a single substrate (Christensen et al. 2002). The degradation of benzyl alcohol by

Acinetobacter sp. C6 resulted in the accumulation of benzoate that was preferentially used by *Pseudomonas putida* R1. Similar results were also observed when TCE was applied to methanotrophic enrichments (Uchiyama et al. 1992), where the aerobe *Xanthobacter autotrophicus* metabolized glyoxylic and dichloroacetic acid intermediates generated from TCE by *Methylocystis* sp. Since the reactor communities were diverse, and many non-phenol degraders were sustained at low densities, it is very likely that cross feeding is a common event in these single substrate fed communities.

Amplification with primers that target conserved regions within the alpha subunit of the multicomponent phenol hydroxylase family revealed that this gene was present, but that there were differences at the amino acid level among the isolates, since sequences identities ranged between 72 to 100 % (Figure 4.6). Because the region amplified by the primers covers the active site, a binuclear iron cluster that activates molecular oxygen (Fox et al. 1993; Johnson and Olsen 1995; Cadieux et al. 2002), differences in kinetic constants or substrate specificity among the different oxygenases of the isolates could be expected. This hypothesis is partially supported by studies made by Futamata and coworkers (Futamata et al. 1998, 2001), who found that different phenol hydroxylase sequence clusters exhibit different affinities for TCE. Furthermore, directed evolution of the toluene *ortho*-monooxygenase of *Burkholderia cepacia* G4 resulted in one amino acid substitution within the alpha subunit that caused a three fold increase in TCE activity and a six fold increase in naphthalene oxidation (Canada et al. 2002). Detailed studies using purified enzyme

preparations from the isolates and the complete sequences of their respective oxygenases would be necessary to determine if the amino acid differences affect the kinetic coefficients or substrate range of these enzymes.

An unexpected finding was the disparity between the 16S rDNA and the phenol hydroxylase sequences of isolates SBR-T12, P10 and T15. Analysis of almost complete 16S rDNA sequences from these isolates revealed that they form a coherent cluster within the *Comamonadaceae* family of the β -*Proteobacteria* (Figure 4.14), with sequence identities of 99 % (Table 4.5). However, analysis of their corresponding phenol hydroxylases revealed that this enzyme in SBR-P10 and T15 was only 72 % identical in amino acid sequence to the one in SBR-T12, forming distinct clusters in the phylogenetic tree (Figure 4.6). As discussed above, the marked divergence between the phenol hydroxylases of the two isolates suggests that the enzymes could have different kinetic constants or substrate specificities. Thus, it is possible that the three isolates represent two different ecotypes within the community. Typical SBR operational conditions generate sharp substrate gradients and periods of aeration and anoxia, situations that generate multiple ecological niches allowing different ecotypes to coexist (Chiesa et al. 1984; Irvine and Ketchum 1989). In the SBRs used in this study, the alternation between phenol and TCE exposure and their respective concentration gradients, in addition to an 11 hour endogenous decay phase in the phenol-fed reactor provide several alternatives for the coexistence of different ecotypes in the same system.

The SYBR green real-time PCR method was used to quantify a group of selected isolates in the reactor. This method has been successfully used to quantify the abundance of bacteria (Rantakokko-Jalava and Jalava 2001; Riley-Buckley 2001), viruses (Wang et al. 2002), and cysts (Limor et al. 2002) from different sources. Since the target gene for quantification was the 16S rDNA, calibration curves were constructed using known numbers of lysed cells as the template to account for differences in genome size and rRNA operon copy number in the different isolates. Calibration curves constructed using this approach resulted in linear correlations over a range of five orders of magnitude, with a limit of detection of one cell per reaction (Figure 4.7). Similar results were observed for *Ralstonia solanacearum* calibration curves, where the limit of detection was 0.2 cells per reaction (Weller et al. 2000), a value observed with some of the calibration curves of the isolates. One of the possible reasons for the low detection limit of the assay is the high growth rates of microbes used for the calibration curves. Fast growing microorganisms could have more than one genome copy per cell, a feature that is not accounted for by direct or viable counts, and hence will overestimate the sensitivity of the assay (Ludwig and Schleifer 2000). However, Hristova and coworkers constructed calibration curves for strain PM1 cells harvested at logarithmic and stationary phases of growth, and found only a small difference in the slope of the curves (0.08); with a sensitivity of 0.3 cells per reaction (Hristova et al. 2001). These results suggest that the low sensitivity of SYBR green real-time PCR using 16S rRNA as a target could be caused by the operon copy number, although detailed studies

comparing the quantification using single and multi copy genes are needed to address this question. Nevertheless, SYBR green real-time PCR using cell calibration curves is a sensitive approach to quantify bacterial populations in environmental samples and should not require knowledge of rRNA operon copy number and genome size of the organisms of interest.

The reproducibility of the SYBR green real-time PCR was determined by analyzing eight replicate samples from each reactor. Cell quantifications using two different primer sets yielded 95 % confidence intervals within the same order of magnitude. These findings indicate that the SYBR green real-time PCR method is reproducible and that reactor samples were homogeneous and representative of the microbial communities studied.

The total bacterial density in the reactors was determined using bacterial specific 16S rDNA primers as described previously (Riley-Buckley 2001), but using *Pseudomonas stutzeri* JM300 as the reference microorganism for the cell calibration curves. This microorganism was used as a reference because it has four copies of the rRNA operon and a genome size of approximately four megabases, values that could be considered average for prokaryotes. Although systematic error could occur depending on the microorganism used as a reference, this approach revealed that there were differences in the abundance and dynamics of bacteria in the two reactors (Figures 4.10-4.11). The bacterial abundance in the phenol-fed reactor fluctuated between 10^6 to 10^9 cells x μg of community DNA. In contrast, the phenol plus TCE-fed reactor had more stable values that ranged between 10^7 to 10^8 cells x μg of community DNA⁻¹. The

differences in bacterial density and stability between the two reactors could have been caused by the presence of predatory organisms, i.e. protozoa and rotifers. Schmidt and coworkers studied the interactions between bacteria and microflagellates in SBRs exposed to 2,4-dinitrophenol (DNP) and found that DNP exposure alone resulted in decreased densities of predatory organisms (Schmidt et al. 1992). The SBR that was fed both DNP and glucose had higher densities of bacteria, but their densities oscillated, suggesting that predator-prey interactions must have occurred. Since rotifers and protozoa were observed more frequently in the phenol-fed reactor, it is possible that predator-prey interactions could have played a role determining the total bacterial densities. These results support previous findings that suggest that the community in the phenol-fed reactor was more dynamic than the community in the phenol plus TCE-fed reactor (Chapter 2).

Quantification of selected isolates in the two reactors revealed that the unidentified group of isolates belonging to the *Comamonadaceae* family of the β -*Proteobacteria* class (SBR-T12, P10 and T15) were the predominant group among the isolates enumerated in both reactors (Figures 4.10-4.13). In the phenol-fed reactor the dynamics of this group mimic the total bacterial dynamics, with cell densities that were in the range of 10^6 - 10^7 cells x μ g of community DNA. Interestingly, the abundance of SBR-T12, P10 and T15 increased almost one fold during days 630-729, a period where high TCE degradation rates were registered in the phenol-fed reactor (Chapter 2). This finding suggests that, perhaps, this phylogenetic group could be involved in the increased performance

of the system during that time period. In contrast, the abundance of the SBR-T12, P10 and T15 was relatively stable in the phenol plus TCE-fed reactor with densities that oscillated between 10^6 - 10^7 cells x μ g of community DNA after day 127 of operation. As determined before, this group of microorganisms grows on phenol and cometabolizes TCE when vitamins were supplied in the medium (Table 4.3). Furthermore, when grown in phenol these isolates form aggregates similar to the ones observed in the phenol-fed reactor. This evidence supports the SYBR green real-time PCR data that the group of isolates SBR-T12, P10 and T15 could be one of the predominant TCE degrading groups in both reactors.

When the abundances of the remaining phenol and TCE degraders and the non-phenol degraders were compared, some differences between the two reactors could be observed. The abundance of *Phenylobacter* sp. SBR-T23, a poor phenol degrader, was higher in the phenol plus TCE-fed reactor by one or two orders of magnitude. Members of this genus are not known to degrade simple aromatic rings like phenol, but they do degrade polycyclic aromatic herbicides (Schmidt et al. 1984). *Variovorax* sp. SBR-T4, a phenol and TCE degrader was also more abundant in the phenol plus TCE-fed reactor with densities up to 10^4 cells x μ g of community DNA. In contrast the abundance of the phenol and TCE degrader SBR-T20 was lower in the phenol plus TCE-fed reactor.

The analysis of non-phenol degrading populations revealed that some isolates were as abundant as the phenol degraders described above. For

instance, *Microbacterium* sp. SBR-T14 was one of the most abundant non-degrading isolates tested with cell densities that reached 10^3 - 10^4 cells x μ g of community DNA in the phenol plus TCE-fed reactor (Figure 4.13). Other, slow growing microorganisms such as ammonia oxidizers were also present in both reactors. These results suggest that TCE application could increase the abundance of several microbial populations in the reactor. Some microorganisms could have reduced affinity for TCE, thus giving them a competitive advantage over TCE degraders. Others, might grow on the TCE degradation products or cell constituents following cell death. Since TCE metabolites seem to be toxic to some cells and predation occurs in these communities, substrates from dead cells could have a major effect on maintaining non-phenol degrading populations in the system. Analysis of reactor samples using an alternative electron acceptor, 5-cyano-2,3 ditolyl tetrazolium chloride (CTC), indicated that cells were actively respiring 6 h after phenol was completely depleted, further supporting this hypothesis. Finally other microbes might be responding in a secondary manner to the primary organisms selected by phenol or TCE. For instance, shortly after phenol addition, the suspended solids from the phenol plus TCE-fed reactor briefly turned yellow. This color change was likely caused by the accumulation of 2-hydroxymuconic semialdehyde (2-HMS), a metabolite of the phenol degradation pathway that often briefly accumulates. This intermediate could diffuse out from the cell and can be used by other non-phenol degrading strains for growth. From these results, it is clear that the phenol and TCE degrading characteristics

of the isolates were not sufficient to predict population abundances in the community.

An understanding of the selective pressure exerted by TCE is necessary for the successful use of cometabolism for TCE bioremediation. Several studies on pure cultures revealed that TCE cometabolism yields intermediates that are toxic to the cells, such as a short lived TCE epoxide that alkylates proteins, DNA and RNA (Wackett and Householder 1989; Rasche and Hyman 1991). Furthermore, studies using purified oxygenases from *Pseudomonas putida* F1 and *Burkholderia cepacia* G4 revealed that TCE cometabolism results in enzyme inactivation and covalent modification of the oxygenases (Li and Wackett 1992; Newman and Wackett 1997a). Hence, it is reasonable to hypothesize that TCE exposure will result in a negative selective pressure that will lead to the disappearance of TCE cometabolizing populations and the take over by non-active populations (Fries et al. 1997a; Mars et al. 1998). In fact, Munakata-Marr et al. observed a decrease in TCE removal in aquifer microcosms that were fed lactate and TCE over a period of 280 days (Munakata-Marr et al. 1997). However, after ceasing the bioaugmentation in the microcosms, they still saw steady removal of TCE for at least 150 days in one of them. Studies in mixed cultures of known toluene and TCE degraders suggests that TCE will have a negative effect on the competitive behavior of toluene degraders that cometabolize TCE (Mars et al. 1998). In our study several phenol and TCE degraders were isolated from the phenol plus TCE-fed reactor after one year of TCE exposure. Moreover, the most abundant group of isolates

in both reactors degrade phenol and cometabolize TCE. These results suggest that long-term TCE application will not always result in the disappearance of TCE degraders by the hypothesized negative selection.

The remaining question is how TCE degrading populations successfully persisted in a reactor that was exposed to TCE twice per day. As observed previously (Chapter 3) the addition of TCE resulted in an increase in the amount of extracellular polymeric substances (EPS) in the total suspended solids. Yeager and coworkers observed that some the toxic TCE intermediates could diffuse out from *Burkholderia cepacia* G4 cells exposed to TCE and affect the viability of G4 mutants with inactive toluene monooxygenases (Yeager et al. 2001). Furthermore, studies on chemostats continuously fed phenol, and pulsed with ^{14}C -TCE for 15 days revealed that 42 % of the radiolabeled TCE became soluble transformation products (Shurtliff et al. 1996). Thus, it is possible that EPS could reduce the diffusion of TCE or some of the diffusible toxic intermediates, resulting in the survival of TCE degraders. The most dominant group of phenol and TCE degraders forms granules when grown on phenol or phenol and TCE providing further support to this idea. Another possible explanation for the success of TCE degraders is that continuous TCE application selected for microbes with increased resistance to TCE toxicity. If the microorganisms can resist TCE intermediate toxicity, negative selection will not occur, and the abundances of TCE degraders will be determined by factors such as competition for primary substrate. Experiments on *Ralstonia eutropha* JM134 derivatives revealed that microbes extremely resistant to TCE exist, since this

strain was resistant up to 800 μM TCE, approximately 100 mg/l (Ayoubi and Harker 1998). TCE degradation rates could also be a factor that determines the success of TCE degraders under prolonged TCE exposure. Comparative studies between *Ralstonia* sp. KN1 constructs carrying a monooxygenase or a dioxygenase suggest that the degradation rate of the enzyme will determine the duration of the activity (Ishida and Nakamura 2000). The dioxygenase construct exhibited faster initial TCE degradation rates that rapidly decreased in comparison with the construct that was carrying the monooxygenase that had higher and stable degradation rates. This suggests that fast TCE degraders become inactive because they can not handle product toxicity as well as slow degraders. Finally, the success of TCE degrading populations in a TCE-fed reactor could also be caused by changes in gene expression. The operational cycles of the SBRs include substrate gradients and periods of endogenous decay. Since TCE is fed 6 hours after phenol addition it is possible that some enzymes are inactive by the time TCE is fed, and avoid the toxicity generated from the intermediates. This will allow TCE degraders to be dominant in a system without being affected by toxicity. The answer to the question of how phenol and TCE degraders persist in mixed communities under long-term exposure to TCE is probably a combination of factors.

The results from this study indicate that long-term TCE application does not result in the disappearance of TCE degrading populations. Several TCE degraders with different phenol hydroxylases were isolated from the TCE-fed reactor. Quantification of the TCE degraders and other isolates indicates that

one group of phenol and TCE degraders is a predominant member of both reactor communities. These findings suggest that TCE degraders can persist in natural communities exposed to TCE for a prolonged period of time making cometabolism a feasible treatment for this ubiquitous pollutant.

References

- Altschul, S. F., W. Gish, W. Miller, E. W. Myers and D. J. Lipman. (1990).** Basic local alignment search tool. *J. Mol. Biol.* **215**: 403-410.
- Amman, R. I., W. Ludwig and K. H. Schleifer. (1995).** Phylogenetic identification and in situ detection of individual microbial cells without cultivation. *Microbiol. Rev.* **59**: 143-169.
- ATSDR. (1994).** National exposure registry. Trichloroethylene (TCE) subregistry baseline technical report (revised). Agency for Toxic Substances and Disease Registry, U.S. Public Health Service, Department of Health and Human Services. **NTIS Publication No. PB95-154589**: Atlanta, Georgia.
- Ayoubi, P. J. and A. R. Harker. (1998).** Whole-cell kinetics of trichloroethylene degradation by phenol hydroxylase in a *Ralstonia eutropha* JMP134 derivative. *Appl. Environ. Microb.* **64**: 4353-4356.
- Bond, P. L., R. Erhart, M. Wagner, J. Keller and L. L. Blackall. (1999).** Identification of some of the major groups of bacteria in efficient and nonefficient biological phosphorus removal in activated sludge. *Appl. Environ. Microb.* **65**: 4077-4084.
- Bond, P. L., P. Hugenholtz, J. Keller and L. L. Blackall. (1995).** Bacterial community structures of phosphate-removing and non-phosphate-removing activated sludges from sequencing batch reactors. *Appl. Environ. Microb.* **61**: 1910-1916.
- Cadieux, E., V. Vrajmasu, C. Achim, J. Powlowski and E. Münck. (2002).** Biochemical, Mossbauer, and EPR studies of the diiron cluster of phenol hydroxylase from *Pseudomonas* sp. strain CF 600. *Biochemistry* **41**: 10680-10691.
- Canada, K. A., S. Iwashita, H. Shim and T. K. Wood. (2002).** Directed evolution of toluene ortho-monooxygenase for enhanced 1-naphthol synthesis and chlorinated ethene degradation. *J. Bacteriol.* **184**: 344-349.

- Chiesa, S. C., R. L. Irvine and J. F. Manning. (1984).** Feast/famine growth environments and activated sludge selection. *Biotechnol. Bioeng.* **27**: 562-569.
- Christensen, B. B., J. A. J. Haagensen, A. Heydorn and S. Molin. (2002).** Metabolic commensalism and competition in two-species microbial consortium. *Appl. Environ. Microb.* **68**: 2495-2502.
- Collantes-Fernández, E., A. Zaballos, G. Alvarez-García and L. M. Ortega-Mora. (2002).** Quantitative detection of *Neospora caninum* in bovine aborted fetuses and experimentally infected mice by real-time. *J. Clin. Microbiol.* **40**: 1194-1198.
- Corless, C. E., M. Guiver, R. Borrow, V. Edward-Jones, E. B. Kaczmarek and A. J. Fox. (2000).** Contamination and sensitivity issues with real-time universal 16S rRNA PCR. *J. Clin. Microbiol.* **38**: 1747-1752.
- De Preter, K., F. Speleman, V. Combaret, J. Lunec, G. Laureys, B. H. J. Eussen, N. Francotte, J. Board, A. D. J. Pearson, A. De Paepe, N. Van Roy and J. Vandesompele. (2002).** Quantification of MYCN, DDX1, and NAG gene copy number in neuroblastoma using a real-time quantitative PCR assay. *Mod. Pathol.* **15**: 159-166.
- Denner, E. B. M., S. Paukner, P. Kampf, E. R. B. Moore, W. R. Abraham, H. J. Busse, G. Wanner and W. Lubitz. (2001).** *Sphingomonas pituitosa* sp. nov., an exopolysaccharide-producing bacterium that secretes an unusual type of sphingolipid. *Int. J. Syst. Evol. Microbiol.* **51**: 827-841.
- Dhar, A. K., M. M. Roux and K. R. Klimpel. (2002).** Quantitative assay for measuring the taura syndrome virus and yellow head virus load in shrimp by real-time RT-PCR using SYBR Green chemistry. *J. Virol. Methods* **104**: 69-82.
- Eberspacher, J. (2002).** The genus *Phenylobacterium*. In *The Prokaryotes*. M. Dworkin. <http://link.springer-ny.com/link/service/books/10125/tocs.htm>, Springer verlag.
- Ehrt, S., F. Schirmer and W. Hillen. (1995).** Genetic organization, nucleotide sequence and regulation of expression of genes encoding phenol hydroxylase and catechol 1,2-dioxygenase in *Acinetobacter calcoaceticus* NCIB8250. *Mol. Microbiol.* **18**: 13-20.
- Folsom, B. R., P. J. Chapman and P. H. Pritchard. (1990).** Phenol and trichloroethylene degradation by *Pseudomonas cepacia* G4 - kinetics and interactions between substrates. *Appl. Environ. Microb.* **56**: 1279-1285.

- Fox, B. G., J. Shanklin, C. Somerville and E. Münck.** (1993). Stearoyl-acyl carrier protein Δ^9 desaturase from *Ricinus communis* is a diiron-oxo protein. *Proc. Natl. Acad. Sci* **90**: 2486-2490.
- Fredrickson, J. K., D. L. Balkwill, G. R. Drake, M. F. Romine, D. B. Ringelberg and D. C. White.** (1998). Aromatic-degrading *Sphingomonas* isolates from the deep subsurface. *Appl. Environ. Microb.* **61**.
- Fries, M. R., L. J. Forney and J. M. Tiedje.** (1997a). Phenol- and toluene-degrading microbial populations from an aquifer in which successful trichloroethene cometabolism occurred. *Appl. Environ. Microb.* **63**: 1523-1530.
- Fries, M. R., G. D. Hopkins, P. L. McCarty, L. J. Forney and J. M. Tiedje.** (1997b). Microbial succession during a field evaluation of phenol and toluene as the primary substrates for trichloroethene cometabolism. *Appl. Environ. Microb.* **63**: 1515-1522.
- Futamata, H., S. Harayama and K. Watanabe.** (1998). Diversity in kinetics of trichloroethylene-degrading activities exhibited by phenol-degrading bacteria. *Appl. Microbiol. Biotech.* **55**: 248-253.
- Futamata, H., S. Harayama and K. Watanabe.** (2001). Group-specific monitoring of phenol hydroxylase genes for a functional assessment of phenol-stimulated trichloroethylene bioremediation. *Appl. Environ. Microb.* **67**: 4671-4677.
- Garrity, G. M., M. Winters and D. B. Searles.** (2001). Taxonomic outline of the prokaryotic genera bergey's manual of systematic bacteriology. [Online] Bergey's manual of systematic bacteriology. Second edition. <http://www.cme.msu.edu/bergeys/april2001-genus.pdf>.
- Giovannoni, S. J.** (1991). The polymerase chain reaction. *In* Nucleic acids techniques in bacterial systematics. E. Stackebrandt. New York, John Wiley & Sons 177-201.
- Grüntzig, V., S. C. Nold, J. Z. Zhou and J. M. Tiedje.** (2001). *Pseudomonas stutzeri* nitrite reductase gene abundance in environmental samples measured by real-time PCR. *Appl. Environ. Microb.* **67**: 760-768.
- Hall, T. A.** (1999). BioEdit: a user-friendly biological sequence alignment editor and analysis program for Windows 95/98/NT. *Nucl. Acids. Symp. Ser* **41**: 95-98.
- Heinaru, E., J. Truu, U. Stottmeister and A. Heinaru.** (2000). Three types of phenol and p-cresol catabolism in phenol- and p-cresol-degrading bacteria isolated from river water continuously polluted with phenolic compounds. *FEMS Microbiol. Ecol.* **31**: 195-205.

- Hopkins, G. D., J. Munakata, L. Semprini and P. L. McCarty.** (1993a). Trichloroethylene concentration effects on pilot field-scale in-situ groundwater bioremediation by phenol-oxidizing microorganisms. *Environ. Sci. Technol.* **27**: 2542-2547.
- Hopkins, G. D., L. Semprini and P. L. McCarty.** (1993b). Microcosm and in-situ field studies of enhanced biotransformation of trichloroethylene by phenol-utilizing microorganisms. *Appl. Environ. Microb.* **59**: 2277-2285.
- Hristova, K. R., C. M. Lutenecker and K. M. Scow.** (2001). Detection and quantification of methyl tert-butyl ether- degrading strain PM1 by real-time TaqMan PCR. *Appl. Environ. Microb.* **67**: 5154-5160.
- Hugenholtz, P., B. M. Gobel and N. R. Pace.** (1998). Impact of culture-independent studies on the emerging phylogenetic view of bacterial diversity. *J. Bacteriol.* **180**: 4765-4774.
- Irvine, R. L. and L. H. Ketchum.** (1989). Sequencing batch reactors for biological wastewater treatment. *CRC crit. Rev. Env. Cont.* **18**: 255-294.
- Ishida, H. and K. Nakamura.** (2000). Trichloroethylene degradation by *Ralstonia* sp. KN1-10A constitutively expressing phenol hydroxylase: transformation products, NADH limitation and product toxicity. *J. Biosc. Eng.* **5**: 438-445.
- Johnson, G. R. and R. H. Olsen.** (1995). Nucleotide sequence analysis of genes encoding a toluene/benzene-2-monooxygenase from *Pseudomonas* sp. strain JS150. *Appl. Environ. Microb.* **61**: 3336.
- Juretschko, S., A. Loy, A. Lehner and M. Wagner.** (2002). The microbial community composition of a nitrifying-denitrifying activated sludge from an industrial sewage treatment plant analyzed by the full-cycle rRNA approach. *System. Appl. Microbiol.* **25**: 84-99.
- Kämpfer, P., R. Erhart, C. Beimfohr, J. Böhringer, M. Wagner and R. I. Amman.** (1996). Characterization of bacterial communities from activated sludge: culture-dependent numerical identification versus in situ identification using group and genus specific rRNA-targeted oligonucleotide probes. *Microb. Ecol.* **32**: 101-121.
- Kim, I. C. and P. J. Oriel.** (1995). Characterization of the *Bacillus stearothermophilus* BR219 phenol hydroxylase gene. *Appl. Environ. Microb.* **61**: 1252-1256.
- La Scola, B., L. Barrassi and D. Raoult.** (2000). Isolation of new fastidious α *Proteobacteria* and *Afipia felis* from hospital water supplies by direct plating and amoebal co-culture procedures. *FEMS Microbiol. Ecol.* **34**: 129-137.

- Li, S. Y. and L. P. Wackett.** (1992). Trichloroethylene oxidation by toluene dioxygenase. *Biochem. Biophys. Res. Commun.* **185**: 443-451.
- Limor, J. R., A. A. Lal and L. H. Xiao.** (2002). Detection and differentiation of *Cryptosporidium* parasites that are pathogenic for humans by real-time PCR. *J. Clin. Microbiol.* **40**: 2335-2338.
- Ludwig, W. and K. H. Schleifer.** (2000). How quantitative is quantitative PCR with respect to cell counts? *System. Appl. Microbiol.* **23**: 556-562.
- Maidak, B. L., J. R. Cole, T. G. Lilburn, C. T. J. Parker , P. R. Saxman, R. J. Farris, G. M. Garrity, G. J. Olsen, T. M. Schmidt and J. M. Tiedje.** (2001). The RDP-II (Ribosomal Database Project). *Nucleic. Acids. Res.* **29**: 173-174.
- Mars, A. E., J. Houwing, J. Dolfing and D. B. Janssen.** (1996). Degradation of toluene and trichloroethylene by *Burkholderia cepacia* G4 in growth-limited fed-batch culture. *Appl. Environ. Microb.* **62**: 886-891.
- Mars, A. E., G. T. Prins, P. Wietzes, W. de Koning and D. B. Janssen.** (1998). Effect of trichloroethylene on the competitive behavior of toluene-degrading bacteria. *Appl. Environ. Microb.* **64**: 208-215.
- Munakata-Marr, J., V. G. Matheson, L. J. Forney, J. M. Tiedje and P. L. McCarty.** (1997). Long-term biodegradation of trichloroethylene influenced by bioaugmentation and dissolved oxygen in aquifer microcosms. *Environ. Sci. Technol.* **31**: 786-791.
- Nadkarni, M. A., F. E. Martin, N. A. Jacques and N. Hunter.** (2002). Determination of bacterial load by real-time PCR using a broad- range (universal) probe and primers set. *Microbiology* **148**: 257-266.
- Nelson, M. J. K., S. O. Montgomery, W. R. Mahaffey and P. H. Pritchard.** (1987). Biodegradation of trichloroethylene and involvement of an aromatic biodegradative pathway. *Appl. Environ. Microb.* **53**: 949-954.
- Newman, L. M. and L. P. Wackett.** (1997a). Trichloroethylene oxidation by purified toluene 2- monooxygenase: products, kinetics, and turnover-dependent inactivation. *J. Bacteriol.* **179**: 90-96.
- Newman, L. M. and L. P. Wackett.** (1997b). Trichloroethylene oxidation by purified toluene 2-monooxygenase: products, kinetics, and turnover dependent inactivation. *J. Bacteriol.* **179**: 90-96.
- Olsen, G. J., H. Matsuda, R. Hagstrom and R. Overbeek.** (1994). FastDNAmI : a tool for construction of phylogenetic trees of DNA sequences using maximum likelihood. *Comput. Appl. Biosci* **10**: 41-48.

- Rademaker, J. L., F. J. Louws and F. J. de Bruijn.** (1998). Characterization of the diversity of ecologically important microbes by rep-PCR fingerprinting. *In* Molecular microbial ecology manual. A. D. L. Akkermans, J. D. van Elsas and F. J. de Bruijn. Dordrecht, The Netherlands, Kluwer Academic Publishers.
- Rantakokko-Jalava, K. and J. Jalava.** (2001). Development of conventional and real-time PCR assays for detection of *Legionella* DNA in respiratory specimens. *J. Clin. Microbiol.* **39**: 2904-2910.
- Rasche, M. E. and Hyman.** (1991). Factors limiting aliphatic chlorocarbon degradation by *Nitrosomonas europaea*-cometabolic inactivation of ammonia monooxygenase and substrate specificity. *Appl. Environ. Microb.* **57**: 2986-2994.
- Rhodes, A. N., J. W. Urbance, H. Youga, H. Corlew-Newman, C. A. Reddy, M. J. Klug, J. M. Tiedje and D. C. Fisher.** (1998). Identification of bacterial isolates obtained from intestinal contents associated with 12,000-year-old mastodon remains. *Appl. Environ. Microb.* **64**: 651-658.
- Riley-Buckley, M.** (2001). Microbial communities in pristine and tetrachloroethylene-contaminated aquifer sediment. Ph. D. Dissertation. Michigan State University, East Lansing, MI.
- Ririe, K. M., R. P. Rasmussen and C. T. Witter.** (1997). Product differentiation by analysis of DNA melting curves during the polymerase chain reaction. *Anal. Biochem.* **245**: 154-160.
- Schmidt, S., R. Muller and R. Lingens.** (1984). Chloridazon-catechol dioxygenases, a distinct group of meta-cleaving enzymes. *Hoppe Seyler's Z. Physiol. Chem.* **365**: 143-150.
- Schmidt, S. K., R. Smith, D. Sheker, T. F. Hess, J. Silverstein and P. M. Radehaus.** (1992). Interactions of bacteria and microflagellates in sequencing batch reactors exhibiting enhanced mineralization of toxic organic chemicals. *Microb. Ecol.* **23**: 127-142.
- Shurtliff, M. M., G. F. Parkin, L. J. Weathers and T. J. Gibson.** (1996). Biotransformation of trichloroethylene by a phenol-induced mixed culture. *J. Env. Eng.* **122**: 581-589.
- Stackebrandt, E. and B. M. Goebel.** (1994). Taxonomic note: a place for DNA-DNA reassociation and 16S rRNA sequence analysis in the present species definition in bacteriology. *Int. J. Syst. Bacteriol.* **44**: 846-849.
- Strunk, O. and W. Ludwig.** (1995). ARB: a software environment for sequence data. Department of Microbiology **Technical University of Munich, Munich Germany**: <http://www.mikro.biologie.tu-muenchen.de>.

- Stubner, S., T. Wind and R. Conrad.** (1998). Sulfur oxidation in rice field soil: activity, enumeration, isolation and characterization of thiosulfate-oxidizing bacteria. *System. Appl. Microbiol.* **21**.
- Thompson, J. D., T. J. Gibson, F. Plewniak, F. Jeanmougin and D. G. Higgins.** (1997). The clustalX windows interface: flexible strategies for multiple sequence alignment aided by quality analysis tools. *Nucleic. Acids. Res.* **24**: 4876-4882.
- Uchiyama, H., T. Nakajima, O. Yagi and T. Nakahara.** (1992). Role of heterotrophic bacteria in complete mineralization of trichloroethylene by *Methylocystis* sp. strain M. *Appl. Environ. Microb.* **58**: 3067-3071.
- Wackett, L. P. and D. T. Gibson.** (1988). Degradation of trichloroethylene by toluene dioxygenase in whole-cell studies with *Pseudomonas putida* F1. *Appl. Environ. Microb.* **54**: 1703-1708.
- Wackett, L. P. and S. R. Householder.** (1989). Toxicity of trichloroethylene to *Pseudomonas putida* F1 is mediated by toluene dioxygenase. *Appl. Environ. Microb.* **55**: 2723-2725.
- Wagner, M., R. I. Amman, H. Lemmer and K. H. Schleifer.** (1993). Probing activated sludge with oligonucleotides specific for proteobacteria: inadequacy of culture-dependent methods for describing microbial community structure. *Appl. Environ. Microb.* **59**: 1520-1525.
- Wang, C. Y. J., J. J. Giambrone and B. F. Smith.** (2002). Detection of duck hepatitis B virus DNA on filter paper by PCR and SYBR green dye-based quantitative PCR. *J. Clin. Microbiol.* **40**: 2584-2590.
- Watanabe, K., M. Teramoto, H. Futamata and S. Harayama.** (1998). Molecular detection, isolation, and physiological characterization of functionally dominant phenol-degrading bacteria in activated sludge. *Appl. Environ. Microb.* **64**: 4396-4402.
- Watanabe, K., M. Teramoto and S. Harayama.** (1999). An outbreak of nonflocculating catabolic populations caused the breakdown of a phenol-digesting activated-sludge process. *Appl. Environ. Microb.* **65**: 2813-2819.
- Weller, S. A., J. G. Elphinstone, N. C. Smith, N. Boonham and D. E. Stead.** (2000). Detection of *Ralstonia solanacearum* strains with a quantitative, multiplex, real-time, fluorogenic PCR (TaqMan) assay. *Appl. Environ. Microb.* **66**: 2853-2858.
- Wilmotte, A., G. Van der Auwera and R. De Wachter.** (1993). Structure of the 16S ribosomal RNA of the thermophilic cyanobacterium *Chlorogloeopsis* HTF (*Mastigocladus laminosus* HTF) strain PCC7518, and phylogenetic analysis. *FEBS Lett.* **317**:96-100.

Wolin, F. A., M. J. Wolin and R. S. Wolfe. (1963). Formation of methane by bacterial extracts. *J. Biol. Chem* **238**: 2882-2886.

Yeager, C. M., P. J. Bottomley and D. J. Arp. (2001). Cytotoxicity associated with trichloroethylene oxidation in *Burkholderia cepacia* G4. *Appl. Environ. Microb.* **67**: 2107-2115.

CHAPTER 5

CONCLUSIONS, SYNTHESIS AND FUTURE DIRECTIONS

Conclusions

Microbial communities are probably the least studied but most important component of bioreactors. Knowledge about bioreactor community structure can likely lead to improved design and operation of these systems. The aim of this dissertation was to determine the long-term effects of TCE application on the microbial community of a particular type of reactor system, sequencing batch reactor. The major findings of this research can be summarized as follows:

1. Long-term TCE application selected a microbial community with low but stable TCE degradation rates.
2. Community succession was dependent on the substrates applied and random factors. When phenol was the only substrate applied, the community never reached stability. On the other hand, when both phenol and TCE were applied a relatively stable microbial community was selected.
3. TCE application resulted in an increase in EPS accumulation and the formation of "star-like" flocs. The EPS was mainly composed of neutral six carbon sugars, with rhamnose being the most abundant.
4. Sequencing batch reactors fed a single growth substrate harbor diverse microbial communities. A major proportion of the isolates belonged to the *Proteobacteria* phylum.

5. Phenol did not enrich for phenol degraders exclusively since the majority of the isolated strains did not grow on phenol as the sole carbon source. Cross-feeding interactions must have occurred between and among different populations in the reactors.
6. Phenol hydroxylases of different phylogenetic groups were present in the SBR communities. Unknown oxygenase diversity apparently exists in the phenol degraders whose degradative genes could not be amplified with the “conserved” phenol hydroxylase primers.
7. A novel group of phenol and TCE degraders from the *Comamonadaceae* family of the β -*Proteobacteria* were among the predominant populations in both reactors.
8. Long-term TCE application did not result in the extinction of TCE degrading populations.

Synthesis

In this dissertation complementary community analysis approaches were used to address the research questions centered on discerning relationships between community structure and function. Nucleic acids analyses, kinetic measures, isolation and characterization of strains, and community physiological measurements were the methods used to determine the effects of long-term TCE application on the SBR microbial community. This polyphonic community analysis approach allows the establishment of interrelationships between community structure, function and the member organisms' physiology, providing

a more comprehensive overview of the communities studied. The results of several of these measures are combined in Figure 5.1 so that they can be better compared and interpreted together.

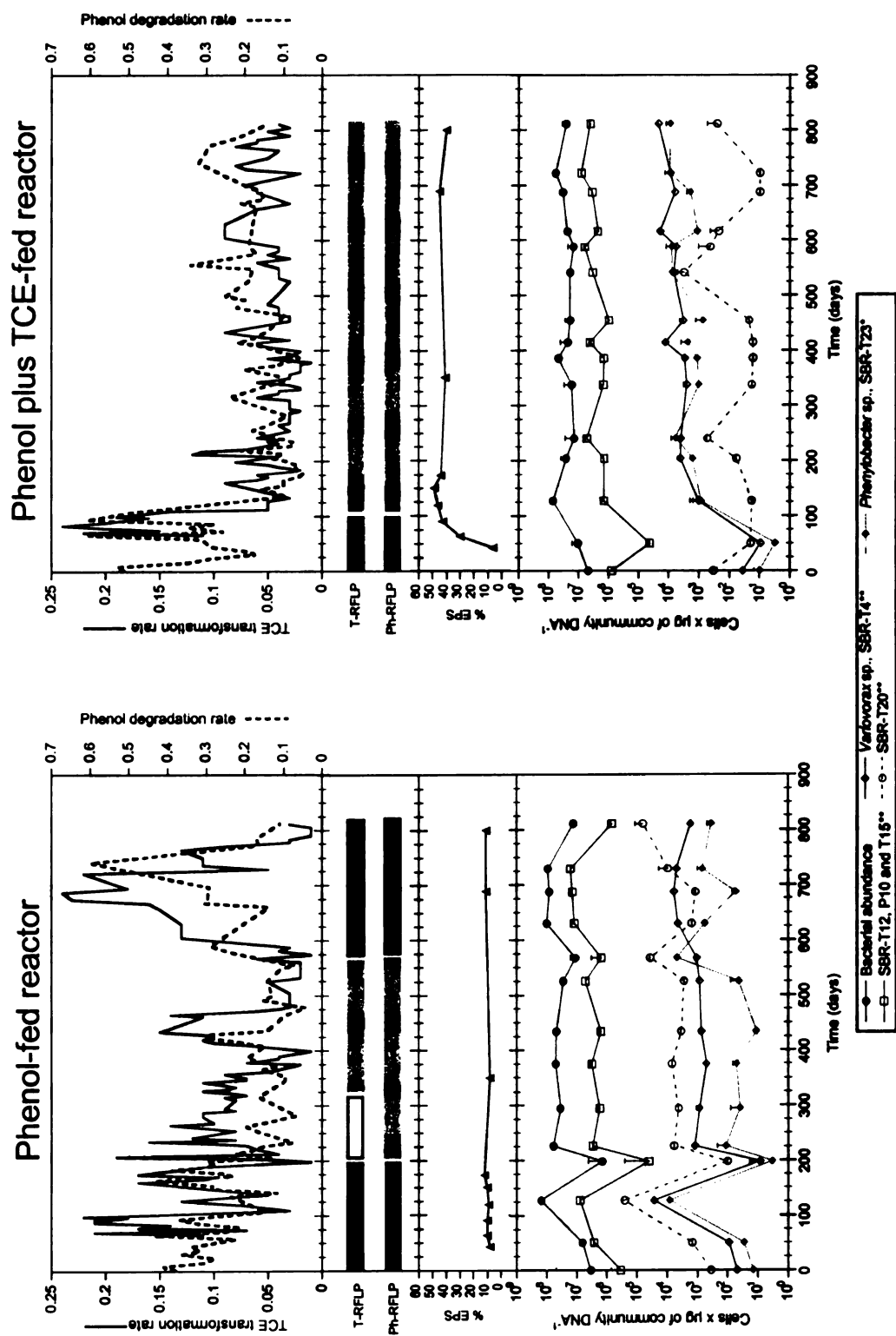


Figure 5.1. Summary of community analysis results. Ph-RFLP, phenol hydroxylase restriction fragment length polymorphism analysis. *, phenol degrader; **, phenol and TCE degrader. Grey, white and black bars represent time periods when the community structure was similar within and between reactors, based on multivariate analysis (T-RFLP), and cluster analysis (Ph-RFLP).

As presented earlier, long-term phenol application (phenol-fed reactor) resulted in a microbial community with dynamic structure and function (Figure 5.1). TCE transformation rates were also variable during 800 days of operation. The highest TCE transformation rates were observed during days 0 to 190 and 567-750 in the phenol fed reactor. The community structure during these two periods was very similar, suggesting that some of the community members were necessary for high TCE degradation rates. Cell densities of several strains, including the predominant group of phenol and TCE degraders, increased during these two periods of high TCE transformation rates. These results suggest that the particular community structure observed during these periods favor phenol and TCE degrading populations.

Major changes in community structure and function occurred after 198 days in the phenol-fed reactor. TCE transformation rates on that day decreased to the lowest values observed followed by rapid increases and decreases. Marked changes in community structure were also observed after 198 days of operation while a significant decrease in total bacterial abundance and strain specific abundance was observed in day 198. Analysis of a second replicate sample of day 198 yielded similar cell densities, further supporting the observed decrease in bacterial abundance. These results suggest that the microbial community was severely perturbed at this point in time. The microbial community structure changed at least one more time during days 198 to 567. TCE degradation rates were variable but not to the degree previously observed. Total bacterial and isolate specific abundances were relatively stable during this

period suggesting that the community structure and function were not closely linked during this period of reactor operation.

TCE application resulted in rapid changes in community structure and function in the phenol plus TCE-fed reactor (Figure 5.1). TCE degradation rates decreased during the first 100 days of operation suggesting that the microbial community was sensitive to TCE exposure. The abundance of isolates SBR-T12, P10 and T15, an important group of TCE degraders, decreased one order of magnitude during the first 50 days of operation. Changes in community structure were also observed during the first 100 days of operation, corroborating that TCE exposure affected the community structure and hence likely the function in the bioreactor.

Although TCE caused some initial changes in community structure, a relatively stable microbial community was selected. The community structure from day 127 to 811 was different from the community structure observed during the first 100 days, and was relatively stable. During this lengthy period, TCE degradation rates were low but relatively stable, suggesting that TCE selected for a community with low TCE transformation rates. The abundance of several phenol and TCE degraders was also relatively stable during this period suggesting that although TCE transformation rates were low, TCE degraders were present in the community in stable densities.

A remaining question is why the microbial community exposed to TCE exhibited high stability compared to the phenol-fed community? An unexpected finding that could explain the survival of TCE degraders and the general stability

of the system was the increase in relative amounts of EPS. During the first 100 days of TCE exposure, the relative abundance of EPS in the total suspended solids increased from 10 to 50 %. EPS concentrations remained relatively stable afterwards, ranging between 40 to 50% during 650 days of operation. The increased EPS resulted in the formation of "star-like" flocs which resemble biofilms. It is possible that EPS protect cells from the toxic effects of TCE and simultaneously causes changes in the spatial distribution of bacteria in the floc, generating a structure that resembles a biofilm. Biofilm communities are more resistant to toxics and the structure is more stable than planktonic communities such as the granular flocs in the phenol-fed reactor.

Future research

Although the aforementioned research provided new insights about the effects of long-term TCE application on the dynamics and physiology of bioreactor communities, new questions emerged that should be intriguing for future investigations.

Community analysis by TRFLP revealed that changes in community structure occurred in both reactor communities. However, the successional patterns in each reactor were different. The data suggests that the community in the phenol plus TCE-fed reactor reached stability after some initial changes, while the community in the phenol-fed reactor never stabilized. Since both of these successional patterns support pre-established ecological theories, further experimentation is needed to determine their generality. Furthermore, the

effects of stressors, such as TCE, on successional patterns and on the resilience of microbial communities to perturbations should be assessed to understand stress responses at the community level. This research should contribute to the development of generalized theory about succession in microbial systems, and to test some of the theories originated in macroecology.

An increase in EPS content was observed in the phenol plus TCE fed reactor. Although the data suggests that TCE induced this response, further work is needed to assess whether the EPS and the resulting “star-like” flocs serve a protective function (Chapter 3). Experiments that assess the effects of TCE or some of its stable intermediates on the accumulation of EPS and the viability of the cultures should test this hypothesis. Isolated strains that produce EPS and degrade TCE will help to better define the role of TCE inducing EPS, and to more accurately determine if the EPS is protecting the cell. Strains from a community producing EPS could also help to determine which populations besides EPS producers are involved in the response. For instance, EPS production does not have to be from phenol and TCE degraders, but could be from non-TCE degrading populations sensitive to TCE intermediates. Such a response could be controlled by quorum sensing. My preliminary tests revealed that the most abundant isolates by real-time quantitative PCR were positive for homoserine lactone production when assayed using *Chromobacterium violaceum* as the reporter strain. To assess which populations are involved in this process, pure and mixed cultures of TCE active and inactive populations should be evaluated in the presence of TCE or similar toxic compounds. These

experiments will increase our knowledge on how individuals or microbial communities respond to toxic stress, a common phenomenon in contaminated sites or when a toxicant is added to a community.

The microbial communities in the SBRs were phylogenetically diverse. The majority of the strains isolated did not degrade phenol under the conditions tested. Abundance data suggests that although they were in low numbers, these populations were constantly present during the 2 years of operation. An important, but difficult to evaluate question is the role of these apparently non-phenol degrading populations. Are these populations necessary for efficient reactor operation, are they detrimental, or are they neutral? For instance, some of these populations could grow on the intermediates of TCE degradation pathway. This will result in the complete mineralization of TCE and detoxification of the system if the TCE metabolites are toxic to other cells. On the other hand, the non-phenol degrading populations could be growing on intermediates from the phenol pathway, resulting in decreased energy for phenol degraders. These phenol inactive populations could also be growing on dead or excreted cell material, or could be involved in the production of vitamins consumed by other populations. To address some of these alternatives, reactor samples can be exposed to ^{13}C -labeled substrates, e.g. phenol, TCE, glyoxylic acid, to generate ^{13}C -labeled cells. The analysis of labeled ribosomal RNA could reveal if the non-phenol degraders consume any of the primary compounds or their derivatives. If the ^{13}C analysis reveals that some of the non-phenol degrading populations consume the primary compounds or the

intermediates then, co-culture experiments could be performed to more accurately determine the metabolic interactions. Ultimately, the bioreactors could be bioaugmented with key non-phenol degrading populations to assess their effect on reactor function and community dynamics.

Phenol and TCE degraders from the *Comamonadaceae* family of the β -*Proteobacteria* were the most abundant population in both reactor communities (Chapter 4). Pure culture studies suggest that TCE degraders are severely affected by TCE metabolites resulting in oxygenase inactivation and reduced viability. Hence, these successful strains should be further characterized to understand why they predominate under TCE exposure. It is possible that these strains possess toxicity resistance mechanisms that allow them to tolerate TCE mediated toxicity. On the other hand, it has been proposed that strains with reduced TCE degradation rates are less prone to TCE metabolite toxicity. These strains should be tested for TCE toxicity, using TCE and the stable TCE metabolites at different concentrations and under different growth conditions to assess if they are more resistant than known strains. Determination of the kinetic constants for TCE and phenol degradation in combination with the toxicity experiments should help to elucidate what phenotypes are selected from long-term TCE application and why.

In a typical SBR system, cells alternate between growth and endogenous decay phases within each cycle. Hence, the SBR cycling could have an effect on the dynamics of cellular components such as RNA and protein. The addition of growth substrates like phenol will trigger the expression of genes involved in

the metabolism of this compound, leading to the synthesis of the necessary proteins. However, the modified SBR cycle used in this study included the addition of TCE, a non-growth substrate that induces its own degradation in pure cultures. To evaluate the effects of the SBR cycles and TCE on the RNA and protein content of the microbial communities, these parameters should be measured during the reactor cycle. This will provide information about how the feeding cycle affects the physiology of the community and as a consequence the function of the system. For instance, the expression of the phenol hydroxylase genes from the dominant phenol and TCE degraders could be studied to evaluate the effects of TCE, and the cycles on the expression of the active enzyme. This information can be related to kinetic measurements to understand the dominance or extinction of different microbes over long-term SBR selection. These experiments will provide more understanding of how microbial communities respond and change under these growth alternating conditions.

APPENDIX A

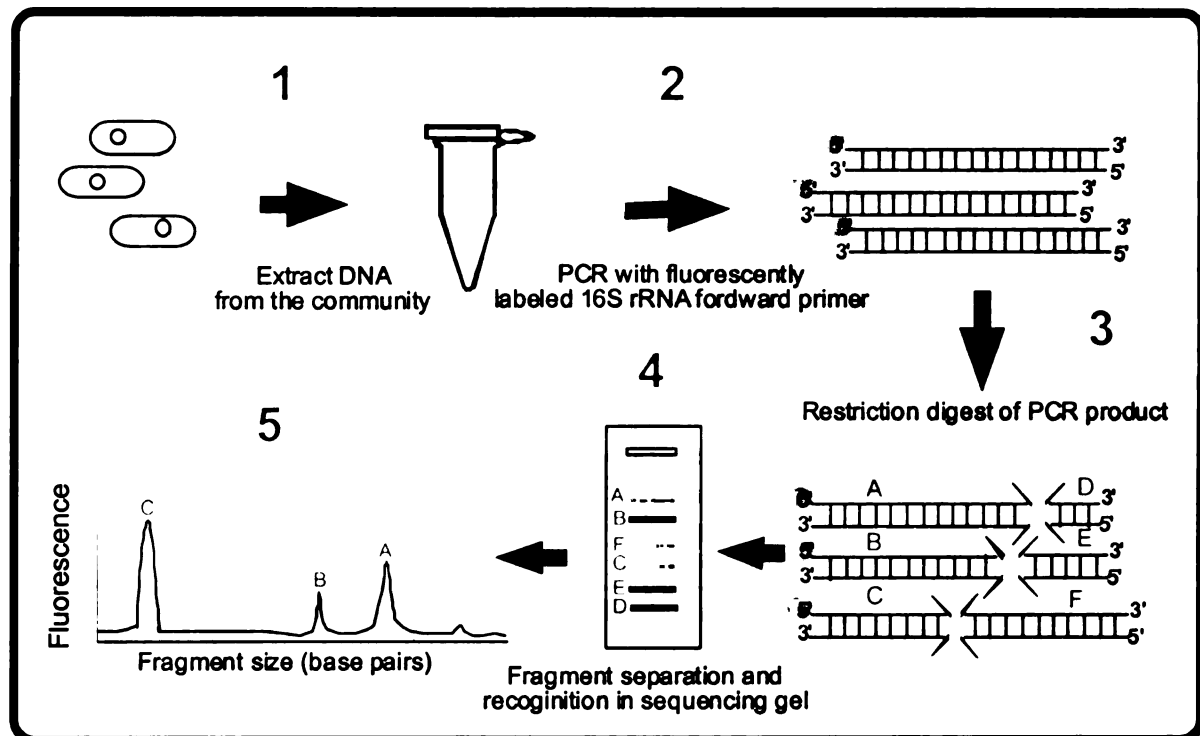
PROTOCOL FOR T-RFLP ANALYSIS OF MICROBIAL COMMUNITIES

This protocol was used for the community structure analysis described on Chapter 2 and in the following published article: Braker, G., H. L. Ayala-del-Río, A. H. Devol and J. M. Tiedje. 2001. Community structure of denitrifiers, bacteria, and archaea, along redox gradients in Pacific Northwest marine sediments by terminal restriction fragment length polymorphism analysis of amplified nitrite reductase (*nirS*) and 16S rRNA genes. *Applied and Environmental Microbiology*. 67:1893-1901. A version modified for use with capillary electrophoreses-based sequencers has been posted on the web as: Improved protocol for T-RFLP by capillary electrophoresis. V. Grüntzig, B. Stres, H. L. Ayala-del-Río, and J. M. Tiedje. http://rdp.cme.msu.edu/html/t-rflp_jul02.html

T-RFLP Protocol

I Principle

Terminal Restriction Eragment Length Polymorphysim (T-RFLP) is a reproducible and high throughput method for the analysis of microbial communities. This method resolves complex microbial communities based on size differences of the terminal fragments of different populations. The figure below illustrates the procedure and the rationale of the method.



First, DNA is harvested from the sample of interest i.e., enrichment cultures, soil, sediment or reactor material (1). The gene of interest is amplified from the community DNA using the polymerase chain reaction (PCR) with a fluorescently labeled primer (2). The mixture of amplicons is purified and digested with a restriction enzyme (3). The different fragments (A-F) are separated in a sequencing gel generating a series of bands (4). A laser reader will recognize only the labeled fragments, and the computer software will calculate the size of the identified fragments and their relative intensity (5).

II. Procedure

A. DNA Extraction

The DNA from the sample should be a uniform representation of the microbial community studied. Therefore, it is important to select an extraction method that allows efficient lysis of the sample and recovery of the DNA. The quality of the DNA is also very important, since DNA contaminated with humic acids will be difficult to amplify. The procedure that I used to extract the DNA from the Sequencing Batch Reactors was a combination of enzymatic digestion with several freeze-thaw cycles.

B. PCR amplification

Primer Selection: The T-RFLP method can be applied to any gene, therefore primer selection will depend on the user's interest and the availability of sufficient sequences to identify conserved regions for primers. For microbial community analysis the 16S rDNA gene is the most commonly used gene since it provides an overview of the microbial community. Several different primers targeting conserved regions of the 16S rDNA molecule have been developed (Amann et al. 1995). Since much of the variability in the 16S rDNA molecule is present in the first 500bp it is recommended to fluorescently label the forward primer. Although there are several different fluorochromes that could be used to label primers, phosphoramidite dye 5-hexachlorofluorescein (HEX) is one of the most commonly used dyes for T-RFLP. The primers I have used to study bacterial and archaeal communities are listed below. The only labeled primers that I have used were forward primers (F), labeled with HEX.

E. coli positioning	Specificity	Sequence (5'→3')	Reference
8→27F	Domain (Bacteria)	AGA GTT TGA TCM TGG CTC AG	(Giovannoni 1991)
1392-1407R	Universal	ACG GGC GGT GTG TAC A	(Amann et al. 1995)
21→40F	Domain (Archaea)	TTC YGG TTG ATC CYG CCR GA	(Moyer et al. 1998)
958→976R	Domain (Archaea)	YCC GGC GTT GAM TCC AAT T	(DeLong 1992)

Composition of the PCR mixture. The following is a modified version of the standard master mix provided by Gibco (Gibco BRL, Gaithersburg, Md.). This mixture could be modified to accommodate different polymerases or to amplify difficult samples by changing the amounts of the different components.

5	10X PCR Buffer (Gibco)
3	50 mM MgCl ₂ (Gibco)
4	2.5 mM dNTP mix (1:1:1:1)
1	Forward primer (10 pMol/μl)
1	Reverse Primer (10pMol/μl)
0.5	BSA (20 mg/ml)
0.5	Taq polymerase (5U/μl) (Gibco)
34	Sterile filtered Mili-Q water
49	Total

Usually 1 μl of template (≈ 20-100ng) is added to each PCR reaction. Since PCR is very sensitive to initial template concentrations, bias can occur between replicate reactions from the same sample. In order to reduce the variability between PCR reactions, at least 3 replicate reactions from each DNA sample should be performed and combined together before further purification.

PCR cycles

The following cycles were used for amplification

95°C 3min	Hot Start/denaturation	} 25-30 cycles
94°C 45 sec	Denaturation	
57°C 1 min	Annealing	
72°C 2 min	Elongation	
72°C 7min	Final Extension	
4°C forever		

The number of cycles to be used will depend on the difficulty of the samples and the specificity of the PCR product. Lower cycles (25) will result in less PCR product but more specific.

C. Purification of the PCR product.

PCR products should be purified before digestion to remove any excess of primer or non-specific PCR products. I recommend the following two methods for product clean up: Microcon concentration or gel extraction. The micron concentration columns will remove any excess of primer but they will not remove any non-specific PCR products. Gel purification will remove both, excess primers and non-specific products. Gel purification is performed by loading all PCR products on an agarose

gel to separate them. The band of the proper size is excised from the gel, and the PCR product is recovered with a gel purification kit (QIAquick gel extraction kit, Qiagen, Chatsworth, Calif.) following the manufacturers recommendations. Is important to check the amount of recovered PCR product on a gel, since a portion of the product will be lost during the purification procedure.

D. Restriction digest of the PCR products

The purified PCR products are digested with a restriction enzyme, usually a four base pair cutter. Restriction enzymes that recognize more than four bases do not cut frequently, resulting in poor resolution of different populations in the community. *HaeIII*, and *HhaI* (*CfoI*) are some of the most effective restriction enzymes for community analysis, although the user is recommended to test several enzymes in order to determine which is the best enzyme for the samples to be studied. The master mix for the restriction reaction is as follows:

1	10X Buffer
1	BSA (1mg/ml)
0.5	Restriction enzyme (10U/μl)
2.5	H ₂ O
5	Total

Add 5 μl of purified PCR product and digest for 2-3 hours at 37°C. Inactivate the enzymes by heating the digest to 65°C for 20 minutes. Store digests at -20°C.

Note: The PCR product should be quantified before being added to the digestion. It is important to use similar amounts of PCR product in order to compare the profiles obtained. However, if a uniform amount of DNA is added to each PCR reactions the amount of product generated should be similar. Quantification can be performed with UV spectrophotometry or gel quantification.

E. Gel separation

An aliquot of the digested PCR products (2 μl) is combined with the TAMRA GS 2500 marker (Perkin Elmer). The mixture is separated in a 6% polyacrylamide gel in a slab gel DNA sequencer (373 ABI Stretch) for 14 hours at 1680 volts. The data are viewed and normalized using GeneScan software version 2.1.

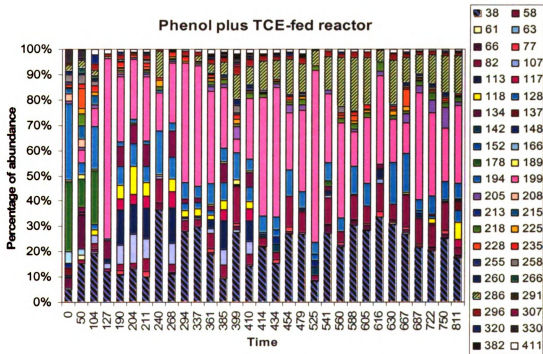
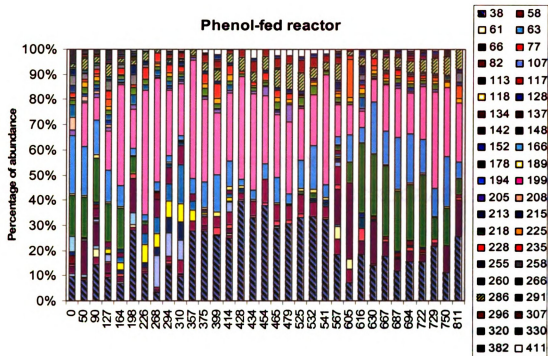
III. References

- Amann, R. I., W. Ludwig and K. H. Schleifer.** (1995). Phylogenetic identification and in situ detection of individual microbial cells without cultivation. *Microbiol Rev* **59**: 143-69.
- Braker, G., H. L. Ayala-del-Rio, A. H. Devol, A. Fesefeldt and J. M. Tiedje.** (2001). Community structure of denitrifiers, Bacteria, and Archaea along redox gradients in pacific northwest marine sediments by terminal restriction fragment length polymorphism analysis of amplified nitrite reductase (*nirS*) and 16S rRNA genes. *Appl. Environ. Microbiol.* **67**: 1893-1901.
- Bruce, K. D.** (1997). Analysis of *mer* gene subclass within bacterial communities in soils and sediments resolved by fluorescent-PCR-restriction fragment length polymorphism profiling. *Appl. Environ. Microbiol.* **63**: 4914-4919.
- Brunk, C. F., E. Avaniss-Aghajanni and C. A. Brunk.** (1996). A computer analysis of primer and probe hybridization potential with small-subunit rRNA sequences. *Appl. Environ. Microbiol.* **62**: 872-879.
- Clement, B. G., L. E. Kehl, K. L. DeBord and C. L. Kitts.** (1998). Terminal restriction fragment patterns (TRFPs), a rapid, PCR-based method for the comparison of complex bacterial communities. *Journal of Microbiological Methods* **63**: 4516-4522.
- DeLong, E. F.** (1992). Archaea in costal marine environments. *Proceedings of the National Academy of Science* **89**: 5685-5689.
- Giovannoni, S. J.** (1991). The polymerase chain reaction. *In* *Nucleic acids techniques in bacterial systematics*. E. Stackebrandt. New York, John Wiley & Sons 177-201.
- Liu, W. T., T. L. Marsh, H. Cheng and L. J. Forney.** (1997). Characterization of microbial diversity by determining terminal restriction fragment length polymorphisms of genes encoding 16S rRNA. *Appl. Environ. Microbiol.* **63**: 4516-4522.
- Marsh, T. L.** (1999). Terminal restriction fragment length polymorphism (T-RFLP): an emerging method for characterizing diversity among homologous populations of amplification products. *Curr. Opin. Microbiol.* **2**: 323-327.
- Moyer, C. L., J. M. Tiedje, F. C. Dobbs and D. M. Karl.** (1998). Diversity of deep-sea hydrothermal vent Archaea from Loihi Seamount, Hawaii. *Deep-Sea Research II* **45**: 303-317.

APPENDIX B

***HA*III T-RFLP DATA**

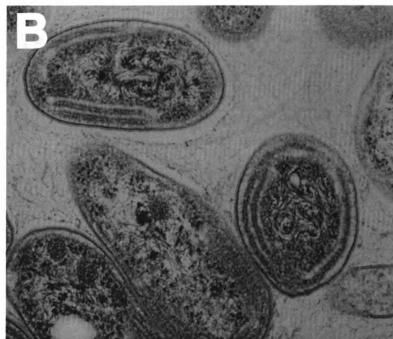
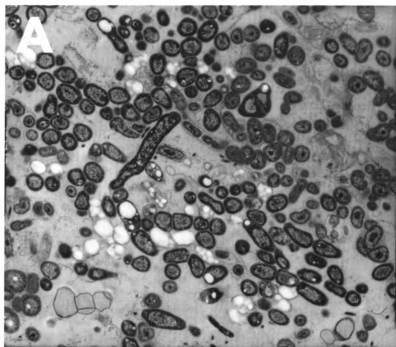
Relative abundance of Bacterial T-RF's from reactor samples after digestion with *Ha*III. Numbers in the legend indicate the sizes of the T-RF's in base pairs.

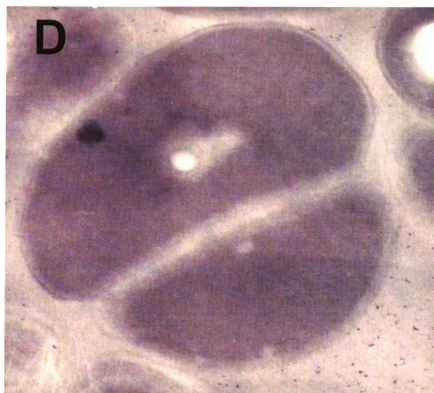
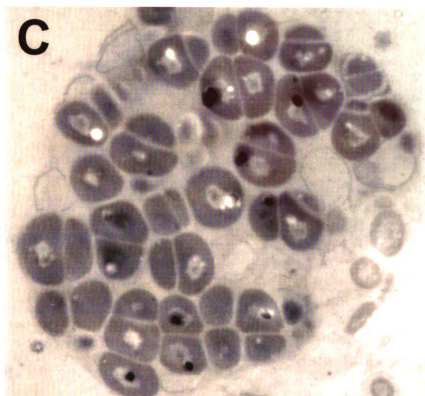


APPENDIX C

TRANSMISSION ELECTRON MICROGRAPHS

Sampling was performed as described in Chapter 3. Samples were processed by the Center for Electron Microscopy at Michigan State University. A, phenol-fed reactor diversity of morphotypes. B, microorganisms with internal membrane systems that resemble ammonia oxidizers in the phenol-fed reactor. C-D, phenol plus TCE-fed reactor images that suggest that some accumulation of storage polymers could be occurring in this community (clear areas inside the cells).





MICHIGAN STATE UNIVERSITY LIBRARIES



3 1293 02327 0774